CT5060 Master of Science Thesis

The influence of flow acceleration on the stability of stones

October 2006 M.A. Huijsmans

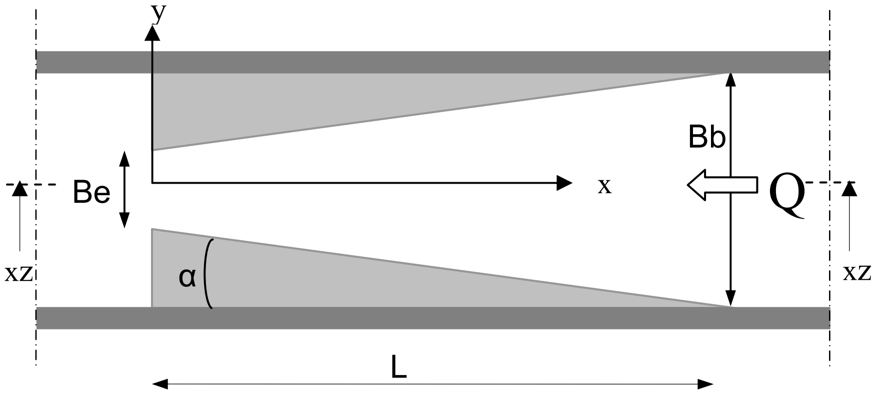

Graduation Committee:
Prof. dr. ir. M.J.F. Stive
Ir. H.J. Verhagen
Dr. Ir. H.L. Fontijn

Faculty of Civil Engineering and Geosciences
Department of Hydraulic Engineering and Geotechnical Engineering
Hydraulic Engeneering Section

Preface

Part of the graduation process of becoming a civil engineer is writing a Master of Science thesis for the Faculty of Civil Engineering and Geosciences of the Delft University of Technology. The work has been carried out for the Hydraulic Engineering Section. The experiments were conducted in the Fluid Mechanics Laboratory under the supervision of the chief of the laboratory dr. ir. H L Fontijn.

Two studies on the subject have already been completed by two former fellow students; ir M M A Tromp and ir M Dessens. This thesis can be seen as an extension on the previous findings by Dessens (2004).

I would like to thank my graduation committee, professor dr ir M J F Stive, ir H J Verhagen and dr ir H L Fontijn, for their assistance and patience.
I would like to thank MSc H Nguyen for the experiments he did. Hoan helped me when I was immobilised after having injured my leg.
I would also like to thank ir M Dessens for his support and advice during the project.
Without the staff of the laboratory, who constructed the tapering of the canal and guided the experiments, this work would not have been possible. My thanks also go out to them.

Markus Huijsmans

Delft
October, 2006

Abstract

Bed protections are often made of granular material and are used to prevent erosion of the bottom or the development of scour holes near hydraulic structures. Failure of the bed protection can undermine the foundations of a hydraulic structure and in the worst case lead to total failure of the hydraulic structure.

Damage of the bed occurs when the top layer of a bed protection isn't able to withstand the hydraulic forces caused by the flow. The threshold of motion is reached and stones will start to move. The threshold conditions are described in terms of the critical flow velocity or shear stress. Current design methods for bed protections are valid for situations where uniform flow exists.

In situations where the uniform flow is interrupted, velocity gradients develop. It is found in experiments and in practice that, when a flow is accelerated stones start to move before the critical velocity has been reached. Scientists ascribe this movement to the existence of flow accelerations.

To find out more about this phenomena experiments are carried out in a flume containing a tapered section. In the tapered section the flow is accelerated and flow conditions can be created so that the threshold of motion will be reached. If the assumptions are correct the stones should move before the critical flow velocity is reached.

Dessens (2004) showed that for combinations of the same velocity with different accelerations there were differences in the movement of stones. More movement was detected for situations were the acceleration was higher yet with the same velocity.

More experiments will be conducted with conditions that vary from those of Dessens to establish the area of influence of acceleration and velocity on the threshold of motion.

An attempt is made to quantify the difference in velocity of the accelerated situation with the velocity of a uniform situation for which the same amount of stone movement would occur.
With the help of the 7 stages of movement defined by Breusers (1969) a translation is made from the amount of moved stones in the experiments to the Shields number that represents this amount of movement.
With this Shields (1936) parameter the critical velocity can be calculated for which this amount of movement occurs in uniform flow conditions. This velocity will be compared with the velocity measured in the experiments. A shift in velocities should occur between the average velocity of the accelerated flow and the average calculated velocity for a uniform flow.

Table of contents

1 Introduction

The movement of bed material from bed protections has been the subject of research for quite some years. The current methods for calculations on the threshold of motion use the velocity of the horizontal flow and the stone size as the main contributing parameters for stone movement. These methods are valid for situations where uniform flow exists.
In situations where a flow is accelerated, stones start to move before one would expect.
The main investigation of this thesis is to quantify the effect that flow acceleration has on the threshold of motion of stones.
Chapter 1 gives background information of the problem, then formulates objectives for this research program and explains the further approach to quantify the effect that flow acceleration has on the stability of stones.

1.1 Problem description

Bed protections made of granular material are often used to prevent erosion of the bottom or the development of scour holes near hydraulic structures. Failure of the bed protection can undermine the foundations of a hydraulic structure and in the worst case lead to total failure of the hydraulic structure.
Damage of the bed occurs when the top layer of stones of a bed protection isn't able to withstand the hydraulic forces. The threshold of motion is reached and the stones will start to move. So we need to know the hydraulic forces that are acting on the stones and we need to know what the resisting forces of the stones are.

The strength of a bed is largely determined by the weight of the stones. This gravitational force is aided by frictional and contact forces by adjacent stones. These forces work to keep a stone in place.
The hydraulic forces acting on a stone are caused by pressure gradients and viscous skin friction. These cause a lift force and a drag force. With an increase of the flow velocity these forces increase. In a uniform flow the stability of the bed is directly related to the mean longitudinal flow velocity.

In practice there are situations where the uniform flow is interrupted and velocity gradients develop. Under certain conditions stones start to move before the critical velocity is reached. Scientists ascribe this type of movement to the existence of flow accelerations.
Schokking (2002) found in an experimental model of jet wash on a slope that more damage occurred at the location of maximum acceleration then at the location of maximum flow velocity.

Acceleration of flow exists in a number of ways in open water. Accelerations of flow develop in waterways, lakes and estuaries because of restrictions in flow by groin fields, bridge pillars or other abutments. Acceleration of flow occurs when water flows through hydraulic structures like locks, barrage dams or closure gaps.
Flow acceleration also occurs when water flows along strong bends in a river or when waves hit a slope.

An example of a hydraulic structure where the flow through the construction is accelerated can be seen in *Figure 1.1*.

Figure 1.1 *Acceleration of flow through a closure gap*

The fact that stones start to move before the critical flow velocity is reached is a point of interest for the Hydraulic Engineering section of the Faculty of Civil Engineering and Geosciences, Department of Hydraulic and Geotechnical Engineering of the Delft University of Technology.
To find out more about these events the section of Hydraulic Engineering started a research program. Two former students, ir. M. Dessens (2004) and ir. M.M.A. Tromp (2004), carried out experiments where local flow accelerations occurred.
Dessens did so by carrying out experiments in a flume containing a local tapered section. He investigated the stability of different stone sizes where the flow was accelerated due to the tapering of the side walls of the flume.
Tromp carried out experiments in a flume under the influence of waves. A wave creates a local acceleration of flow. Tromp looked at the movement of stones at these locations where local accelerations occur.
Dessens pointed out that there is a relation between acceleration of flow and the flow velocity regarding the threshold of motion. In order to get the full picture more experiments needed to be conducted, so that a larger range of data would be covered.

Understanding the consequences of acceleration of flow on the stability of stones will have its influence on bed protection design. Efficient designing will be the reward.

1.2 *Review of existing literature*

Izbash (Schiereck, 2001 after Izbash, 1930) uses the forces that act on a single grain to define a critical flow velocity for which a grain with a certain diameter and density will start to move. The critical velocity in this case is the local velocity just above the bed without knowing its relation to the water depth. This method can be used if the velocity just above the bed is known.
Using this method in case of accelerated flow does not indicate the amount of acceleration that takes place. But it can be used as an indication for a threshold of motion.

Shields (Schiereck, 2001 after Shields, 1936) uses empirical formulae as a basis for the design method for incipient motion. With the use of graphs a threshold of motion can be found. Shields assigns the movement of stones to the exceeded critical value of the shear stress. The shear stress is related to the height above the bed by the logarithmic velocity flow profile for a uniform undisturbed flow (Van Rijn, 1984). This threshold of motion is valid only for a uniform flow. In the case of this thesis the uniform flow will be disturbed and the empirical relations will no longer be applicable.

King (1991) showed that the boundary layer does not fully develop in an accelerated flow as it does in a uniform flow. The boundary layer thickness is less in an accelerated flow than in a uniform flow. This could mean that the bed shear stress in an accelerated flow is higher than that of a uniform flow. This would result in more movement of stones.

Fluid accelerations have also been related to sandbar morphology by Elgar and Hoefel (2003) where it was shown that the peak in acceleration skewness of the surf zone flows was well correlated to onshore sandbar motion.

Calantoni and Drake (2001) investigated the effect of fluid acceleration on bed load transport in highly unsteady flows typical of near shore marine environments. They believe that the movement of stones, before the required critical velocity is reached, can be ascribed to the existence of flow accelerations. Flow accelerations are present in non-uniform flows or in the orbital wave motion under waves.

However, there is not yet a clear empirical definition of the influence of acceleration on the stability of stones.

1.3 Problem formulation

The previous experiments have been conducted in a flume with tapered sections of L = 1.50 m and L = 2.00 m. In both cases the upstream end of the tapered section had a width of B_b = 0.50 m and the downstream end a width of B_e = 0.15 m, *figure 1.2*.

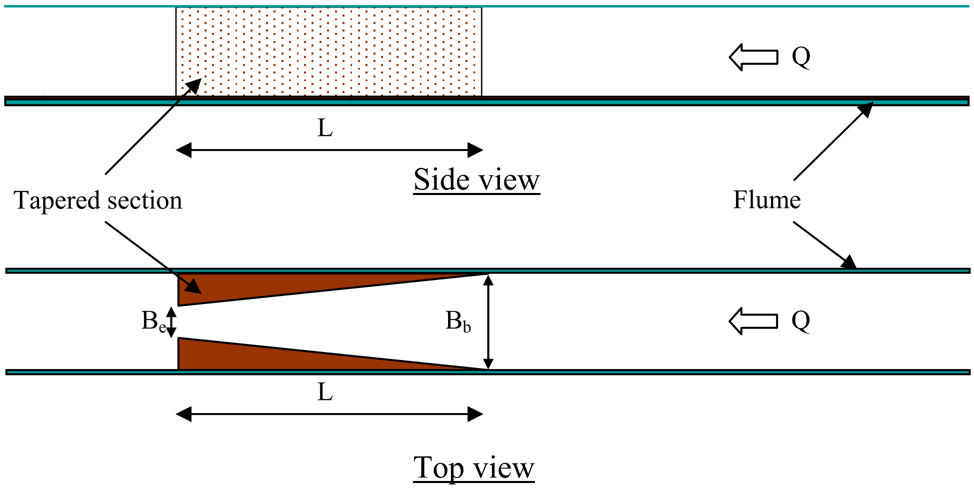

Figure 1.2 *Sketch of the flume with a tapered section*

With this set-up Dessens conducted a number of experiments as listed in the table below:

Table 1.1 *Number of experiments by Dessens*

	Large stones	Small stones
No. of experiments with L = 2.00m	28	58
No. of experiments with L = 1.50m	28	67
No. of experiments used	46	114
No. of u/a combinations	32	66

For the tapered section the flow velocities can be determined by measuring the water depth or by measuring the velocity profile in the xz-plane with an EMS. The value for the average velocity can be calculated using the measured water depth and the width of a certain cross-section, since the discharge is known, *section 4.1.1*.
The average velocity, $\bar{u}$, of a cross-section can also be determined by measuring the velocity profile of the flow, *section 4.1.2*. This is done for certain locations in the tapered section known as the measuring area, *section 3*.3.
The measuring area is divided up into strips. The average acceleration, $\bar{a}$, of the flow over a strip can be determined, *section 4.2*. Each strip of the measuring area creates certain velocity-acceleration combinations. The velocity-acceleration combinations for the small stones found by Dessens can be seen in *figure 1.3*.

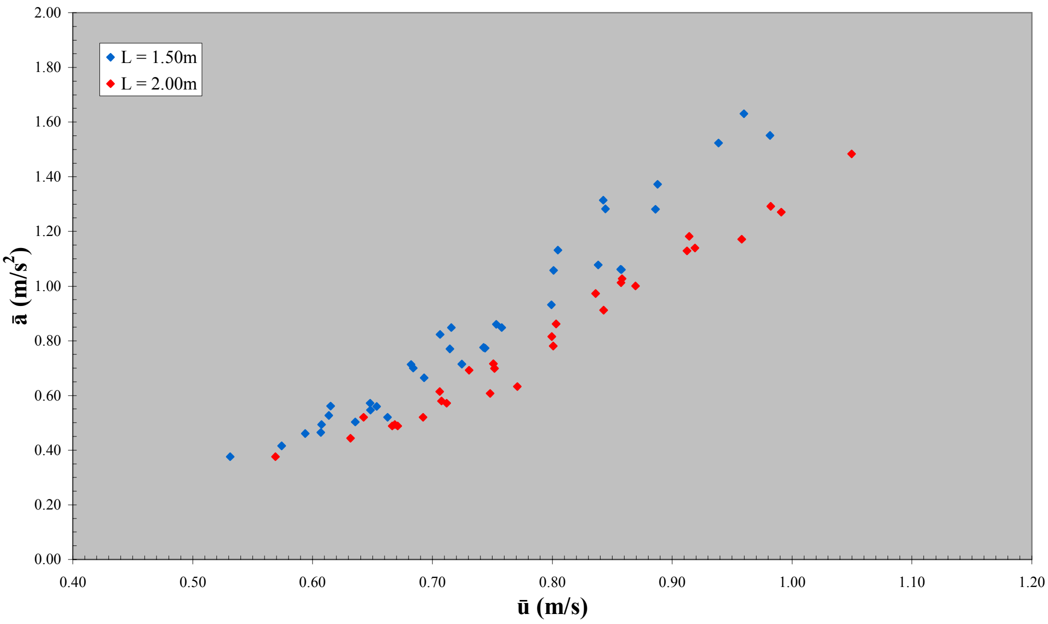

Figure 1.3 *Velocity-acceleration, combinations for small stones (Dessens, 2004)*

The amount of stones that move from a strip during an experiment are documented. Each data point in the graph resembles a certain amount of moved stones with flow conditions with a certain average flow velocity and a certain acceleration of flow.

Assumption 1: The stability of stones only depends on the flow velocity and not on flow acceleration.
If acceleration of flow does not have any influence on the movement of stones, the amount of stones, which move from their strips, will remain the same for a certain velocity regardless of the acceleration that takes place. This is visualized in *figure 1.4*. The lines represent certain amounts of moved stones. Along a line the same amount of stone movement occurs.

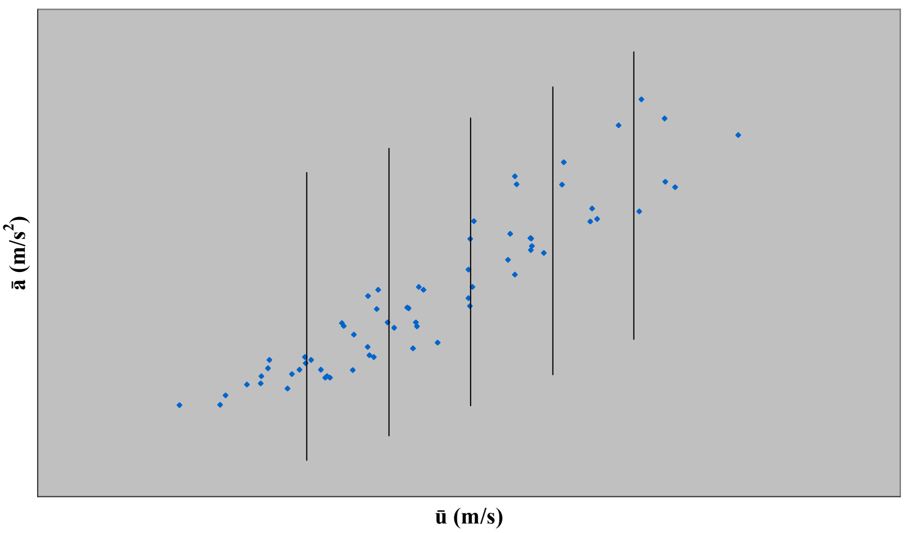

Figure 1.4 *Stability of stones only depends on ū and not on ā*

Assumption 2: The stability of stones depends on the flow velocity and on the acceleration of the flow.
If the stability of the stones is influenced by the flow acceleration this should be visible in the velocity-acceleration graph. For a low velocity and high acceleration combination the same amount of movement should occur as for a higher velocity yet lower acceleration combination. This can be seen in *figure 1.5*.

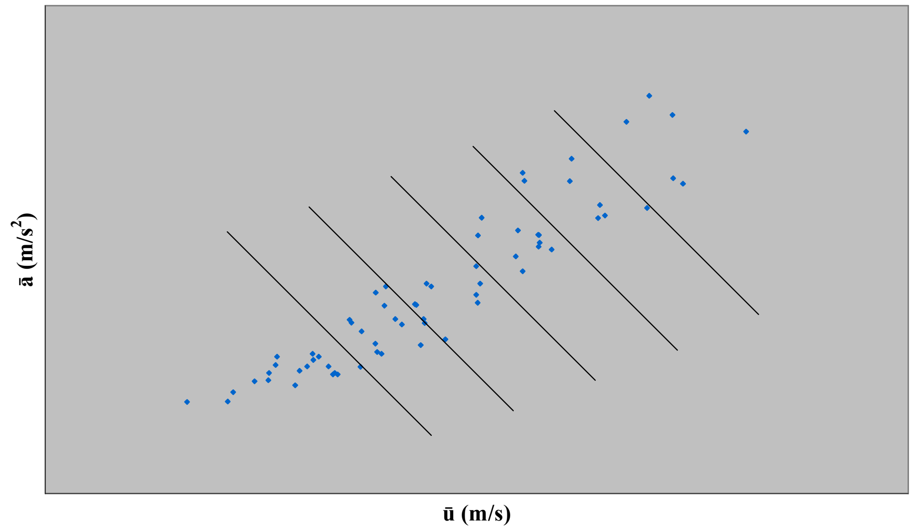

Figure 1.4 *Stability of stones only depends equally on ū as on ā*

The data gathered in the experiments by Dessens are in a "narrow" belt; therefore it is difficult to observe these influences of flow acceleration. More experiments need to be conducted to obtain a broader data belt.
In *figure 1.5* the regions of interest for flow conditions are shown.

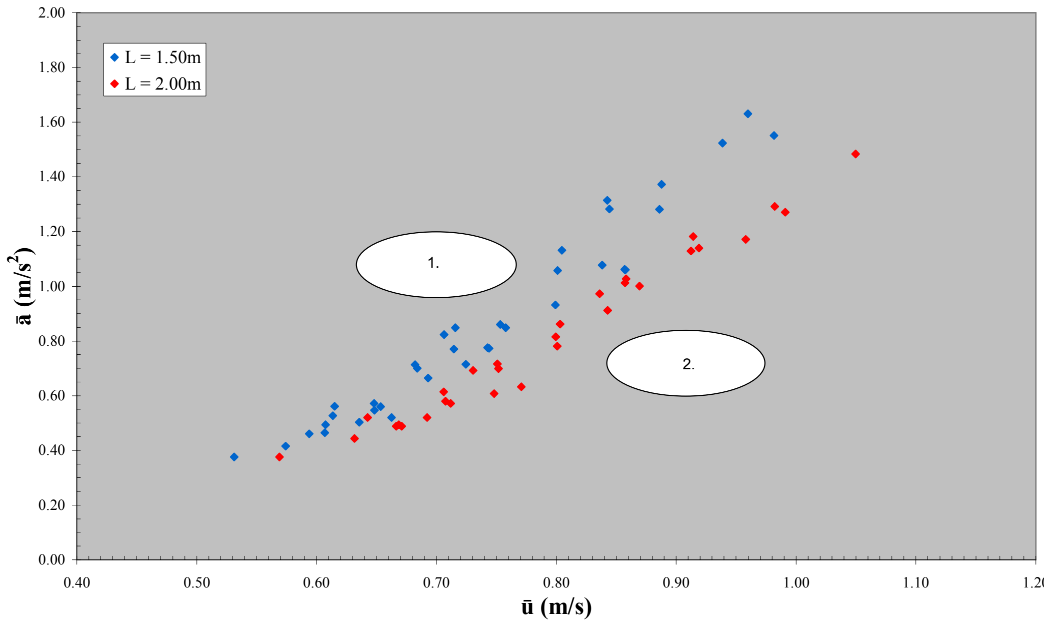

Figure 1.5 *Velocity-acceleration combinations by Dessens and regions of interest for more data gathering*

When the flow velocity is low and the acceleration of the flow is high, the effect that acceleration of flow has on the stability of stones should be the most visible, *region 1* in *figure 1.5*.
The more the flow velocity increases the more likely it is that the stones start to move because the critical flow velocity has been reached, not due to the acceleration of the flow, *region 2* in *figure 1.5*.
Gathering data in situations where flow conditions exist as shown in *figure 1.5*, *region 1* and *region 2* might show the extent of the influence that flow acceleration has on the stability of stones.

Another way to show the influence of flow acceleration on the stability of stones is by determining the flow velocity of a uniform flow ($a = 0$) for a given amount of moved stones with a standard computational method (according to Shields). The difference in velocities between the accelerated flow and the uniform flow, for which the same amount of stones move, can be ascribed to the influence of flow acceleration. *Figure 1.6* shows the expected change in velocities.

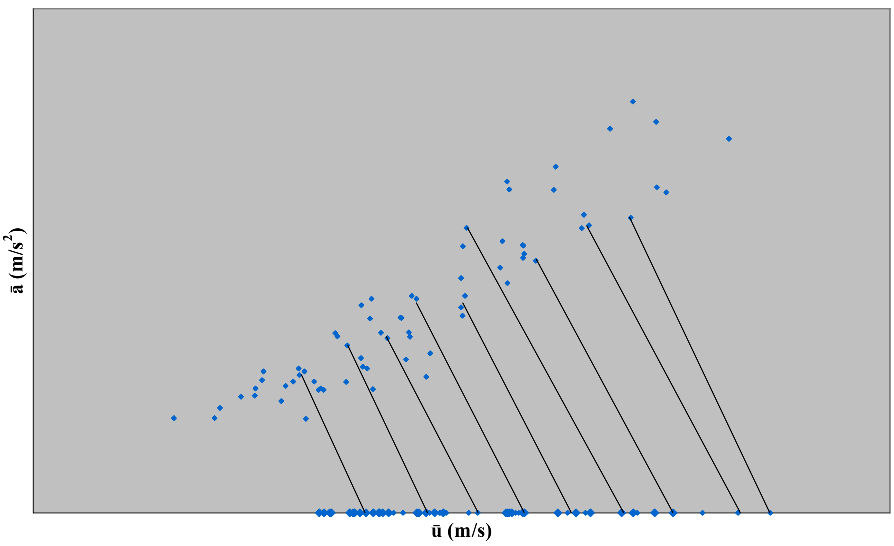

Figure 1.6 *Comparing the velocity of the accelerated flow with the velocity of a uniform flow for which the same amount of stone movement occurs*

1.4 Objectives

The objective for following experiments is to record the movement of stones in situations with flow conditions that lie in the interesting regions as shown in *figure 1.5*.

The objective for the analysis of the data is to compare the average flow velocity of an accelerated flow with the average flow velocity of a uniform flow for which the same amount of transport of stones occurs, to show the influence of acceleration of flow on the stability of stones.

1.5 Approach

In chapter 2 relevant theories on stone stability and flow characteristics that will be used to examine to the effect of flow acceleration on a uniform flow is presented.

Chapter 3 presents a description of the experimental set-up and experimental procedures. This includes specifics on the flume, the granular bed, the measuring devices used including their accuracy of measurement and the sequence of activities in an experiment.

The data which was gathered in the experiments and the methods that were used to convert the data from the experiments to representative values are given in chapter 4.

The data will be analysed in chapter 5 and will be compared to the situation where there is no acceleration of flow. The idea is to translate the data in such a way that it can be compared to the average velocity that normally would be needed to move the same amount of stones.

In chapter 6, the last chapter, the conclusions that can be deduced from the data analysis are summarised. Restrictions of the validity of the conclusions are presented and recommendations for further research are given.

Finally, in the appendices of this report one can find technical specifications, additional experimental data, characteristics of the stones and other specifics.

2 Stone stability and flow characteristics

The purpose of this thesis is to determine the area of influence of flow acceleration on the stability of the stones in a bed.
A bed is stable when the stones are settled in their positions without being swept away by the current. Stones in a bed are not uniformly positioned due to the irregular dimensions of the stones. The stability of a stone in the bed varies depending on its position and its protrusion into the flow. If one looks at the stability of one stone, one can observe that the stone will start to move when the stone is not in equilibrium with the forces acting on it. In a uniform flow stones will start to move when a certain critical average flow velocity is reached.

There are a number of ways to calculate the critical velocity of the flow at which the stability of the bed is no longer secured. Izbash and Shields have studied the stability of stones in flowing water where the flow is considered to be a uniform current (Schiereck, 2001). They found a relation between a stone with a certain diameter and density and the critical flow velocity at which the stone becomes instable. With velocities higher than the critical velocity stones will start to move and for values lower than the critical velocity the stones will remain static.

It is hard to define a clear threshold of motion. Some stones may find themselves in unfavourable positions and after increasing the flow velocity will move a certain distance. Increasing the velocity even more will eventually lead to movement across the whole bed. The movement of one or a small number of stones does not indicate that the threshold of movement has been reached. There are a number of ways to define the movement of a stone. Depending on the definition used and the amount of movement allowed a critical flow velocity can be determined.

This chapter will outline the movement of stones using classical methods and will explain the problem of using these methods for an accelerated flow.

2.1 Forces on a single grain

If one is to understand the stability of stones, it is necessary to know which forces cause a stone to move. A stone will move when the forces acting on it dominate the forces resisting movement. *Figure 2.1* shows the forces acting on a single grain. There are forces acting on the grain: a drag force (F_D), a shear force (F_S) and a lift force (F_L). The drag force is caused by the protrusion of the stone in the flow. The lift force is caused by the curvature of the flow lines. The gravitational force (F_G) and either the moment around *A* or the friction force (F_F) are the two resisting forces keeping the stone in place.

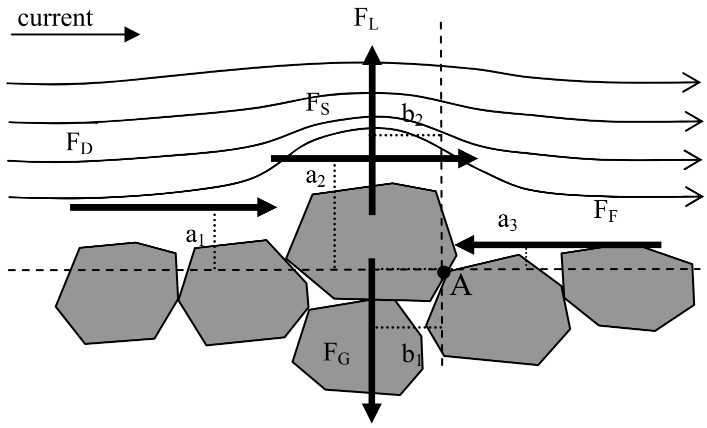

Figure 2.1 *Forces on a grain in flow*

Acting forces:

$$F_D = \frac{1}{2} C_D \rho_w u_b^{\,2} A_D \tag{2.1}$$

$$F_S = \frac{1}{2} C_D \rho_w u_b^{\,2} A_S \tag{2.2}$$

$$F_L = \frac{1}{2} C_L \rho_w u_b^{\,2} A_L \tag{2.3}$$

F_D:	drag force	[N]
F_S:	shear force	[N]
F_L:	lift force	[N]
C_D:	drag coefficient	[-]
C_S:	shear coefficient	[-]
C_L:	lift coefficient	[-]
ρ_w:	density of water	[kg/m^3]
u_b:	velocity of the flow near the bottom	[m/s]
A_D:	exposed surface area	[-]
A_L:	exposed surface area	[-]
A_S:	exposed surface area	[-]

Resisting forces:

$$F_G = (\rho_s - \rho_w) g V \tag{2.4}$$
$$F_F = C_F (\rho_s - \rho_w) g V \tag{2.5}$$

F_G:	gravity force	[N]
F_F:	friction force	[N]
C_F:	friction coefficient	[-]
ρ_s:	density of stone	[kg/m^3]
g:	gravitational acceleration	[m/s^2]
V:	volume of the stone ($\propto d_n^3$)	[m^3]
d_n:	nominal diameter	[m]

$$\sum V = 0 \Rightarrow F_L = F_G \tag{2.6}$$
$$\sum H = 0 \Rightarrow F_D + F_S = C_F \cdot F_G \tag{2.7}$$
$$\sum M\big|_A = 0 \Rightarrow F_D \cdot a_1 + F_S \cdot a_2 + F_L \cdot b_2 = F_G \cdot b_1 + F_F \cdot a_3 \tag{2.8}$$

The weight of the stone is proportional to the diameter, d, by the third power. If one considers the horizontal, vertical or moment equilibrium, one proportionality remains:

$$\rho_W \cdot u_c^2 \cdot d^2 \propto (\rho_s - \rho_w) \cdot g \cdot d^3 \tag{2.9}$$

Here the critical velocity is used: u_c. A dimensionless relation between load and strength can now be deducted.

$$u_c^2 \propto \left(\frac{\rho_s - \rho_w}{\rho_w} \right) \cdot g \cdot d = \Delta \cdot g \cdot d \rightarrow u_c^2 = K \cdot \Delta \cdot g \cdot d \tag{2.10}$$

Δ:	relative density (= $(\rho_s - \rho_w) / \rho_w$)	[-]

All the formulae on grain stability follow this proportionality. The constant K has to be determined empirically.
There are a number of formulae used for this purpose of which two formulae will be considered in the next two sections: Izbash and Shields.

2.2 Stone stability in a uniform flow

2.2.1 Izbash

Izbash, 1930, expressed *equation (2.10)* as:

$$u_c = 1.2 \cdot \sqrt{2 \cdot \Delta \cdot g \cdot d} \tag{2.11}$$

u_c:	critical velocity	[m/s]
d:	diameter	[m]

In this formula depth is not considered as a contributing factor. Izbash did not define a velocity distribution profile. This formula can be used as an indication when the velocity near the bottom is known, without knowing its relation to the water depth, for instance when a jet enters a body of water. In other cases Shields is recommended.
In case of a very rough protection (h/d_{n50}< 5; h: waterdepth [m], d_{n50}: median nominal diameter [m]) the Shields formula is not very reliable. In that situation one may use the Izbash formula.

2.2.2 Shields

The most commonly used formula for stability of stones is the Shields formula. Shields found a relation between the initiation of motion of grains and the occurring critical shear stress.
Shields described the initiation of motion by relating the dimensionless critical value of the shear stress (ψ_c) to the particle Reynolds-number (Re_*) (Schiereck, 2001).

$$\psi_C = \frac{\tau_C}{(\rho_S - \rho_W)gd} = \frac{u_{*C}^2}{\Delta gd} = f(\mathrm{Re}_*) \tag{2.12}$$

ψ_c:	Shields parameter	[-]
τ_c:	critical shear stress	[N/m^2]
d:	stone diameter	[m]
u_{*c} :	critical shear velocity	[m/s]

$$\mathrm{Re}_* = \frac{u_{*c}d}{\upsilon} \tag{2.13}$$

Re_*:	particle Reynolds number	[-]
υ:	kinematic viscosity	[m^2/s]

Shields uses shear stress, τ_c, as the active force. Shear stress is not necessarily the active force in every situation, but for the purposes of this study using the shear stress as an active force is the right choice. For small water depths the concept of a shear stress on the grains is no longer valid. The flow exerts only a drag force on the grain. However this is not the case in these experiments, since h/d_{n50} > 20 is the lower limit in the conducted experiments.

The critical shear velocity, u_{*c}, is an algebraic expression with which the critical shear stress can be found through iteration in the empirical Shields graph, *figure 2.2.*
The particle Reynolds number, Re_*, tells you whether the grain is protruding in the turbulent boundary layer or whether it is still covered by a viscous sub-layer. The grain size used in these experiments is of such proportion that a high Re_* is reached (Re_*> 500). For a high Re_* a constant value of ψ_c = 0.055 is found as the boundary between transport and no transport.

Figure 2.2 shows the relation between ψ and Re_*. The Shields curve shows the change between no transport and transport. Transport occurs for values of ψ above the curve.

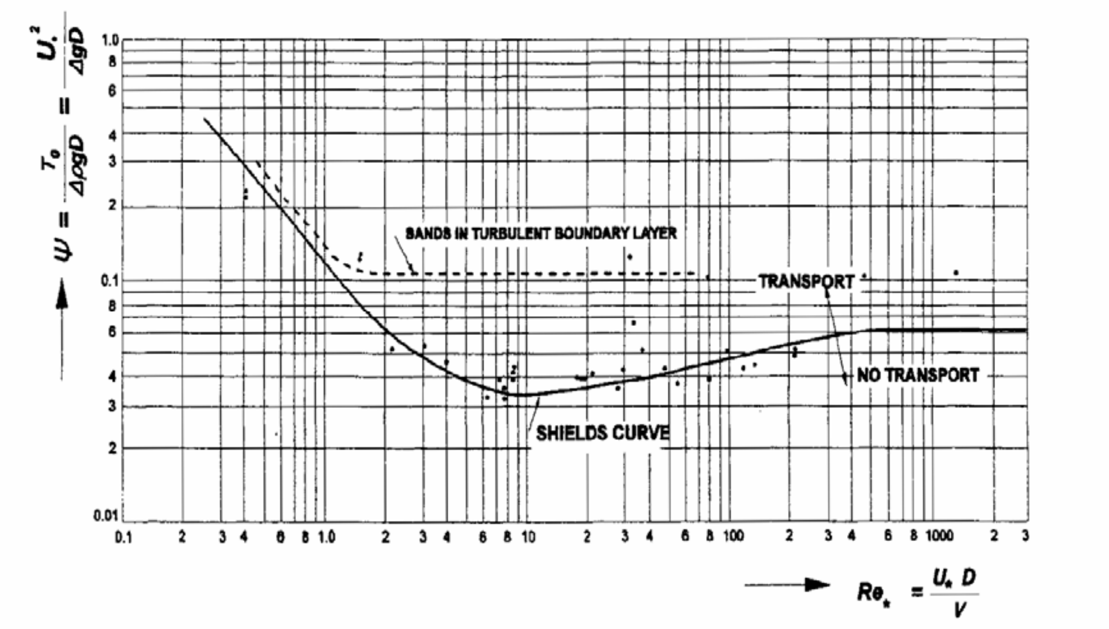

Figure 2.2 *Critical shear stress according to Shields*

It is difficult to define a clear threshold of motion. Some stones may move because of unfavourable positioning in the bed or unfavourable shapes. Increasing the velocity even more will eventually lead to movement across the whole bed. The movement of one or a small number of stones does not indicate that the threshold of movement has been reached.

A study done by Delft Hydraulic Laboratory (DHL) into incipient motion defined 7 stages of transport (Breusers, 1969). These reflect the transition between no movements at all to total movement across the whole bed. The different stages are related to the Shields stability parameter, ψ as can be seen in *figure 2.3*.

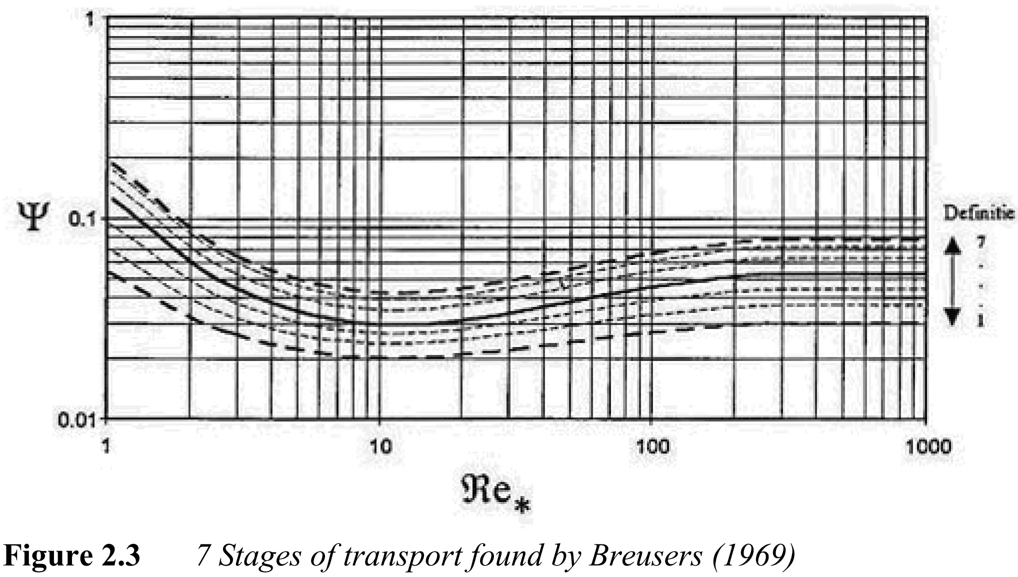

Figure 2.3 *7 Stages of transport found by Breusers (1969)*

Seven stages of transport as defined by Breusers:

stage 0 - no movement at all
stage 1 - occasional movement at some locations
stage 2 - frequent movement at some locations
stage 3 - frequent movement at several locations
stage 4 - frequent movement at many locations
stage 5 - frequent movement at all locations
stage 6 - continuous movement at all locations
stage 7 - general transport of the bed

The theory described in this section is valid for a uniform stationary flow.
In case of an accelerated flow it will be shown in the experiments that the uniform logarithmic flow profile changes, so the relation found by Shields on stone stability is no longer valid.

In a uniform current the velocity of the flow is affected by the bottom friction. The shear velocity is used to describe the bottom stress. The shear stress at the bottom, τ_0, is the developed shear force per unit wetted area.

In the next section the theoretical approach for the velocity distribution of a logarithmic flow profile is given.

2.3 Velocity distribution in a uniform flow

Bottom friction in a uniform current affects the velocity of the flow. The bottom friction creates a boundary layer. As a fluid moves past the bottom, molecules stick to the surface of the bottom. The molecules just above the surface are slowed down in their collisions with the molecules sticking to the surface. These molecules in turn slow down the flow just above them. The farther one moves away from the surface, the fewer the collisions are affected by the object surface. This creates a thin layer of fluid near the surface in which the velocity changes from zero at the surface to the free current velocity away from the surface and this layer is logarithmic in shape.
The logarithmic part of the flow profile exists from a distance of 2 or 3 times the grain diameter above the bed up to at least 0.2 times the water depth, *h.*

A theoretical approach is used for the flow profiles measured in the experiments.
For an undisturbed 2-dimensional flow with a free surface area and a water depth, *h*, the logarithmic flow profile is given by Nikuradse (Schiereck, 2001 after Nikuradse, 1932):

$$\frac{u}{u_*} = \frac{1}{\kappa} \ln \frac{z}{z_0} \qquad (2.14)$$

Integration over the depth h gives the discharge per width:

$$q = \int_0^h u dz \cong \frac{u_*}{\kappa} \int_{z_0}^h \ln \frac{z}{z_0} dz \qquad (2.15)$$

q:	discharge per width	[m^2/s]
u:	velocity	[m/s]
κ:	von Kàrmàn constant (= 0.4)	[-]
h:	water-depth	[m]
z:	height above the bed	[m]
z_0:	the position above the bottom where the velocity is zero	[m]

With $\int \ln x dx = x \ln x - x$ this becomes:

$$q = \frac{u_* h}{\kappa}\left[\ln\frac{h}{z_0} - 1 + \frac{z_0}{h}\right] \approx \frac{u_* h}{\kappa}\left[\ln\frac{h}{z_0} - 1\right] \text{, with } z_0 << h \tag{2.16}$$

This can be written as:

$$\bar{u} = \frac{q}{h} = \frac{u_*}{\kappa}\ln\left(e^{-1}\frac{h}{z_0}\right) \rightarrow \frac{\bar{u}}{u_*} = \frac{1}{\kappa}\ln\left(e^{-1}\frac{h}{z_0}\right) \tag{2.17}$$

$\bar{u}$:	depth-averaged flow velocity	[m/s]

Figure 2.4 shows the logarithmic flow profile near the bottom due to the bottom shear stress, given in *equation (2.14)*. This equation resembles the relation between the shear velocity and the mean velocity. This relation is valid for an undisturbed flow.

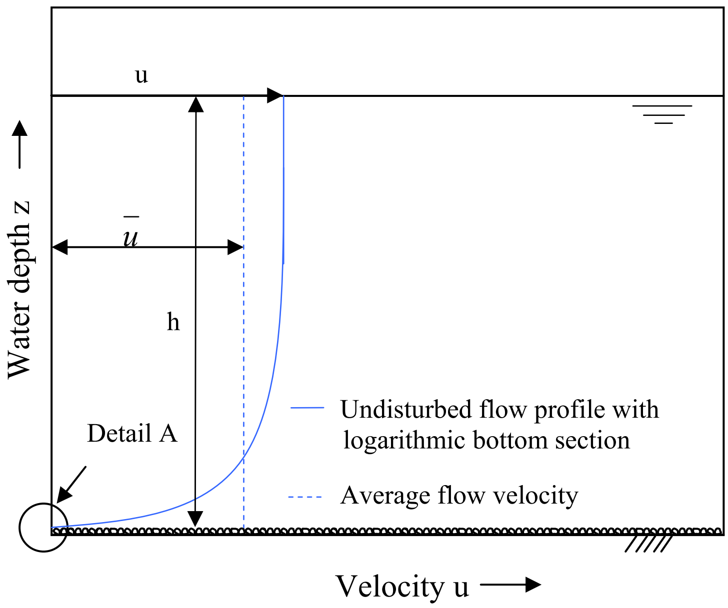

Figure 2.4 *Logarithmic velocity profile of an undisturbed flow. Detail A: see figure 2.5*

Figure 2.5 shows *Detail A* of *figure 2.4*, the level of the bed. The velocity reaches zero just above the level of the bed. This point is known as z_0, ($u = 0$ at $z = z_0$).

The level of the bed (z = 0m) and z_0 are levels that need to be determined when the experimental set-up is in place and the flow conditions are studied. *Chapter 4* will look into this.

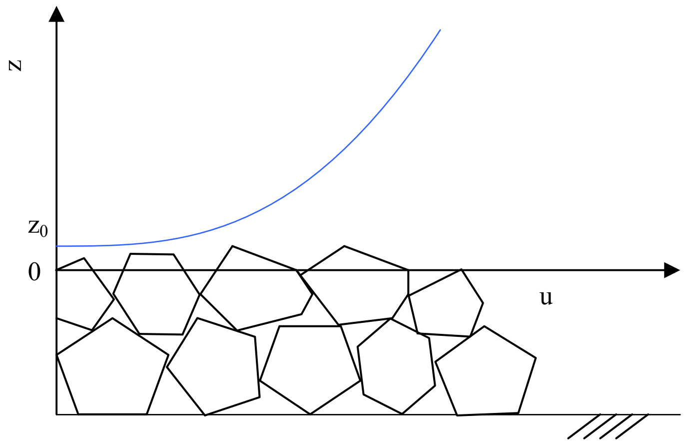

Figure 2.5 *Detail A: level of the bed, z = 0; u = 0 at $z = z_0$*

The flow is undisturbed and uniform as flow enters the tapering. This logarithmic flow profile will be measured and used to determine z_0.

2.4 Velocity profile in an accelerated flow

Gradients in the velocity distribution cause the uniform logarithmic flow profile to change. Acceleration causes reduction of the boundary layer thickness. When a flow is accelerated the velocity profile becomes fuller. $\partial u / \partial z$ increases near the bottom which causes an increase of shear stress (Schiereck, 2001).
Figure 2.6 shows the change in velocity profile for an accelerated flow and decelerated flow.

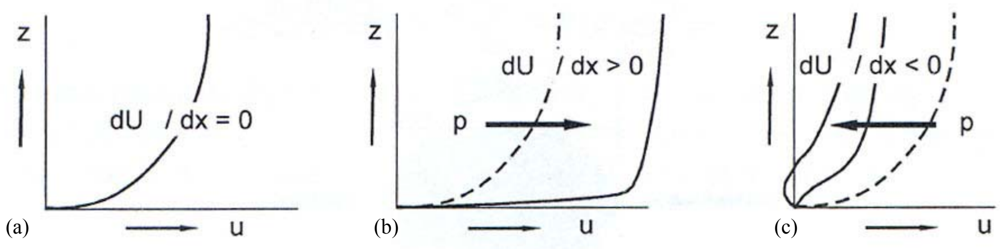

Figure 2.6 *Change in velocity profile due to velocity gradients in x-direction, (a) stationary uniform flow, (b) accelerated flow, (c) decelerated flow (Schiereck, 2001)*

In the experiments conducted for this thesis the flow in the flume will be accelerated. The flow profiles measured in the experiments will resemble the velocity profile given in *figure 2.6b*.

3 Experimental set-up and procedure

In a flume at the Fluid Mechanics Laboratory of the Department of Hydraulic and Geotechnical Engineering of the Faculty of Civil Engineering and Geosciences, Delft University of Technology, conditions are created so that acceleration of flow occurs. A locally tapered section in the flume will cause flow accelerations. Varying the dimensions of the tapering will create different combinations of velocity and acceleration.

One of the objectives of this thesis is to obtain data that can be added to the data gathered in the experiments conducted by Dessens (2004). The experimental set-up used by Dessens must be followed. In this chapter this setup will be explained as well as the chain of activities

3.1 The flume

The flume which was used for the experiments has a length of approximately 14m, a width of 0.50m and a height of 0.70m. Water is pumped from a basin to the flume through the inlet pipe, Q_{in}.
The discharge entering the flume is regulated by an inlet valve and is measured with an orifice plate. The difference in water pressure before and after the orifice plate can be translated in a difference in piezometric head on a pressure gauge. The difference in piezometric head is related to a value for the discharge.
The water enters the flume through a diffuser. As the water leaves the diffuser it is still very turbulent, so a flow stabilizer has been placed in the flume. Water flows under these conditions remain turbulent; however a uniform flow profile will develop if the large turbulent structures in the flow are subdued. The flow profile needs to be fully developed before it enters the tapered section in the flume.

The water level in the flume can be regulated by adjusting the height of a gate at the end of the flume.
The gate works as a Rehbock-gate. The related discharge calculations will not be used, since these discharge calculations are based on a logarithmic flow profile. In the tapered section the logarithmic flow profile will change.

A visualization of the flume is given in *figure 3.1*. The picture is not to scale.

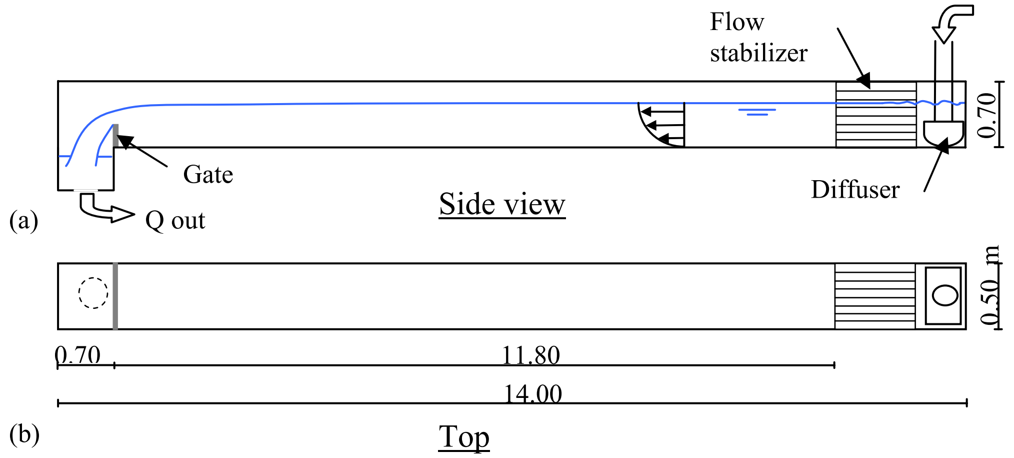

Figure 3.1 *The flume: (a) side view; (b) top view (courtesy Dessens, 2004)*

Wooden plates are placed on the bottom of the flume. A granular bed covers these wooden plates. Near the end of the flume a tapered section is made to create acceleration of flow. In the next sections features of the tapered section and the granular bed will be reviewed.

3.2 Tapering of the channel

To create acceleration of flow a tapered section is placed in the flume.
The dimensions and the construction of the tapering are straightforward. It is a symmetrical construction, so that the water streamlines will form a symmetrical flow pattern in a cross section of the flume.
The sidewalls are made of multiplex and have a smooth surface. At the upstream end of the contraction the transition between the glass and the side walls is made as smooth as possible with an additional adhesive, as not to lose any of the discharge behind the walls of the tapered section. The bottom plates cover the length of the flume and will be covered with a granular bed. Parameters and placement of these stones will be covered in *section 3.3*.

The end of the tapered section is placed at a far enough distance from the gate to avoid influence of the gate on the flow in the tapered section. In the experiment a distance of 1.85m was chosen between the outflow and the gate. Considering that the maximum height of the gate in the experiments was 0.20m, it means that the distance between the outflow of the contraction and the gate is over 9 times the height of the gate. For a Rehbock-gate, at a distance of two times the height of the gate there is no influence of the gate on the water height upstream. So it is safe to assume that there is no influence on the flow from the gate.

By changing the length of the tapered section the angle of the sidewall with the flume wall changes. The greater the angle, the more the flow will be accelerated. The dimensions have been selected to create certain velocity-acceleration combinations, *Table 3.1*.

Table 3.1 *Dimensions of the tapered section used in experiments*

Length L (m)	Inflow B_b (m)	Outflow B_e (m)	Height (m)	Angle α (°)	Acceleration	Velocity
1.50	0.15	0.50	0.70	6.65°	high	low
2.00	0.15	0.50	0.70	5.00°	medium	medium
2.50	0.15	0.50	0.70	4.00°	low	high

The areas of high acceleration/low velocity or low acceleration/high velocity are of interest for this study.
The position of the local origin of the xyz-plane is fixed on the surface of the bed at the outflow end of the tapered section and in the middle of the flume. The height of the origin, z = 0, depends on the level of the bed. It depends on the layer of stones that cover the bottom plates.
The bed of stones consists of two layers. With a point gauge the height of the bed needs to be measured in relation to the top of the bottom plates. The average value will give an indication of the height of the level of the bed. This level will be determined in *section 4.1.1.*
In *figure 3.2* the *xy*-plane and the *xz*-plane are shown. The glass walls of the flume are shown in blue and the bottom plates as well as the tapered section are shown in brown.

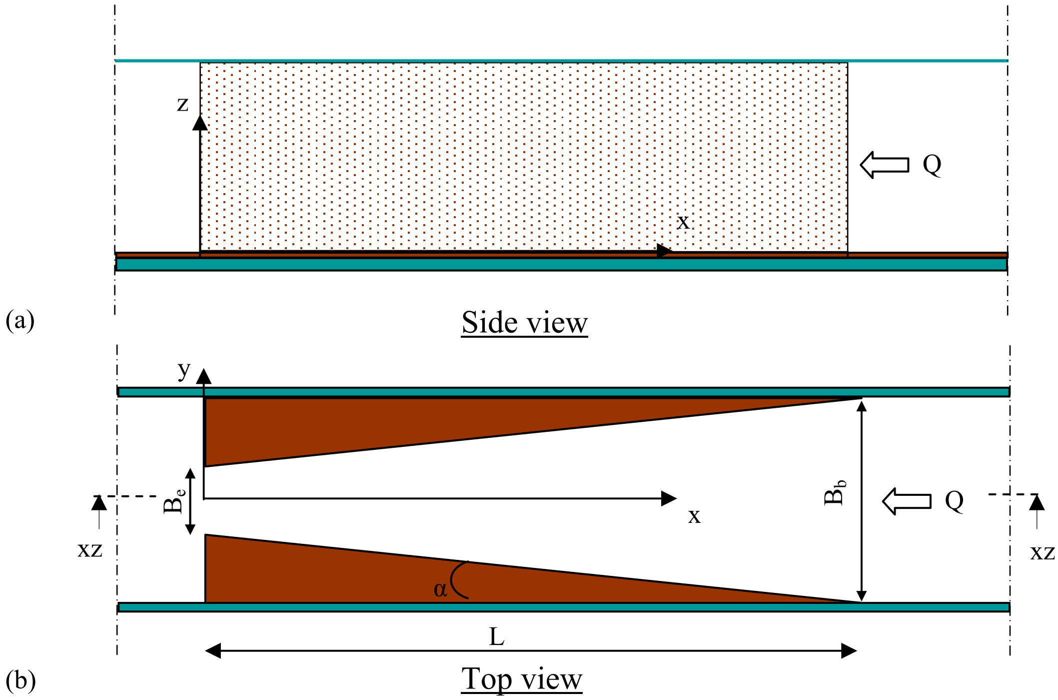

Figure 3.2 *The xz- and xy-plane: (a) side view; (b) top view (courtesy Dessens, 2004)*

The flow accelerates and contracts when it enters the tapered section. When a flow contracts velocity vectors converge. There are converging horizontal velocity vectors in the horizontal xy-plane and converging vertical velocity vectors in the vertical xz-plane.

The locations for velocity measurements are located in the xz-plane in the middle of the, *section 3.4.1*. Here the horizontal velocity vectors are theoretically zero; the converging horizontal velocity vectors cancel each other out due to the symmetry of the tapering.
The converging vertical velocity vectors develop when the flow accelerates and the surface level drops. The vertical velocity vectors cannot be measured with the EMS, *section 3.41*. The actual velocity will be larger than the measured horizontal velocity. This has to be taken into account when the velocity profiles are measured, *section 4.1.2*.

The flume and the tapered section can be seen in *Appendix A, figure A1*.

3.3 Granular bed

In the experiments conducted by Dessens (2004) two grain sizes were used for the tapered section: d_{n50} = 0.0200m ("large" stones) and d_{n50} = 0.0082m ("small" stones). He opted for experiments with two grain sizes to check the influence of flow acceleration on different stone sizes.
This study looks at the influence of flow acceleration on one grain size only, d_{n50} = 0.0082m. With the smaller grain size more movements of the stones can be achieved in the limited flume.

Stone parameters

In the table below the stone parameters for the stones used by Dessens are given:

Table 3.2 *Stone parameters (Dessens, 2004)*

	Small stones	Large stones	Dimension
# stones	250	139	-
M cum.	361.77	2845.6	gr
dn50	0.0082	0.0200	m
ρ av.	2682.2	2682.	kg/m3
W50	1.49	21.422	gr
d85/d15	1.22	1.18	-
Δ	1.67	1.67	-

The number of stones (*# stones*) represents the number of stones measured. The total mass of the stones is given as *M cum*. The average density, ρ_{av}, is the mean value of the dataset. The mean median nominal weight of a stone is given as $W_{50.}$ and the ration between the sieve diameters as d_{85}/d_{15}.
The sieve curves for the mass and d_n are given in *Appendix B*.
A different stone size was used for the approach to the tapered section. The wooden plates before the tapering are covered with a layer of stones with a d_{n50} = 0.015m. More on the placement of the stones can be read in the next section.

Placement of the stones

The wooden plates in the channel are covered with two types of stones. There is a difference in stone sizes for the approach channel and the tapered section of the channel. The way they are placed in the flume can be read in the following section.

A single layer of stones with a d_{n50} = 0.015m covers the bottom plates of the approach channel. The stones are glued to the bottom, so they will not move during the course of the experiments.

The transition between the approach channel and the tapered section changes the boundary layer slightly since there is a difference in roughness. This difference is kept to a minimal by choosing a stone diameter for the approach channel that is approximately 2*d_{n50} of the stones used in the tapered section.

Measuring area

The first layer of small stones covering the wooden plates is glued to the plates to ensure that the smooth surface of the plates does not affect the results of the experiment. This layer is then covered by a second layer of the small stones.
The last 0.40m of the tapering, where movement of the stones most likely occurs, will be known as the measuring area. The colour-coded stones are placed in strips of 0.10m width. Only coloured stones moved from the strips are counted for further analysis.

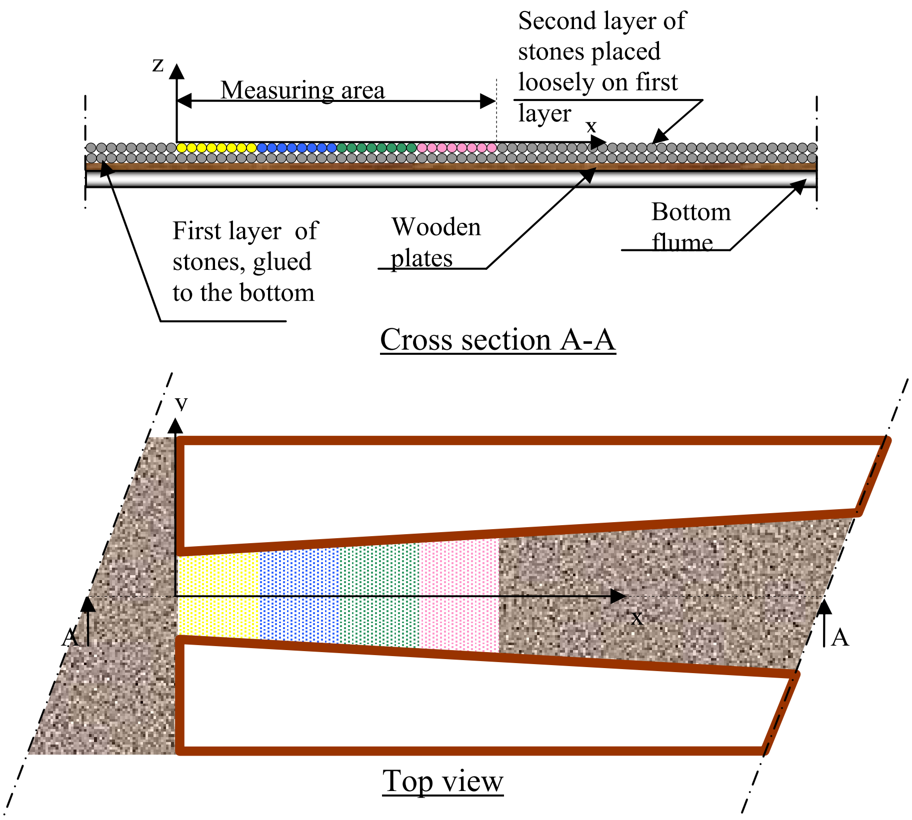

Figure 3.3 *Placement of the stones: a) cross section A-A; (b) top view (courtesy Dessens, 2004)*

The stones in the tapered section are placed by dumping. Estimation is made on how many stones fit a strip. To calculate the amount of stones the assumption is made that the stones are of a cube shape and that they cover the entire surface area between the walls:

$$\#stones = \frac{A_{strip}}{d_{n50}{}^2} \tag{3.1}$$

A_{strip}:	area of a coloured strip	[m^2]
d_{n50}:	median nominal diameter	[m]

This estimation is then compared with the number of stones needed to manually cover up the bottom with one layer of coloured stones.
Dessens found the next relation between the stones used and calculated for small stones:

$$S_{u,small} = 0.92\frac{A_{strip}}{d_{n50}{}^2} \tag{3.2}$$

S_u:	amount of stones in one layer dumped in a strip	[-]

3.4 Experimental procedure

During an experiment relevant parameters need to be measured. In this section the instruments and techniques for these measurements will be taken into account.
The last part of the section deals with the sequence of activities concerning the experiment.

3.4.1 Measurement techniques

The measurements in the experiment can be categorized in four different groups: geometrical, fluid-motion, transport and time-duration measurements.

Table 3.3 *Type of measurement*

Type	To be measured	[ ]	Instrument
Geometrical	Dimensions of the flume	[m]	Tape measure
	Dimensions of the tapering	[m]	Tape measure
	Measuring scheme	[m]	Tape measure
	Water depth	[m]	Point gauge
	Gate height	[m]	Point gauge
	Stone size	[m]	Vernier calliper and balance
Fluid motion	Velocity	[m/s]	EMS
	Discharge	[m/s^3]	Orifice plate
Transport	Number of grains in strip	[-]	Manually
	Number of grains moved from strip	[-]	Manually
Time duration	Duration experiment	[s]	Stopwatch

With the help of a tape-measure and a point gauge a measuring scheme can be set up for the tapered section.
The locations for measurements are located in the xz-plane in the middle of the tapering where the velocities in y-direction are theoretically zero.
Water depth measurements are carried out by measuring the height difference between the water surface and the top of the wooden plates using a point gauge. When the z = 0m level has been determined in the processing stage, this height will be subtracted from the water depths that were measured in the experiment.

The x-positions in the measurement area are located with intervals of 0.10m equal to the width of a strip in the measuring area, as can be seen in *figure 3.4*. Beyond the measuring area the intervals are larger.

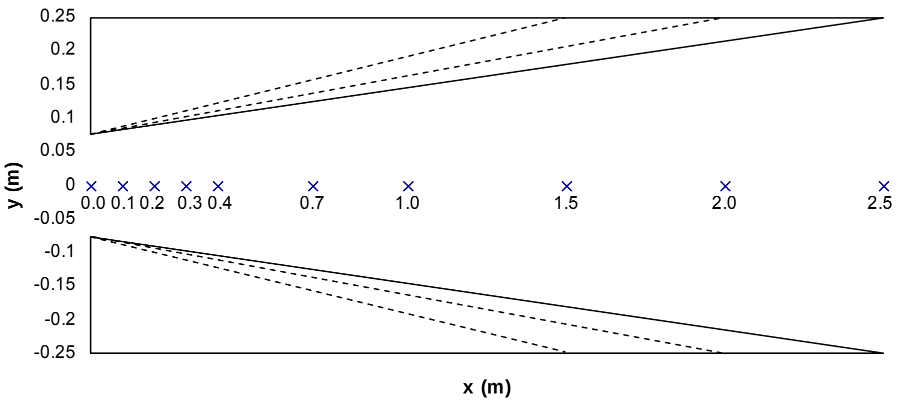

Figure 3.4 *Measuring scheme for water depth measurements, y = 0*

At these locations the water depths need to be recorded as well as the velocity profiles.
The velocity profile will be measured using an EMS.

EMS

Velocity measurements are carried out using an EMS (Electro Magnetic Sensor). The EMS can measure velocities of a flow in x- and y-direction by measuring differences in its magnetic field. The EMS is not capable of measuring velocity gradients in z-direction.

The EMS sensor is sensitive to temperature and humidity changes. Also the distance of the measurement location to a wall, bottom or the water surface level can influence the magnetic field of the EMS.

Because of the sensitivity of the probe of the EMS calibration has to be done between experiments. This calibration is done in still water for all the locations of the measuring scheme. The averaged "zero-measurements" will be subtracted from the averaged measured velocities resulting in a representative velocity of the flow for that specific location.

The measuring scheme for the velocity measurement scheme in the xz-plane is given in *figure 3.5*.

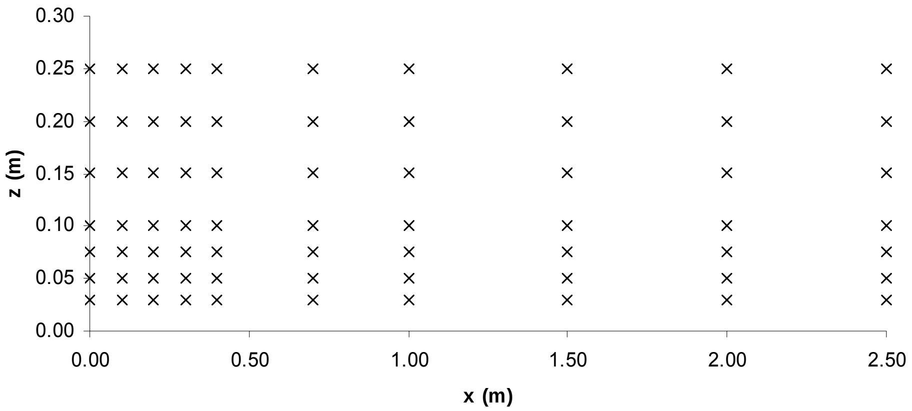

Figure 3.5 *Measuring scheme for velocity measurements*

The location of the lowest measurement is limited to a distance of 0.03m to the z = 0 level. Otherwise the magnetic field is affected and the EMS will not give a proper reading.
If measurements are done too close to the water level the magnetic field might also be affected. In addition vertical velocity gradients exist near the surface. This also needs to be taken into account when the velocity profiles are processed, *section 4.1.2*.

3.4.2 Accuracy and reliability

The accuracy of an experiment largely depends on the instruments used. It is important to know the accuracy of an instrument as to make the right decision on which instrument to use for the experiment.
Incorrect use of an instrument can also affect the outcome of an experiment. Following a tight procedure and double checking the experimental results should eliminate human error.

Although every attempt is made to duplicate every experiment, it can't be avoided that differences in the outcome will exist within a data series. It is inevitable that stones are placed differently during the course of the experiments. When placed in unfavourable positions stones will move earlier.

The number of experiments that is required to acquire a reliable dataset of values has been determined by using a test-retest procedure.
If a standard normal deviation is expected from the obtained data, the student t-test can be used to determine the precision of the mean value of the dataset. The precision, *P*, can be defined as:

$$P = \pm t_{(m,p)} \frac{\sigma}{\sqrt{n}} \tag{3.3}$$

t:	test parameter	[-]
σ:	standard deviation	[-]
n:	number of tests	[-]

In case of this experiment the number of tests taken for obtaining a dataset is 6. To test the significance, you need to set a risk level called the alpha level. In most research, the "rule of thumb" is to set the alpha level at 0.05 ($\alpha = 2p$).
In *table 3*.4 the value for t can be found for different values of p (p = probability). The value of m (m = number of degrees of freedom) is equal to the number of tests minus 1 ($m = n$ -1).

Table 3.4 *Number of test versus the maximum admissible risk*

m \ p	0.1	0.05	0.025	0.01
4	1.533	2.132	2.776	3.747
5	1.476	2.015	2.571	3.365
6	1.44	1.943	2.447	3.143
7	1.415	1.895	2.365	2.998

When assuming a probability p of 2.5%, t will be 2.571. Equation (3.4) can now be written as:

$$P = \pm 1.050\sigma \qquad (3.4)$$

The probability of 2.5% is considered to be acceptable for n = 6 experiments.

The accuracy of measurement for the instruments used is listed in *table 3.5*.

Table 3.5 *Accuracy of the instruments used*

Instrument	Error
Balance	± 0.01 g
Thermometer	± 1º C
Stopwatch	± 1 s
EMS	± 0.02 m/s
Vernier Calliper	± 0.5 mm
Tape measure	± 0.5 mm

3.4.3 The experiment

For a good test result the procedure for the experiment needs to be defined, in order that differences in the results can not be assigned to an inconsequent measuring procedure.
In the experiment a number of things will be measured: the water levels, the flow velocities and the amount of moved stones.

But first the level of the bed needs to be measured. Measure the height of the two layers of stones. The point gauge is lowered until it touches the surface of a stone Then the point gauge is lowered until it touches the top of the bottom plates. The averaged difference in height at 30 arbitrary points will be used to determine the level of the bed in *section 4.11*.

One complete experiment is composed of 7 experiments. In the first experiment the velocities of the flow are measured with the EMS for every location of the measuring scheme. The water depths are also measured.
The velocity measurements only need to be done in the first experiment. Checking that the water levels of the 6 other experiments are equal to the first experiment guarantees that the same flow conditions are met as in the first experiment.
In the first experiment the stone moves are discarded.
In the six experiments, that follow, the emphasis lies on recording the movement of stones. The flow conditions for these experiments must be the same as for the first experiment.

The sequence of activities for measuring the velocity profiles and the water depth in the first flow-velocity experiment is as follows:

1. Set the height of the wooden plates on the bottom as a reference level for the water-depth measurements.
2. Dump the second layer of stones on the first layer.
3. Calibrate the EMS in still water for all the measurement locations.
4. Set the height of the gate, h_{gate}, at the desired height for the experiment.
5. Gradually increase the discharge, Q, to the required value and let the flow stabilize.
6. Measure the water depths, h, with the point gauge.
7. Measure the velocity of the flow at the locations of the measuring scheme with the EMS.
8. Stop the first experiment.

Now the other six experiments start in which the moves of the stones are recorded; for each experiment it holds:

1. Ensure that the colour coded stones are placed in their designated strips and that the rest of the tapered section is covered with a second layer of stones.
2. Set a discharge for the initiation phase. This discharge should lower than the discharge in the actual experiment. The initiation phase lets stones that are lying in unfavourable positions settle in.
3. Stop the flow after 15 minutes and take out all the coloured stones that might have moved from their strips during the initiation phase.
4. Start the actual experiment by slowly increasing the discharge to the same value, Q, as set in the first experiment.
5. Verify that the water level is the same as in the first experiment.
6. Stop the flow after 15 minutes and register the number of displaced stones.

The following series of experiments will be conducted in the flume with a tapered section of L = 2.50m, *table 3.6*.

Table 3.6 *Series of experiments that will be conducted*

Series	Q	h gate
Series 1	0.04	0.1890
Series 2	0.05	0.1890
Series 3	0.05	0.1690
Series 4	0.05	0.1490
Series 5	0.04	0.1490
Series 6	0.04	0.1290
Series 7	0.03	0.1290

4 Measurement data

This chapter will present representative data gathered in the experiments. The measurements done in the experiments consisted of water-depth measurements and EMS flow-velocity measurements. In addition the amount of moved stones during the experiment was registered.

A number of experiments have been done by Dessens. Dessens conducted his experiments with two different stone-sizes. The experiments for this thesis were done using the smaller stones. The larger stones show the same effect by acceleration as the small stones only on a different scale.

Table 4.1 shows the number of experiments that were conducted and used for further analysis.

Table 4.1 *Number of experiments*

Nr of experiments	small stones
Nr. of experiments with L = 2.50m	42
Nr. of experiments with L = 2.00m	58
Nr. of experiments with L = 1.50m	67
Nr. of experiments used for analysis	156
Nr. of u, a combinations	94

The following sections will process the data from the experiments in a way so that they can be used for further calculations and analysis. The analysis of the data is the subject of *Chapter 5*.
With the depth measurements a number of things will be determined. Firstly the average height of the bed of stones is established after which an average flow-velocity can be calculated.
The EMS flow-velocity measurements will be used to plot flow profiles.
The uniform flow profiles at the beginning of the tapered section measured with the EMS will be used to derive a value for z_0.
With the other EMS flow profiles the average EMS flow velocities, $\bar{u}_{EMS}$, in the middle of the flume (y = 0) will be determined. Now that $\bar{u}_{EMS}$ is known at the beginning and at the end of a strip, the average velocity for a strip, $\bar{u}_{strip}$, can be defined.
Combining the average velocity over a coloured strip, $\bar{u}_{strip}$, with the averaged flow acceleration over that strip, $\bar{a}_{strip}$, will result in a velocity-acceleration graph.
For every combination of velocity and acceleration the movement of stones will be observed.

4.1 Flow velocity

In order to calculate the acceleration of the flow one needs to know the change in velocities that occurs in the tapered section of the flume. The velocity of a flow can be determined in two ways.
When the water depth is measured the average velocity, $\bar{u}_h$, can be calculated for a specific cross-section given a certain discharge, *section 4.1.1*.
By measuring the velocity profile using an EMS one can calculate the average velocity provided one knows z_0. In *section 4.1.2* a value for z_0 is determined using the uniform logarithmic flow profiles at the beginning of the tapered section. The average measured EMS flow-velocity, $\bar{u}_{EMS}$, is calculated by dividing the area of the flow profile by its height.

4.1.1 Water depth

Due to irregular dimensions and positioning of the stones at the bottom of the flume, the water depth will vary slightly depending on whether a stone is protruding in the flow or whether one measures the depth in between two adjacent stones. The height of the bed has to be determined to fix the x-axis. The bed consists of two layers of stones and the height of the bed has been measured at different locations. The average value of the measurements gives an indication for the level of the bed.
There is also a calculation method for determining the height of a bed. The calculated height will be compared with the averaged measured height.

The level of the bed

Using a point gauge the height of the bed was measured in relation to the top of the wooden plates, *figure 4.1*. Averaging the obtained values will give an average height for the two layers of stones called the perpendicular layer thickness, t_m.
Bosma (2001) states on the porosity distribution of the layer thickness that the flow will reach between 0.15 and 0.30 times the d_{n50} under the perpendicular layer thickness known as the theoretical thickness layer, t_t. This theoretical thickness layer, t_t, is used for the level of the bed (z = 0.00m).

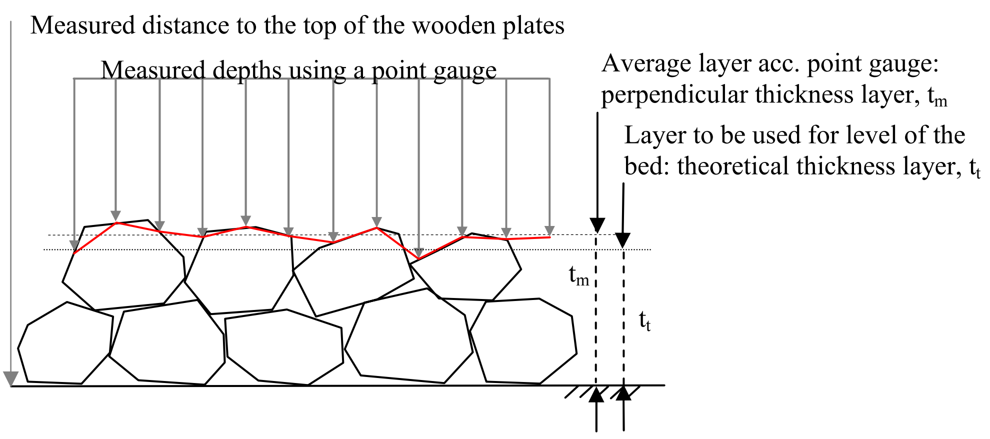

Figure 4.1 *Measuring the perpendicular layer thickness*

Note that the depth measurements were done with a point gauge where a hemispherical probe (with a size of 0.50 d_{n50}) should be used.
The CIRA/CUR (1991) gives a definition for calculating the perpendicular layer thickness:

$$t_c = n \cdot k_t \cdot d_{n50} \tag{4.1}$$

t_c:	calculated thickness layer	[m]
n:	number of layers	[-]
k_t:	thickness layer coefficient	[-]

Bosma found a value for k_t between 0.75 and 0.90.

In *table 4.2* the values for the measured perpendicular, the theoretical and the calculated thickness layers are compared.

Table 4.2 *Level of the bed above wooden plates, t (z = 0m)*

	d_{n50} (m)	***N***	**t_m (m)**	**t_t (m)**		**t_c (m)**	
				t_m–0.30d_{n50}	**t_m–0.15d_{n50}**	**k_t=0.75**	**k_t=0.90**
small stones	0.0082	2	0.0142	0.0117	0.0130	0.0123	0.0148

The first indication is that the height of the level of the bed (z = 0.00m) will between $1.17\text{x}10^{-2}$m and 1.30 $\text{x}10^{-2}$m above the bottom plates. These values are according to the theoretical thickness layer and *table 4.2* shows that these values are feasible when compared with the calculated layer thickness.

The choice for the level of the bed will be determined using flow profiles that where measured with an EMS. In *section 4.1.2* the measured EMS velocity-profiles will be plotted versus the measuring height above the bottom plates on a logarithmic scale. This way z_0 can be determined. This will be done for both estimations of the level of the bed. An average value for z_0 will be determined for the two different bed levels for the series of experiments. These values will be examined and a level of the bed as well as a level for z_0 will be established.

Average flow velocity

As *section 4.1.2* will show, the level of the bed will be defined as z = 0.00m at $1.30\text{x}10^{-2}$m above the bottom plates.
With the height of the bed determined, the mean flow velocity in a cross section can be calculated given a discharge and the measured water-depth:

$$Q = \bar{u} \cdot h \cdot B \tag{4.2}$$

Q:	discharge	[m^3/s]
$\bar{u}$:	cross section averaged velocity	[m/s]
B:	width of cross section	[m]
h:	water depth	[m]

Figure 4.2 is a graph of the water depths for series 6 of the experiments conducted in the tapering with a length of L = 2.50m. Series 6 was chosen at random. The graph shows the decline of the water depth due to the tapering in the flume.

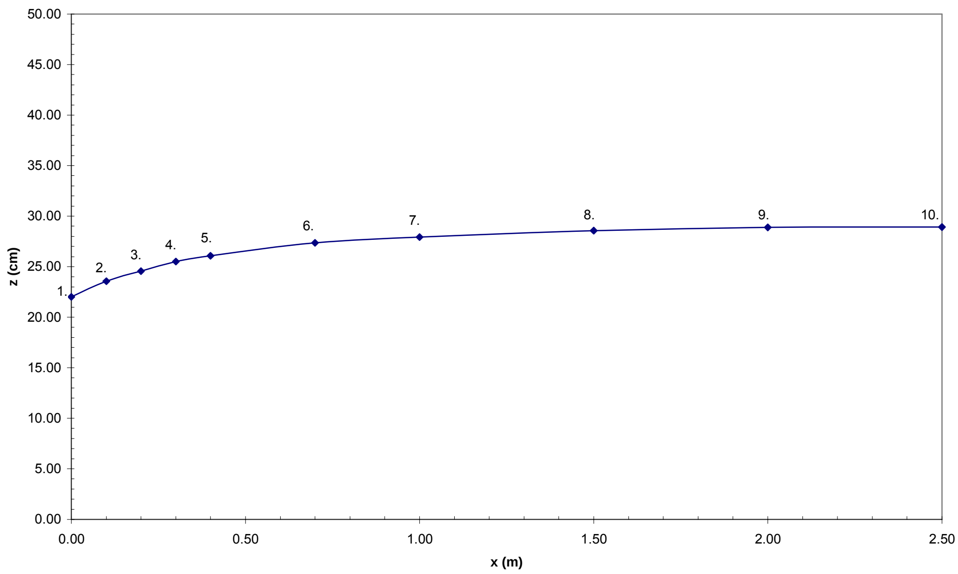

Figure 4.2 *Water depths h: series 6, L = 2.50m, Q = 0.04m³/s,* h_{gate} *= 0.1290m*

In the table below the water-depths that were measured in the experiments, h_{exp}, are displayed. Subtracting the height of the bed ($1.30\text{x}10^{-2}$m) from h_{exp} will give the actual water depth *h*. For each location in the flume the width and the discharge are known so the mean velocity for that cross-section can be calculated.
As one can see the average velocity increases as the flow goes through the tapering.

Table 4.3 *Calculated average velocity,* $\bar{u}_h$*, using the measured water depths Series 6: L = 2.50m, Q = 0.04m³/s,* h_{gate} *= 0.1290m*

#	1	2	3	4	5	6	7	8	9	10
x (m)	0.00	0.10	0.20	0.30	0.40	0.70	1.00	1.50	2.00	2.50
B (m)	0.150	0.164	0.178	0.192	0.206	0.248	0.290	0.360	0.430	0.500
h_m (m)	0.233	0.249	0.259	0.268	0.274	0.286	0.292	0.299	0.302	0.302
h (m)	0.220	0.236	0.246	0.255	0.261	0.273	0.279	0.286	0.289	0.289
$\bar{u}_h$ (m/s)	1.21	1.03	0.91	0.82	0.74	0.59	0.49	0.39	0.32	0.28

Calculating the mean velocity in this way does not tell you about the velocity distribution of the flow. With the flow being tapered the flow profile changes and loses its logarithmic shape. The boundary layer is reduced and the velocities near the bottom will increase. It is believed that this causes stones to move before the critical velocity is reached. To find out more about the change in flow profile the velocities will need to be measured with the EMS.

4.1.2 EMS data

Flow velocities can be measured with the help of an EMS at a specific location. Taking a number of measurements in the vertical will provide you with a flow profile. For this flow profile the mean velocity can be calculated
The EMS measurements also show the change in flow profile as the flow accelerates.

Determination of z_0

Where the flow touches the bed the flow velocity is equal to zero. For calculation purposes a height above the bed is defined, $z = z_0$, where the velocity is considered to be zero. This height is the where the logarithmic velocity flow profile intersects with the z-axis. The logarithmic feature of the velocity flow profile at the beginning of the tapered section will be used to determine z_0. The EMS velocity-flow profile will be plotted on a logarithmic scale to find out at which height $z = z_0$.
In case of the experiments by Dessens the flow profiles used to find z_0 were measured at x = 1.50m for $L_{1.50}$ and x = 2.00m for $L_{2.00}$. To determine a value for $z = z_0$ for the experiments under consideration the logarithmic flow profiles at x = 2.50m for $L_{2.50}$ were used.

Equation (2.14) can be written as:

$$\frac{u}{u_*} = \frac{1}{\kappa}(\ln z - \ln z_0) \tag{4.3}$$

$$\ln z = \kappa \frac{u}{u_*} + \ln z_0 = \kappa \frac{1}{u_*} u + \ln z_0 = au + b \tag{4.4}$$

Plotting the velocity measurements, u, versus the height, z, above the bed level on a logarithmic scale gives a and b. This is done in *Appendix C2* for the undisturbed flow profiles for both estimations of the level of the bed, respectively 1.17×10^{-2}m and 1.30×10^{-2}m above the bottom plates. The average values of z_0 for the undisturbed flow profiles from the experiments by Dessens and Huijsmans are given in the table below.

Table 4.4 *Average values of z_0 for two estimations of the level of the bed*

Level of the bed	$z_{0\text{ - Dessens}}$	$z_{0\text{ - Huijsmans}}$
1.17×10^{-2}m	1.56×10^{-3}m	1.72×10^{-3}m
1.30×10^{-2}m	1.17×10^{-3}m	1.57×10^{-3}m

The level of the bed can be fixed now so that the values for z_0 are processed. The level of the bed is chosen at z = 0 at 1.30×10^{-2}m above the bottom plates for reasons which will now be explained.

The value of z_0 should be approximately:

$$z_0 \cong 0.033 k_r \tag{4.5}$$

k_r: Nikuradse's roughness coefficient [-]

Van Rijn, 1986, proposed $k_r \approx 4 - 5\ d_{n50}$. Lammers, 1997, and Boutovski, 1998, found for a flat bed in a flume experiment: $k_r \approx 6\ d_{n50}$. This would result in a range for z_0 of $z_0 = 1.08\text{x}10^{-3}$m - $1.62\text{x}10^{-3}$m.
With a level of the bed at $1.30\text{x}10^{-2}$m the value for z_0 ($z_0 = 1.17\text{x}10^{-3}$m, Dessens; $z_0 = 1.57\text{x}10^{-3}$m, Huijsmans) is closer to the calculated z_0 than with the level of the bed set at $1.17\text{x}10^{-2}$m ($z_0 = 1.56\text{x}10^{-3}$m, Dessens; $z_0 = 1.72\text{x}10^{-3}$, Huijsmans).

Secondly the perpendicular thickness layer was measured using a point gauge, where a hemispherical probe should be used. Using the hemispherical probe would have resulted in a higher average level of the bed. The higher level of the bed is favourable.

With the level of the bed defined at $1.30\text{x}10^{-2}$m above the bottom plates the following log profiles, *figures 4.3 and 4.4*, can be made using the average values of z_0 as calculated in *Appendix C2*

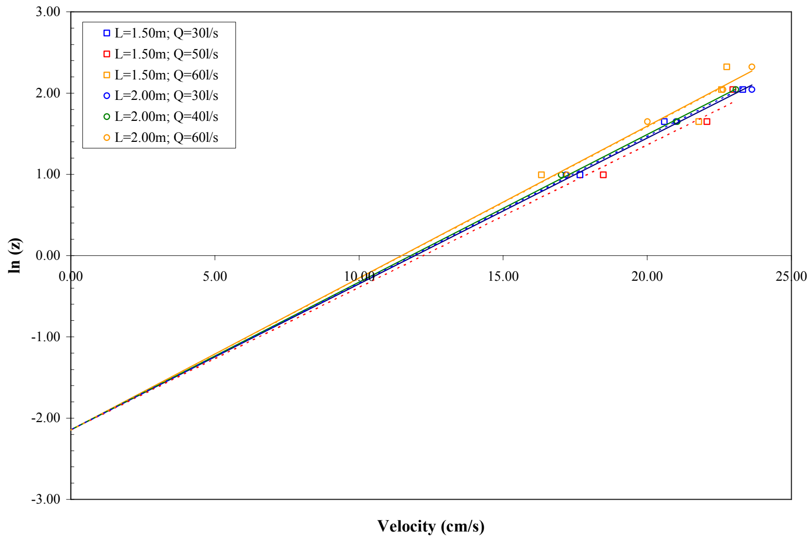

Figure 4.3 *Log profiles of 6 different datasets for the undisturbed flow with an average value for* $z_0 = e^{-2.145} = 1.17\text{x}10^{-1}cm = 1.17\text{x}10^{-3}m$ *(Dessens)*

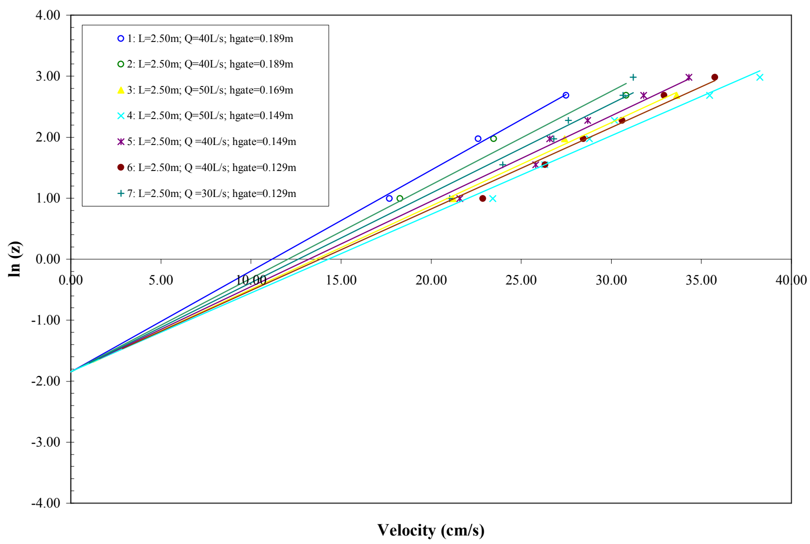

Figure 4.4 *Log profiles of 7 different datasets for the undisturbed flow with an average value for* $z_0 = e^{-1.852} = 1.57\text{x}10^{-1}cm = 1.57\text{x}10^{-3}m$ *(Huijsmans)*

The value of $z_0 = 1.17\text{x}10^{-3}$m by Dessens is safely within the boundaries of the theoretical approaches. Since the same stone parameters were used in the latter experiments as in the experiments by Dessens, it is assumed that the roughness conditions are similar.
Also for calculation purposes it is better to use the same value for z_0 as used by Dessens so that the results can be compared.

The value of z_0 is chosen at $z_0 = 1.17\text{x}10^{-3}$m for further analysis of the data. The levels of the bed and of z_0 are depicted in *figure 4.5*.

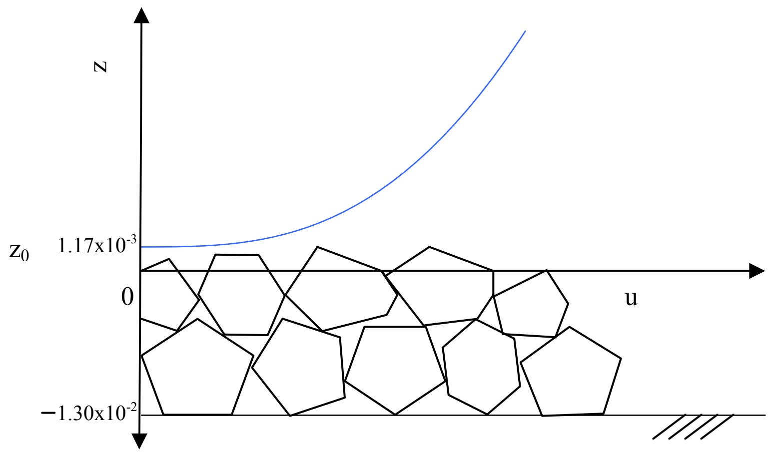

Figure 4.5 *Level of the bed: z = 0 at 1.30x10*$^{-2}$*m above bottom plates;*
$z = z_0 = 1.17\text{x}10^{-3}m$

The flow profile changes as the flow accelerates. It loses its logarithmic feature which is needed to plot the log profile. It is not possible to determine the height of z_0 for the disturbed flow. The height of z_0 in the accelerated flow is considered to be the same as in the undisturbed situation at the beginning of the tapered section for now. In *Appendix C4* a different z_0 will be used for the data analysis to see what the effect of choosing a different z_0 has on the shift in velocities.

$\overline{U}_{EMS}$

Now that the level of the bed and the level for z_0 are known the z-coordinates for the measurements with the EMS are fixed. The velocity measurements taken in the xz-plane are plotted versus its height

Through these plotted velocity measurements the velocity profile is plotted. From the velocity profile the average measured velocity, $\bar{u}_{EMS}$, has to be determined.

Near the bottom there is a lack of measurement points due to the limitations of the EMS. As you can see in *figure 4.6* the lowest measurement point has a lower velocity than the point just above it. It is hard to determine what the rate of decrease of velocity is near the bottom and at what height this occurs. When a flow is largely accelerated the boundary layer will be quite thin.

The flow profiles of the experiments for L = 2.50m are given in *Appendix C1*.

In *figure 4.7* an example is given of plotted velocity measurements versus their height taken from series 6 out of the experiments. It will now be explained how the velocity profile is plotted through these points.

- A vertical section is plotted as the average velocity of the velocity measurements taken at a height higher than 5 cm, disregarding the velocity measurement taken nearest to the surface.
  This measured horizontal velocity is affected by vertical velocity gradients. The horizontal velocity is lower than the actual velocity occurring at this location. The actual velocity consists of a horizontal velocity vector and a vertical velocity vector.
- The velocity profile also consists of a logarithmic section near the bottom. This section is plotted as a logarithmic profile from z_0 through the lowest measurement at a height of z = 0.03m above the bed. The lowest measurement is low enough to show a decrease in velocity due to the presence of the boundary layer, but is high enough to avoid disruptions to the magnetic field.
- The height, at which the logarithmic section near the bottom reaches the average velocity of the vertical section, is used to calculate the two surfaces of the two sections.
- The average velocity of the flow profile, $\bar{u}_{EMS}$, is determined by adding the area of the vertical section to the area of the logarithmic bottom section and dividing the total surface by the measured water depth.

In *figure 4.7* the flow profile for x = 0.00m from series 6 (L = 2.50m, Q = 0.04m^3/s, h_{gate} = 0.1290m) is shown. It shows the locally measured velocities with the EMS and the plotted flow profile through these.

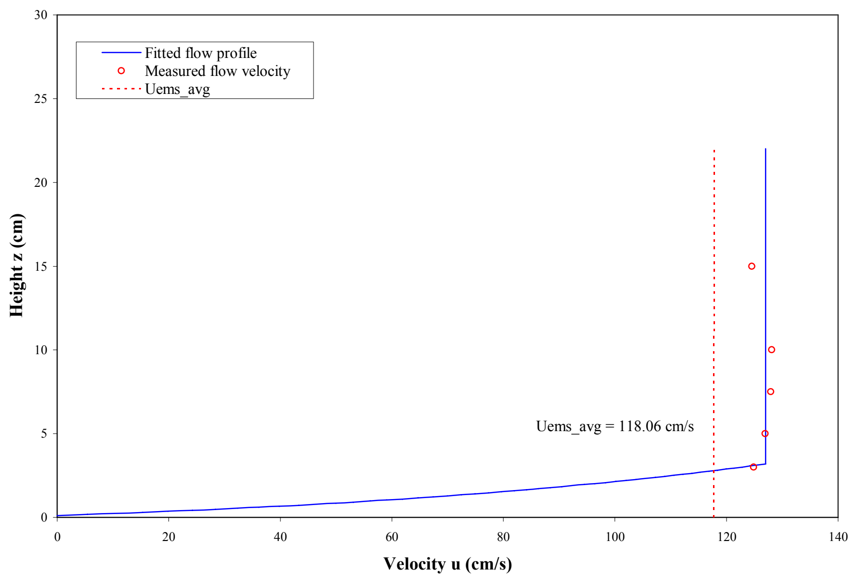

Figure 4.6 *Flow profile series 6 with $\bar{u}_{EMS}$: L = 2.50m, Q = 0.04 m^3/s, h_{gate} = 0.1290m, x = 0.00m, h = 0.22m, $\bar{u}_{EMS,x=0.00}$ = 1.18m/s*

When the average EMS flow velocities are compared with the average calculated velocities using the measured water depth, one notices some differences, *table 4.5*. These differences can be assigned to the change of the uniform flow profile.

Table 4.5 *Measured average EMS flow velocity, $\bar{u}_{EMS}$, and calculated average velocity, $\bar{u}_h$, using the measured water depths*
Series 6: L = 2.50m, Q = 0.04m^3/s, h_{gate} = 0.1290m

x (m)	0.00	0.10	0.20	0.30	0.40
h (m)	0.22	0.24	0.25	0.26	0.26
$\bar{u}_{EMS}$ (m/s)	1.18	1.05	0.96	0.84	0.76
$\bar{u}_h$ (m/s)	1.21	1.03	0.91	0.82	0.74

The average velocities measured with the EMS, $\bar{u}_{EMS}$, are used to calculate the acceleration over a strip.

4.2 Velocity-acceleration combinations

The flow accelerates as it enters the tapered section. The acceleration is given by:

$$a = \bar{u}\frac{d\bar{u}}{dx} \tag{4.6}$$

Here $\bar{u}$ is the average velocity between the beginning and the end of a strip where the movement of the coloured stones can be observed. The velocities that occur in the middle of a cross-section of the flume, measured with the EMS, will be used for calculating the acceleration over a strip.
The average velocity of the accelerated flow in the middle of a strip, $\bar{u}_{strip}$, is defined as:

$$\bar{u}_{strip} = \frac{\bar{u}_{EMS,x} + \bar{u}_{EMS,x+.0.10}}{2} \tag{4.7}$$

The increase in velocity is assumed to be linear. Over a small strip the difference between a linear increase in velocity and a parabolic increase in velocity is negligible. The average acceleration over a coloured strip can now be calculated:

$$\bar{a}_{strip} = \bar{u}_{strip} * \frac{\bar{u}_{EMS,x} - \bar{u}_{EMS,x+0.10}}{\Delta x} \tag{4.8}$$

Figure 4.7 shows the velocity-acceleration combinations for the flow conditions created in the experiments.

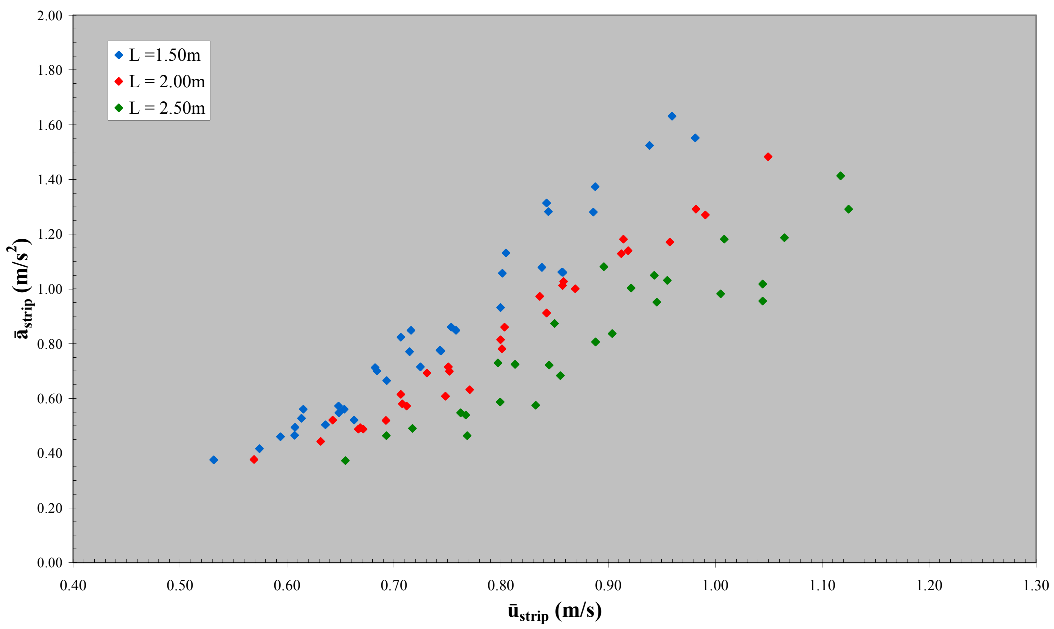

Figure 4.7 *Velocity- acceleration combinations for experiments*

Under flow conditions given by the velocity-acceleration combinations the amount of stones moved from their strips have been documented.

4.3 Stone moves

In case of a uniform flow the movements of stones are linked to a Shields parameter. In these experiments the flow is accelerating which means that the theory by Shields is no longer valid.

Under the flow conditions created in the tapering the amount of moved stones should differ from uniform conditions. The amount of stones moved during an experiment form the basis for the comparison between the uniform situation and the accelerated situation.

After an experiment the amount of stones that moved from their respective strips has been documented. For every experiment the amount of moved stones can be assigned to a velocity-acceleration combination.

Chapter 5 will analyze the stages of transport and the flow conditions for which these stages of transport occur.

In the *table 4.6* the stones that moved from their strips in series 6 of the experiments, are linked to the velocity and acceleration that occurred in that strip.

Table 4.6 *Stone moves*
Series 6, L = 2.50m, Q = 0.04 m^3/s, h_{gate} = 0.1290m

				stone moves in experiment						
x	strip	$\bar{u}_{strip}$	$\bar{a}_{strip}$	1	2	3	4	5	6	avg
0.00-0.10	Yellow	1.12	1.41	132	120	100	112	135	180	129.8
0.10-0.20	Blue	1.01	0.98	71	72	29	36	40	80	54.7
0.20-0.30	Green	0.90	1.08	29	8	5	5	6	12	10.8
0.30-0.40	Pink	0.80	0.59	2	3	2	2	2	0	1.8

For all the stone moves recorded in the experiments see *Appendix C3*

5 Data analysis

In this chapter the data from the experiments will be analyzed. The goal is to compare the movement of the stones in the accelerated situation with that in a uniform situation. It is the expectation that more stones will move from their locations in the accelerated flow than in a uniform situation with the same average flow velocity. Or, for the same amount of transport to occur in a uniform flow one would expect the average uniform flow velocity to be higher compared to the average flow velocity of an accelerated flow.

To compare the two situations a common denominator has to be found since the two situations can't be compared in terms of flow profiles. The two common denominators are the amount of moved stones and the discharge. If the amount of moved stones in the experiments can be linked to the Shields parameter possibly a comparison can be made between accelerated conditions and uniform conditions. With the discharge kept constant the average flow velocity and the water depth for a logarithmic flow profile will differ from an accelerated flow profile.
In this chapter it will be investigated if the two situations can be compared, so that the influence of the flow acceleration on the movement of stones can be visualized.

In the *section 5.1* the amount of moved stones in the experiments will be linked to a Shields parameter. There are a number of ways to define the movement of a stone. In this thesis a stone is considered to have moved when it has moved out of a coloured strip. The movement of a stone that is of interest for this thesis is the movement of a stone that occurs after having been subject to the flow for quite some time.
The classical Shields method uses the critical shear velocity to determine the grain diameter for the stability of a stone with the Shields parameter. It depends on the design criterion which Shields parameter should be used. The use of different Shields parameters for the movement of a stone with a certain diameter results in stages of movement as given in *section 2.2.2*. With the definitions of the different stages of transport defined by Breusers the amount of moved stones in the experiments will be assigned to a Shields parameter.

In *section 5.2* a translation is sought from the accelerated flow to a uniform flow. Two parameters stay unchanged; the Shields parameter and the discharge. The Shields parameter is empirically determined by the amount of stones, moved in the experiments. The discharge remains constant in order to create a new equilibrium for the uniform flow with a logarithmic flow profile.

The velocity-acceleration combinations for the accelerated flow in the experiments are shown in *figure 4.7*. With the translation to a uniform situation a shift in velocities should occur.

The calculated average flow velocity for the uniform flow will be plotted on the x-axis.

5.1 Threshold of motion

The Shields formula for the stability of stones, as given in *section 2.2.2* and *formula 5.1*, is the most commonly used formula for determining the stability of stones.

$$\psi = \frac{u_*^2}{\Delta g d} \tag{5.1}$$

In case of this experiment the Shields parameter is not used to determine the stone diameter of a bed for a critical flow velocity. In this case the Shields parameter is used as a threshold-of-motion parameter. It is used as an indication for the degree of transport. With a low flow velocity some stones might move a little. A value of 0.03 for ψ reflects this type of movement. With an increase of flow velocity the value of ψ will increase. Eventually there will be continuous movement across the whole bed for $\psi > 0.06$ (De Boer, 1998).

A study done by Breusers into incipient motion defined 7 stages of transport, *figure 5.1* (DHL, 1969). The transition between no movements at all to general transport across the whole bed can be seen as ψ increases.

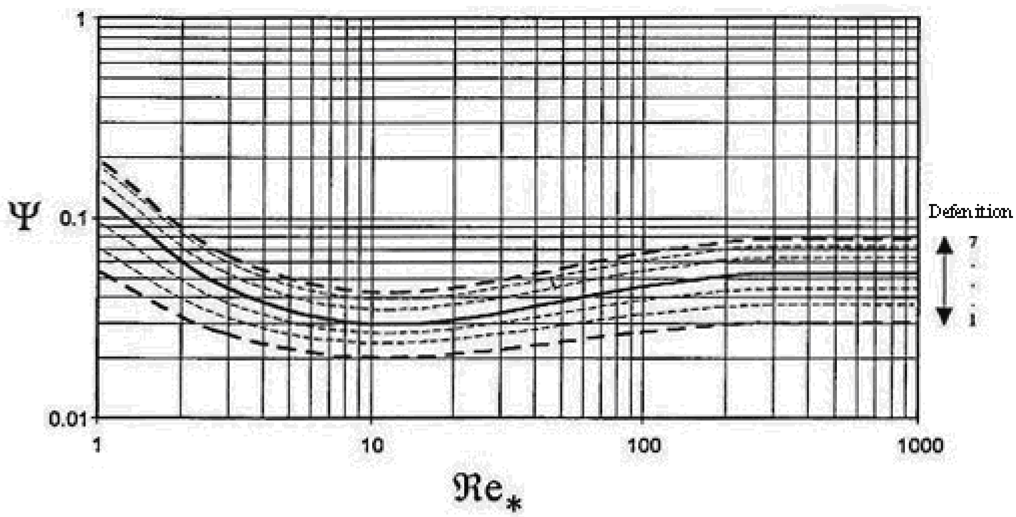

Figure 5.1 *7 Stages of transport found by Breusers (DHL 1969)*

Seven stages of transport (DHL) with the corresponding Shields parameters:

stage 0.	no movement -	$\psi < 0.030$
stage 1.	occasional movement at some locations -	$\psi = 0.030$
stage 2.	frequent movement at some locations -	$\psi = 0.037$
stage 3.	frequent movement at several locations -	$\psi = 0.044$
stage 4.	frequent movement at many locations -	$\psi = 0.053$
stage 5.	frequent movement at all locations -	$\psi = 0.063$
stage 6.	continuous movement at all locations -	$\psi = 0.072$
stage 7.	general transport of the bed -	$\psi = 0.078$

These definitions with the corresponding Shields numbers will be used to quantify a Shields parameter for the amount of stones that moved in the experiments.

Linking the average amount of moved stones from the experiments to a certain Shields parameter using the definitions of the seven stages by Breusers is quite difficult without the experimental data of Breusers. His experimental data could have given more insight into the amount of stones that moved during his experiments for the different stages. In this case the interpretation of his definitions is the only thing to go on. Choices will have to be made concerning how many stone moves are considered to be “occasional”, “frequent” or “continuous movement”.

With the different lengths of the tapered section the amount of dumped stones in a strip will vary according to the area of the strip concerned. To take this variance out of the equation the amount of moved stones from a strip are portrayed in percentages of the total amount of stones dumped in a strip, *st%* (the amount of stone moves in percentages are given in *Appendix C.3*).

A threshold of motion is defined for the experiments and is linked to the Shields parameter according to the definitions given by Breusers for the 7 stages of transport through the percentage of moved stones. *Distribution 1* given in *table 5.1* is a first interpretation of the definitions given by Breusers in terms of stone percentages.

Table 5.1 *Distribution of stone movements over 7 stages of transport by Breusers, (Distribution 1)*

Breusers #	Shields parameter					Stone moves in percentages				
0			ψ	<	0.027			st %	<	0.1
1	0.027	≤	ψ	<	0.033	0.1	≤	st %	<	1
2	0.033	≤	ψ	<	0.040	1	≤	st %	<	4
3	0.040	≤	ψ	<	0.049	4	≤	st %	<	10
4	0.048	≤	ψ	<	0.058	10	≤	st %	<	20
5	0.058	≤	ψ	<	0.068	20	≤	st %	<	35
6	0.068	≤	ψ	<	0.075	35	≤	st %	<	60
7	0.075	≤	ψ			60	≤	st %		

The amount of stone moves are chosen for the stages in this case by considering more than 0.1 % of stone movement as occasional movement in some locations. In the experiments it means that on average 2 stones moved during the six experiments. This is little movement, but if this movement was caused by the acceleration of flow a shift in velocities for the lower stages of movement should be visible.
For the 7th stage of movement 60% of stone movement means that more than half of the second layer of stones would have moved during the experiments. This is considered as general transport of the bed.
The other stages are distributed over the stages following the Shields parameters assigned to the 7 stages of transport by Breusers.

We now have a first interpretation of the amount of stones that moved from their strips to go with Shields parameters of a stage of transport. These Shields parameters will be used to compare the accelerated situation with a uniform situation.

The choice of the boundaries of a distribution is of influence when a uniform flow velocity is calculated.
Choosing the limits of the range for a certain stage of movement is quite equivocal since the experimental data of Breusers is not accessible. This problem is dealt with by applying various distributions to the stages of transport by Breusers in later sections. With a number of distributions a distinction can be made which distribution most likely resembles a correct interpretation of the stages of transport by Breusers

In the next section the algorithm is given how the translation to a uniform model is achieved using *distribution 1*.

5.2 Translation to a uniform flow

Assuming a bed in a uniform flow with the same roughness and the same grain diameter as in the experiments with the accelerated flow, then the amount of moved stones can be compared in terms of a Shields parameter. With this Shields parameter the flow conditions for a uniform flow will be investigated.
There are two parameters which remain the same in order to compare the two situations.

The two constant parameters are:

- The Shields parameter remains constant in both situations and is given by the distribution given in *table 5.1* through the amount of moved stones in the experiments.

- The discharge remains constant for both situations.

With the Shields parameter determined one can calculate the shear velocity, u_*:

$$u_* = \sqrt{\psi \cdot \Delta \cdot g \cdot d} \tag{5.2}$$

with $\Delta = 1.67, g = 9.81 m/s^2, d = 0.0082 m$

With the shear velocity one can calculate the average flow velocity, $\bar{u}_{uniform}$, for a uniform flow profile provided one knows the water depth, h, and height of z_0:

$$u_* = \frac{\bar{u}_{uniform} \cdot \kappa}{\ln\left(e^{-1}\dfrac{h}{z_0}\right)} \tag{5.3}$$

However, as we have seen in the experiments the water depth is different for an accelerated flow profile. Thus it is not possible to take the water depth from a particular velocity-acceleration combination and use it in *equation 5.3* to calculate a new average flow velocity.

As yet $\bar{u}_{uniform}$ and h are unknown to us. In order to calculate a new average flow velocity for the uniform situation a calculation tool is used: B_{strip} and h_{strip} are added to the denominator and the numerator of *equation (5.3)*.

$$u_* = \frac{\bar{u}_{unifrom} \cdot \kappa \cdot B_{strip} \cdot h_{strip}}{\ln\left(e^{-1} \dfrac{h_{strip}}{z_0}\right) \cdot B_{strip} \cdot h_{strip}} \tag{5.4}$$

$\bar{u}_{uniform}$:	calculated average uniform flow velocity	[m/s]
B_{strip}:	width in the middle of a strip	[m]
h_{strip}:	water depth for uniform situation	[m]

The discharge is kept constant in the translation to the uniform model. For the new uniform situation the discharge is defined as:

$$Q = \bar{u}_{uniform} \cdot B_{strip} \cdot h_{strip} \tag{5.5}$$

Q:	discharge set for the experiment	[m^3/s]

Now Q can be substituted in *equation (5.4)*:

$$u_* = \frac{Q \cdot \kappa}{\ln\left(e^{-1} \dfrac{h_{strip}}{z_0}\right) \cdot B_{strip} \cdot h_{strip}} \tag{5.6}$$

With the Shields parameter, given by the amount of moved stones and the distribution over the 7 stages of transport by Breusers, u_* can be calculated, *equation 5.2*.

Q is the set discharge by the discharge valve and the orifice plate.
B_{strip} is the width of a cross section in the middle of a strip, for which the average flow velocity of the accelerated flow, $\bar{u}_{strip}$, and the average acceleration, $\bar{a}_{strip}$, have been determined in *section 4.2*.

h_{strip} can be calculated with *equation 5.6* through iteration.

A new equilibrium exists for a uniform flow by calculating $\bar{u}_{uniform}$ with *equation (5.5)* using the h_{strip} from the iteration.

The average uniform flow velocities, which would cause the same amount of transport as in the experiments, are calculated. The calculated uniform velocities, $\bar{u}_{uniform}$, are plotted on the x-axis, *figure 5.2*.

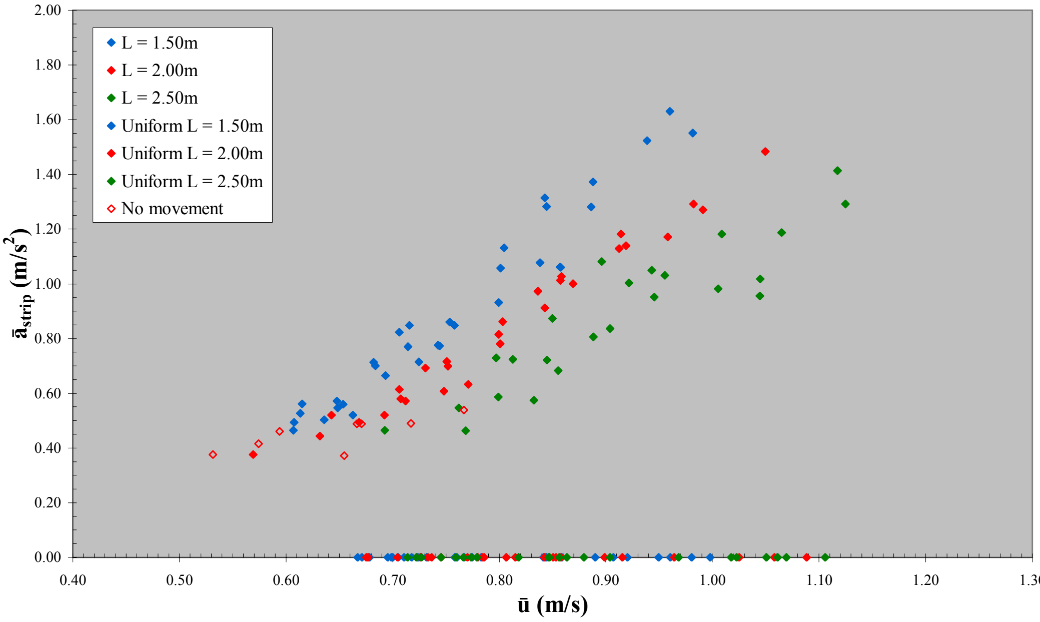

Figure 5.2 *Shift in velocities for a uniform flow profile. The values of the calculated uniform flow velocities are plotted on the x-axis.*

Figure 5.2 does show the shift in velocities, but does not present a clear picture of the influence of acceleration visualized by a shift in velocities.
In the next section it will be checked whether the shift in velocities, when visualized for the stages of transport defined by Breusers, shows a clear difference between the accelerated and the uniform situation.

5.3 Stages of transport

It is not quite clear from *figure 5.2* which velocities increase, if they increase at all or whether they might even decelerate. To get a better understanding of the graph, the velocity-acceleration combinations will be looked at for the different stages of transport defined by Breusers. This results in a graph where the cloud of data is divided up into stages. The shift in velocities might be more visible if the shift is displayed for the 7 stages of movement.

The interpretation of amount of stones that go with the definitions for the stages of transport quantifies the stone movements in terms of Shields parameters. To see if the boundaries are chosen correctly different distributions are made. With different distributions different translations come to the uniform situation.

5.3.1 Breusers

In this section the velocity-acceleration combinations are visualized for the 7 stages of transport by Breusers.

Distribution 1

With *distribution 1* given in *table 5.1* a representation of the velocity-acceleration combinations is made for the 7 stages of transport by Breusers. *Figure 5.3* shows the different stages of transport with the values for the calculated uniform velocities plotted on the x-axis.

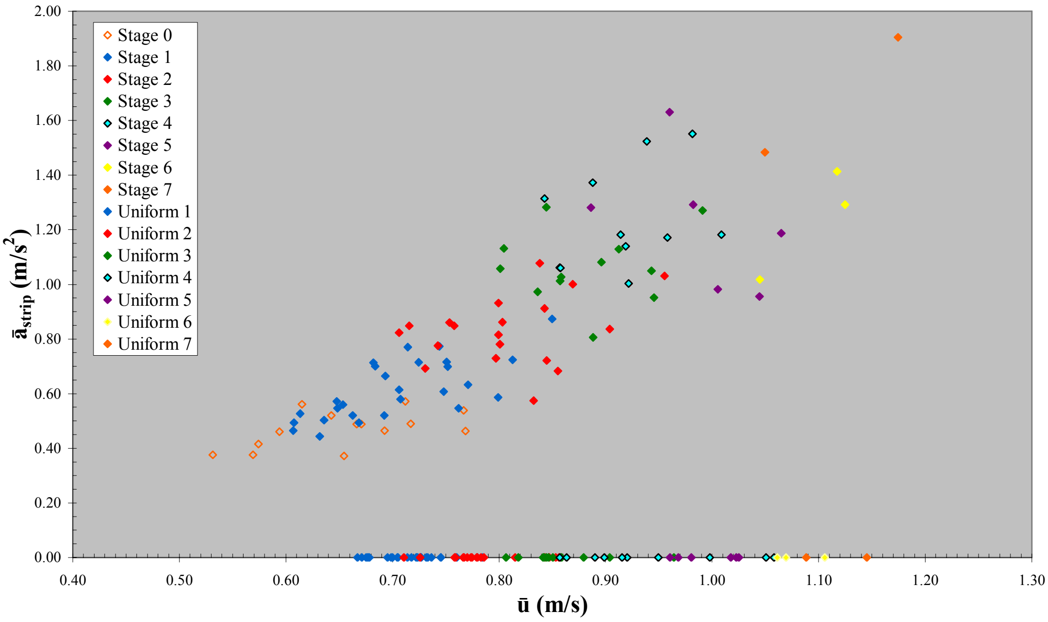

Figure 5.3 *Shift in velocities for 7 stages of transport by Breusers, distribution 1*

The scatter of the uniform flow velocities on the x-axis will be looked at in more detail. *Figure 5.4* shows the shift in velocities for each stage separately. This way the shift in velocities will be more visible.

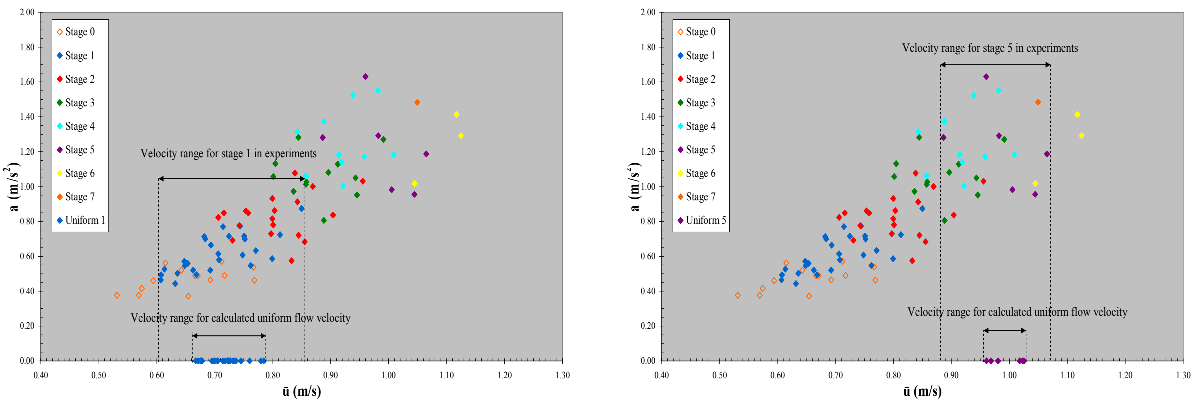

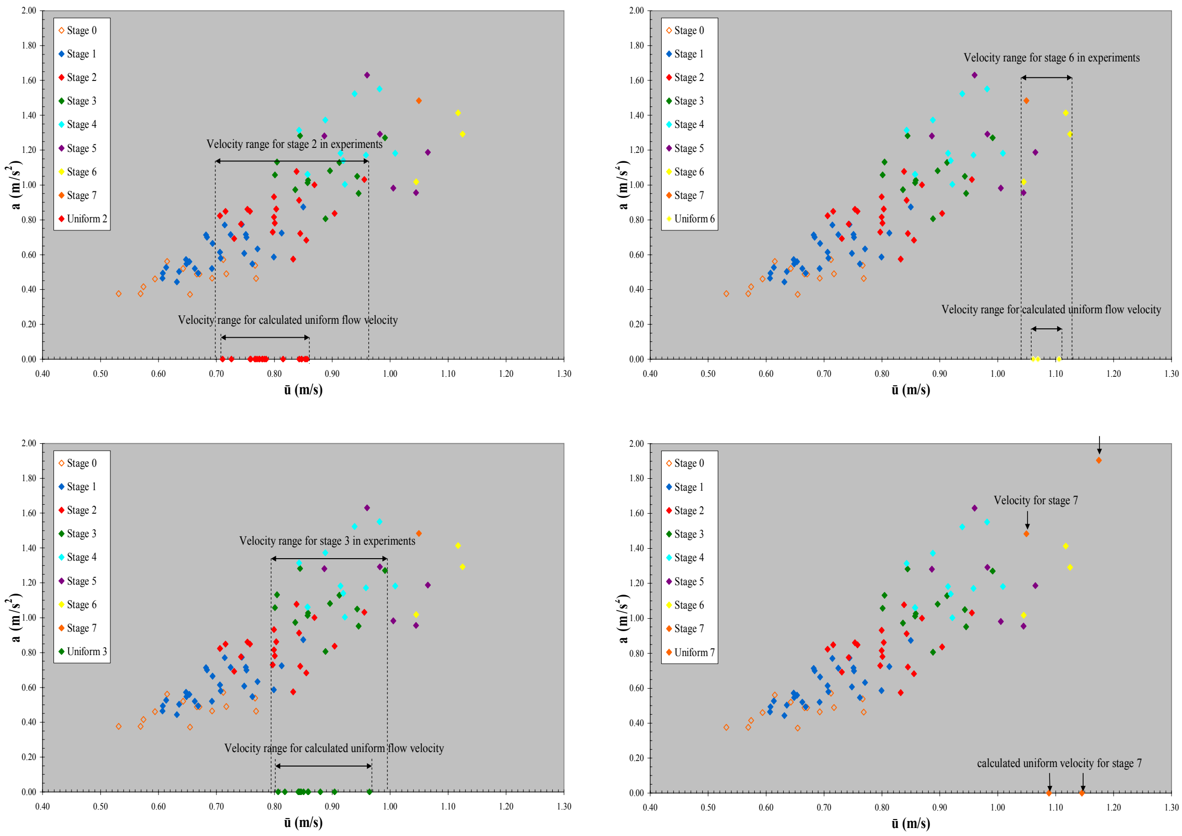

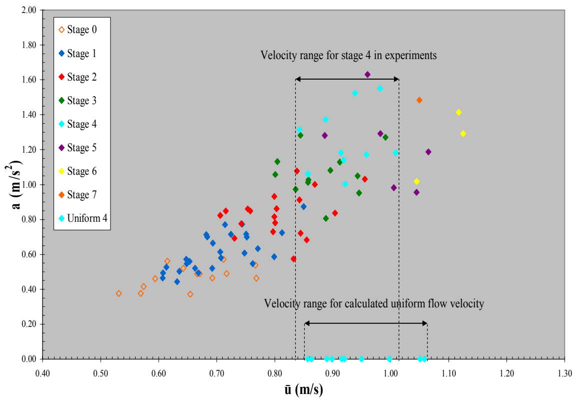

Breusers 7 stages of transport (*distribution 1)*:

- The left column from top to bottom: the shift in velocities for stages 1 to 4 with the calculated uniform velocities plotted on the x-axis.

- The right column: the shift in velocities for stages 5, 6 and 7.

Figure 5.4 *Shift in velocities visualized for each stage of transport, distribution 1*

As can be seen in *figure 5.4*, for every stage of transport there is a shift in velocities to the right noticeable. Even though slightly in some cases, but the left boundary shows a move to the right. With the right boundary it's a different case.
The range of the calculated uniform flow velocities rarely exceeds the range of the velocities as measured in the experiments except for stage 4. It appears, that while some points show an increase in speed other points show a decrease in velocity, when the uniform situation is compared with the accelerated situation.

In order to see which points increase and which points decrease, the velocity-acceleration combinations will be linked to the calculated uniform velocity by connecting them with a line. The line colour tells you the colour of the stones that moved from their strip for that velocity-acceleration combination.

Not every point has been connected, because of close proximity to other points and the danger of cluttering the graph.

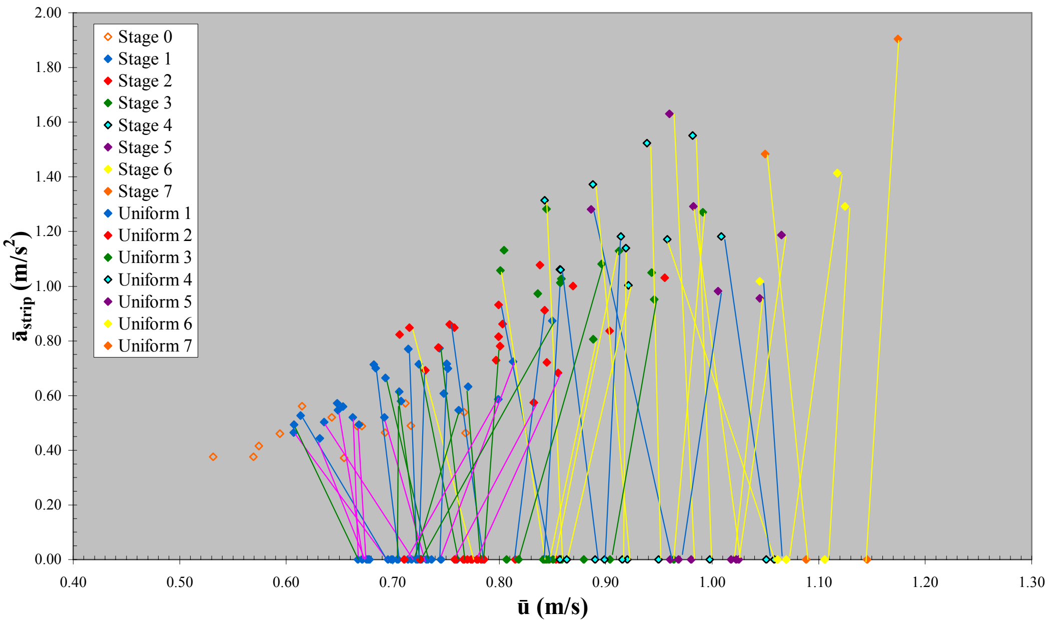

Figure 5.5 *Shift in velocities for data points, distribution 1*

As we can see here in the graph there are some lines showing an increase in velocity and other lines clearly show a decrease in velocity.
It seems that the last strip, the yellow strip, doesn't show that much of an increase in velocity when the accelerated situation is compared with the uniform situation. Perhaps for such amounts of stone moves the differences in velocities are not noticeable.
Stones in the blue strip appear to be influenced by the acceleration of flow. This can be seen by the increase in velocities.
The stone moves from the green and pink strip are of the lower magnitude, so they only appear in the lower stages of movement. They also show some moves forward and some moves backwards.

The data is divided up into the data of the three different tapered lengths to see if a difference in influence can be noted, *figure 5.6*.

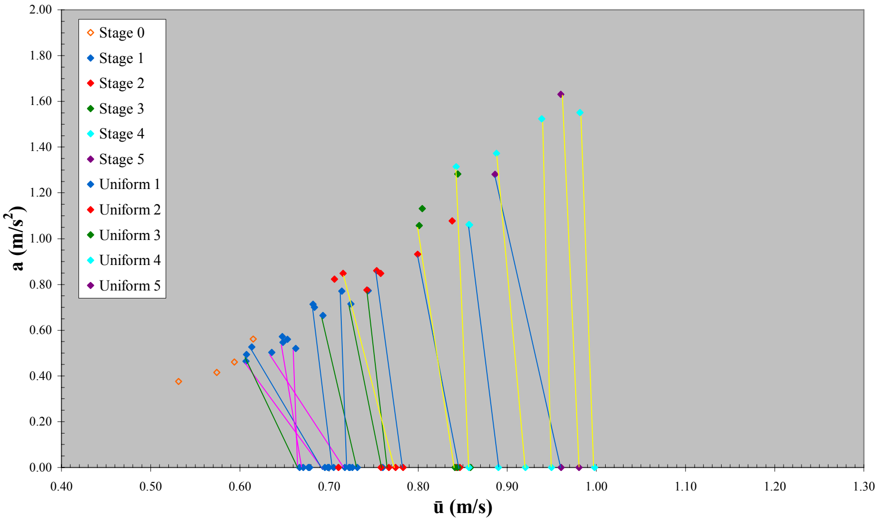

(a) L = 1.50m

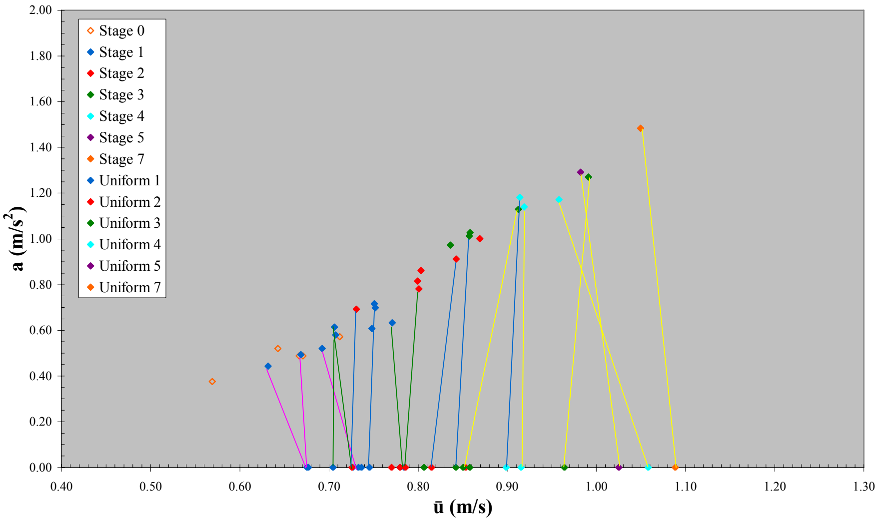

(b) L = 2.00m

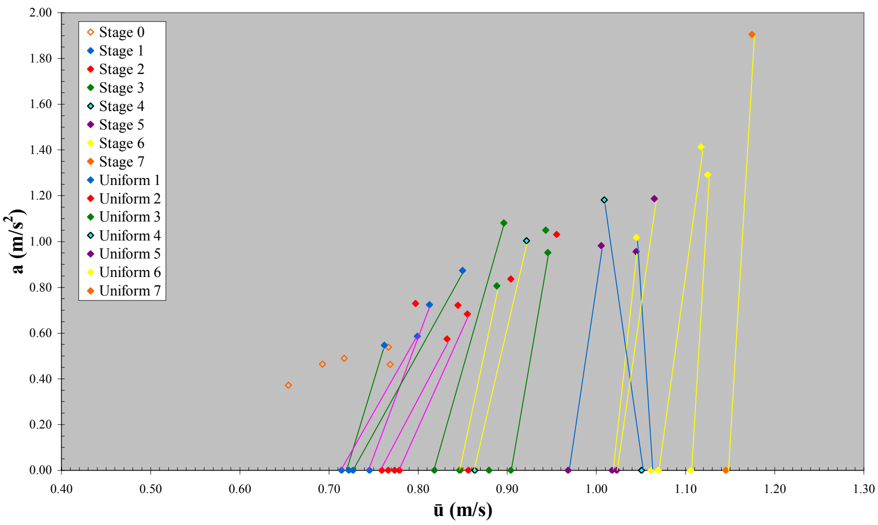

(c) L = 2.50m

Figure 5.6 *Shift in velocities visualized for each length of the tapered section (L = 1.50m, L = 2.00m and L = 2.50m), distribution 1*

In *figure 5.6* the difference in shift in velocities that can be noticed for the different tapered sections is shown. *Figure 5*.6a shows an increase in velocities. For the same amount of stone movement to occur in a uniform flow a higher average flow velocity is required. *Figure 5.6a* shows the most increase in velocities, when compared to *figures 5.6b and 5.6c*. This is what can be expected, since the acceleration is the highest for the shortest tapered section. What is surprising, however, is that *figure 5.6c* mainly shows a decrease in velocities even though the flow has been accelerated. Perhaps this can be assigned to the choices made for *distribution 1*.

Distribution 2

Another distribution is made, where for the 7th stage the movement of 50% of stones from the bed is considered as general transport. to see if the calculated velocities increase if less stone movements are assigned to the stages of transport.
For the tapering with a length of L = 2.50m the acceleration of the flow did not seem to affect the stability of stones in negative way. With this distribution an increase in velocities for the tapering with a length of L = 2.50m are more likely to occur.

Table 5.2 *Distribution 2 for 7 stages of transport by Breusers*

Breusers #	Shields parameter					Stone moves in percentages				
0			ψ	<	0.027			st %	<	0.1
1	0.027	≤	ψ	<	0.033	0.1	≤	st %	<	0.5
2	0.033	≤	ψ	<	0.040	0.5	≤	st %	<	2
3	0.040	≤	ψ	<	0.049	2	≤	st %	<	4
4	0.049	≤	ψ	<	0.058	4	≤	st %	<	10
5	0.058	≤	ψ	<	0.068	10	≤	st %	<	25
6	0.068	≤	ψ	<	0.075	25	≤	st %	<	50
7	0.075	≤	ψ			50	≤	st %		

With this distribution the following shift in velocities can be noticed for the stages of transport, *figure 5.3*.

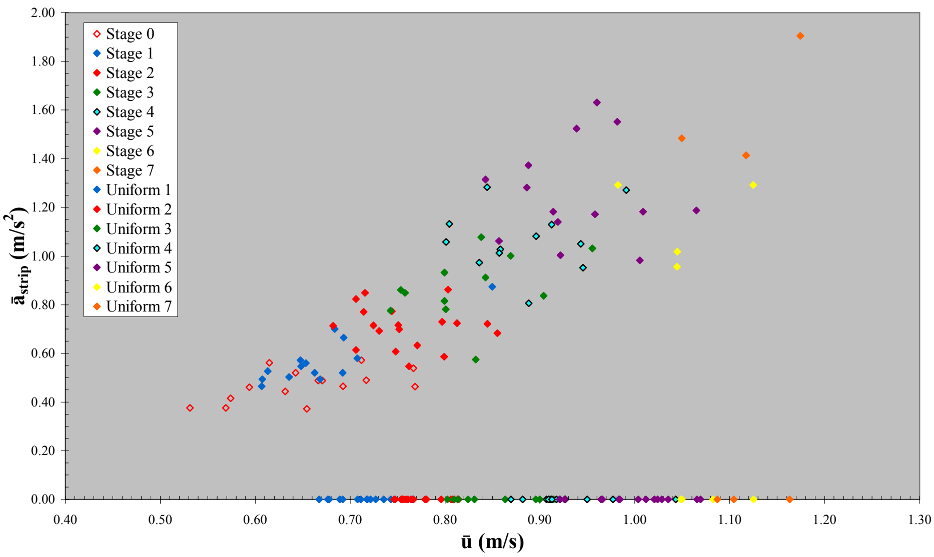

Figure 5.7 *Shift in velocities for 7 stages of transport by Breusers, distribution 2*

The shift in velocities visualized for the stages of transport separately, *figure 5.8*.

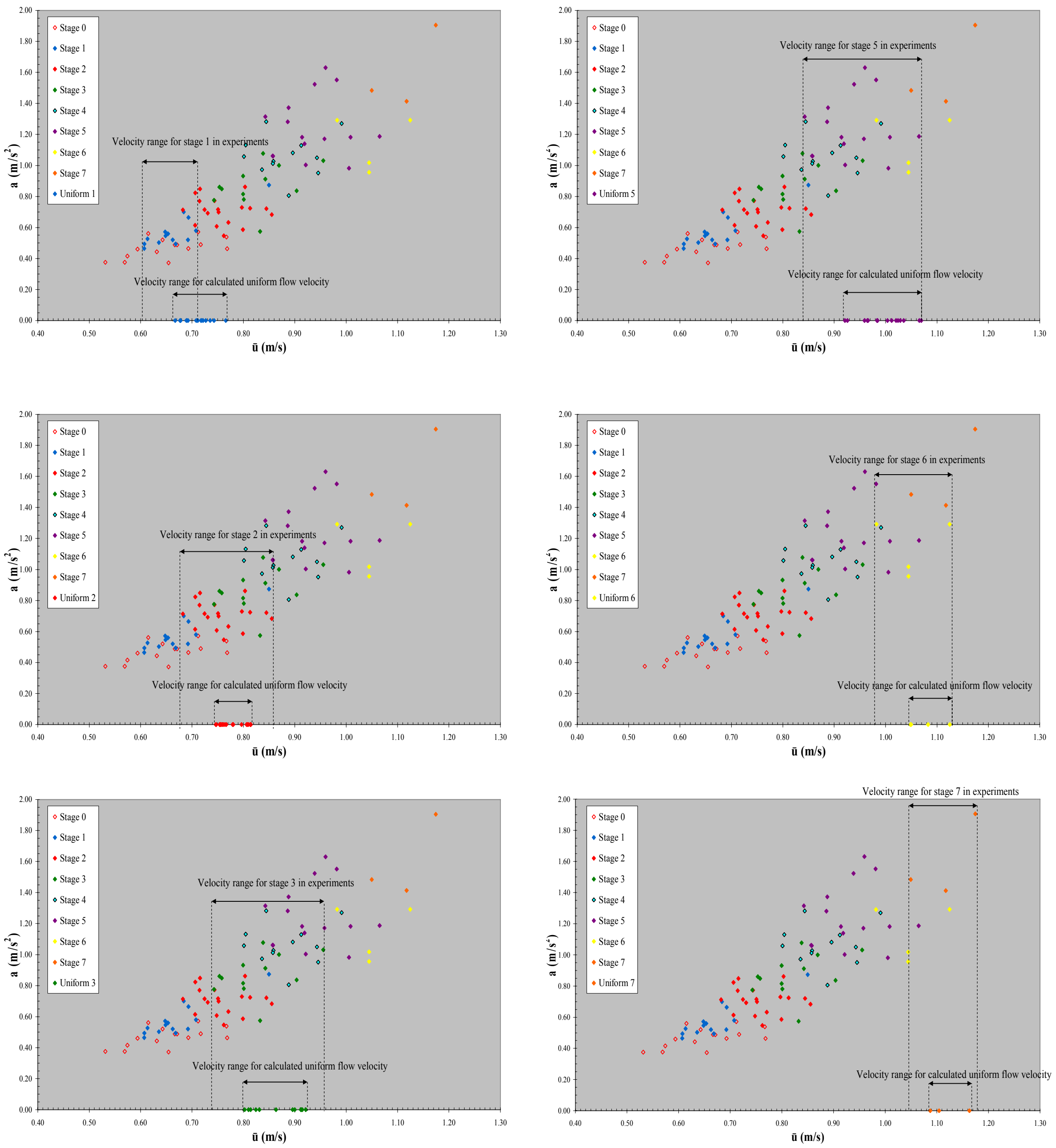

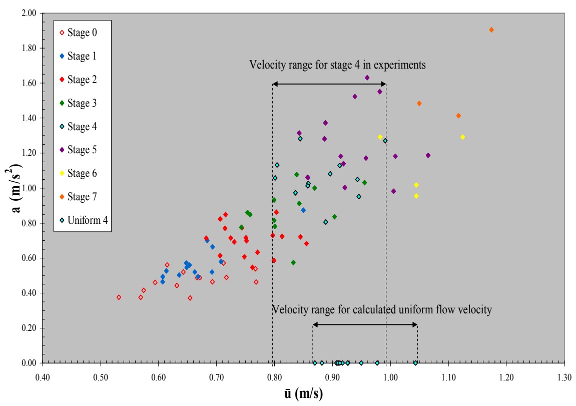

Breusers 7 stages of transport (*distribution 2)*:

- The left column from top to bottom: the shift in velocities for stages 1 to 4 with the calculated uniform flow velocities plotted on the x-axis.
- The right column: the shift in velocities for stages 5, 6 and 7.

Figure 5.8 *Shift in velocities visualized for each stage of transport, distribution 2*

When one compares *figure 5.8* with *figure 5.4,* one notices a bigger shift to the right when the uniform flow velocities are calculated with *distribution 2*.
The range of the uniform flow velocities in two cases exceeds the range of velocities for the stages of movement of the accelerated flow. This is the case for stage 1 and stage 4. The other stages of movement show some increase of the left boundary, but the right boundaries aren’t exceeded. This means that there are some data points that do not increase in velocity.

Figure 5.5 shows the velocity-acceleration combinations of all three tapered sections linked to the calculated uniform flow velocities for *distribution 1*. This graph could also be shown for *distribution 2*; however, this graph does not present a clear picture of the shift in velocities. This graph will therefore not be shown for *distribution 2*.

In *figure 5.9* the shift in velocities is visualized separately for the three different lengths of the tapering.

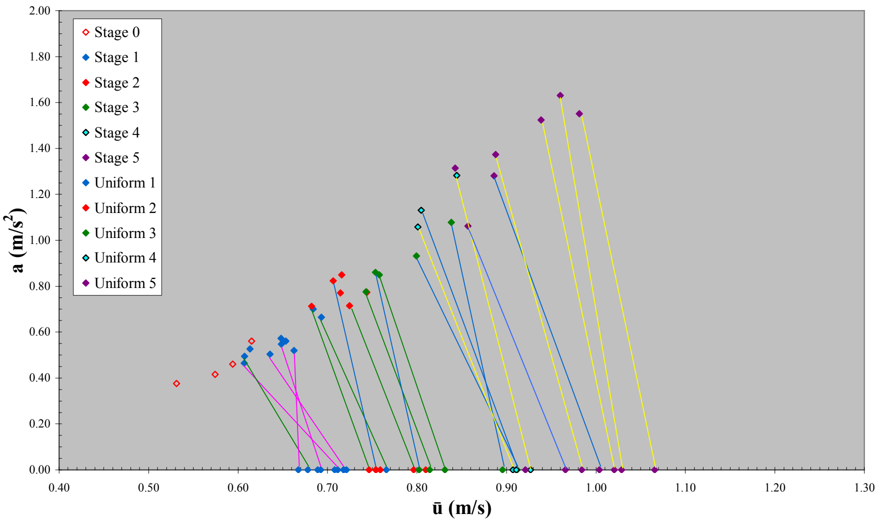

(a) L = 1.50m

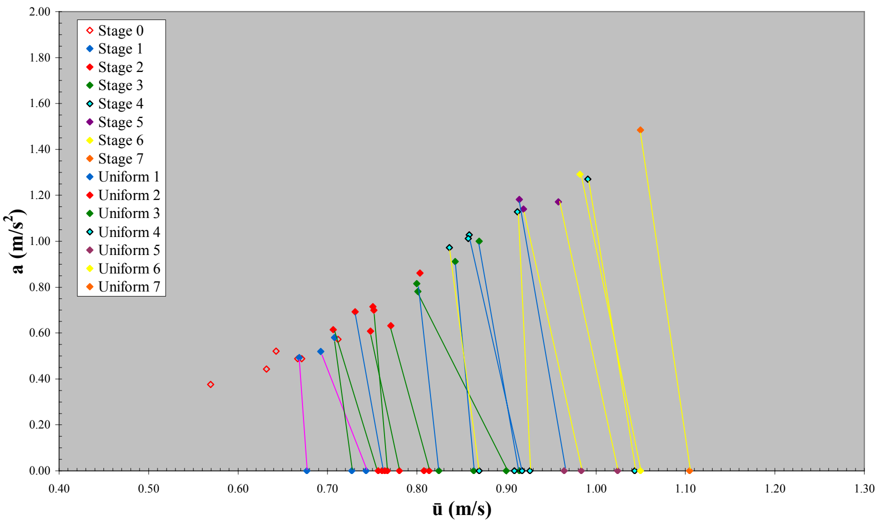

(b) L = 2.00m

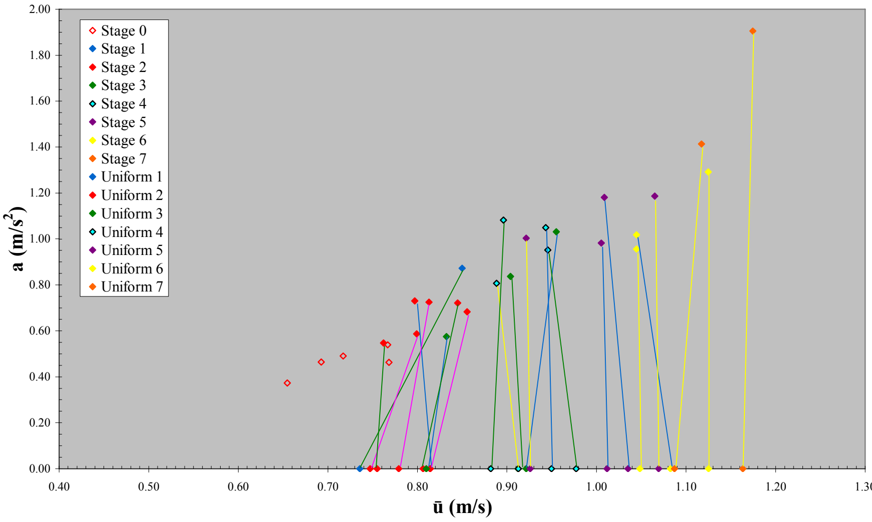

(c) L = 2.50m

Figure 5.9 *Shift in velocities visualized for each length of the tapered section (L = 1.50m, L = 2.00m and L = 2.50m), distribution 2*

What becomes clear from this distribution is that the choice of the boundaries for a stage of transport has a definite influence on the shift in velocities.
Figure 5.8 and *figure 5.9* show a larger increase in velocity in comparison with *distribution 1*. This is what could be expected, since the Shields parameters for the different stages of transport have been assigned to less stone moves resulting in a higher Shields parameter for a data point.
Figure 5.9a gives a proper shift in velocities to the right, which would indicate that the acceleration created in the flume has a destabilizing effect on the stability of the stones.
Figure 5.9b also presents a shift in velocities to the right. With *distribution 2* it appears that the acceleration created in the flume increases stone movements.
Figure 5.9c still shows a decline in velocities when the uniform velocity has been calculated with *distribution 2*.

Where the uniform flow velocities for the two shortest tapered sections show a clear shift to the right, *figure 5.9c* does not show an increase in velocity even with this favourable distribution. This would entail that the acceleration created with a tapered section of L = 2.50m does not cause more stones to move than in a uniform flow.

The next distribution is made in which more stone moves are assigned to the lower stages of transport. The stages of transport for *distribution 2*, while showing a lot of influence by acceleration, have been assigned with very little stone movement in the lower stages of movement. The next distribution will look at the sensitivity of the choices of amount of stones for the lower stages.

Distribution 3

This distribution allows for more stone moves in the lower stages of movement. "Occasional and frequent movement at some/several locations" are in this case allocated to more stone movements when compared to *distribution 1* and *distribution 2*.
This would result in an increase in velocities which are less then for the first two distributions. If the shift in velocity should still be predominantly to the right, then it is safe to assume that acceleration of flow does increase the movement of stones.
The amount of stone moves assigned to stage 7 is kept the same as *distribution 1*.

Table 5.3 *Distribution 3 for 7 stages of transport by Breusers*

Breusers #	Shields parameter	Stone moves in percentages
0	$\psi < 0.027$	$st\ \% < 0.5$
1	$0.027 \leq \psi < 0.033$	$0.5 \leq st\ \% < 3.0$
2	$0.033 \leq \psi < 0.040$	$3.0 \leq st\ \% < 6.0$
3	$0.040 \leq \psi < 0.049$	$6.0 \leq st\ \% < 10.0$
4	$0.049 \leq \psi < 0.058$	$10.0 \leq st\ \% < 20.0$
5	$0.058 \leq \psi < 0.068$	$20.0 \leq st\ \% < 35.0$
6	$0.068 \leq \psi < 0.075$	$35.0 \leq st\ \% < 60.0$
7	$0.075 \leq \psi$	$60 \leq st\ \%$

With this distribution the following shift in velocities can be observed for the stages of transport.

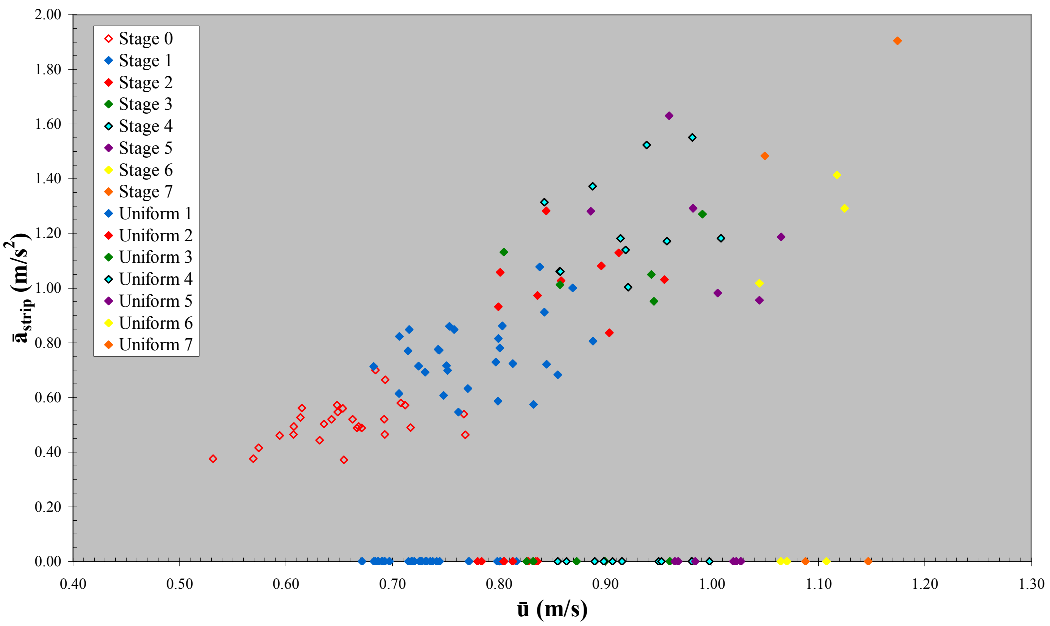

Figure 5.10 *Shift in velocities for 7 stages of transport by Breusers, distribution 3*

In the previous distributions minor stone moves in stage 1 of transport showed erratic shifts in velocities. With this distribution minor stone movements are considered to belong to the stage "no movement".

The shift in velocities visualized for the stages of transport separately, *figure 5.11*.

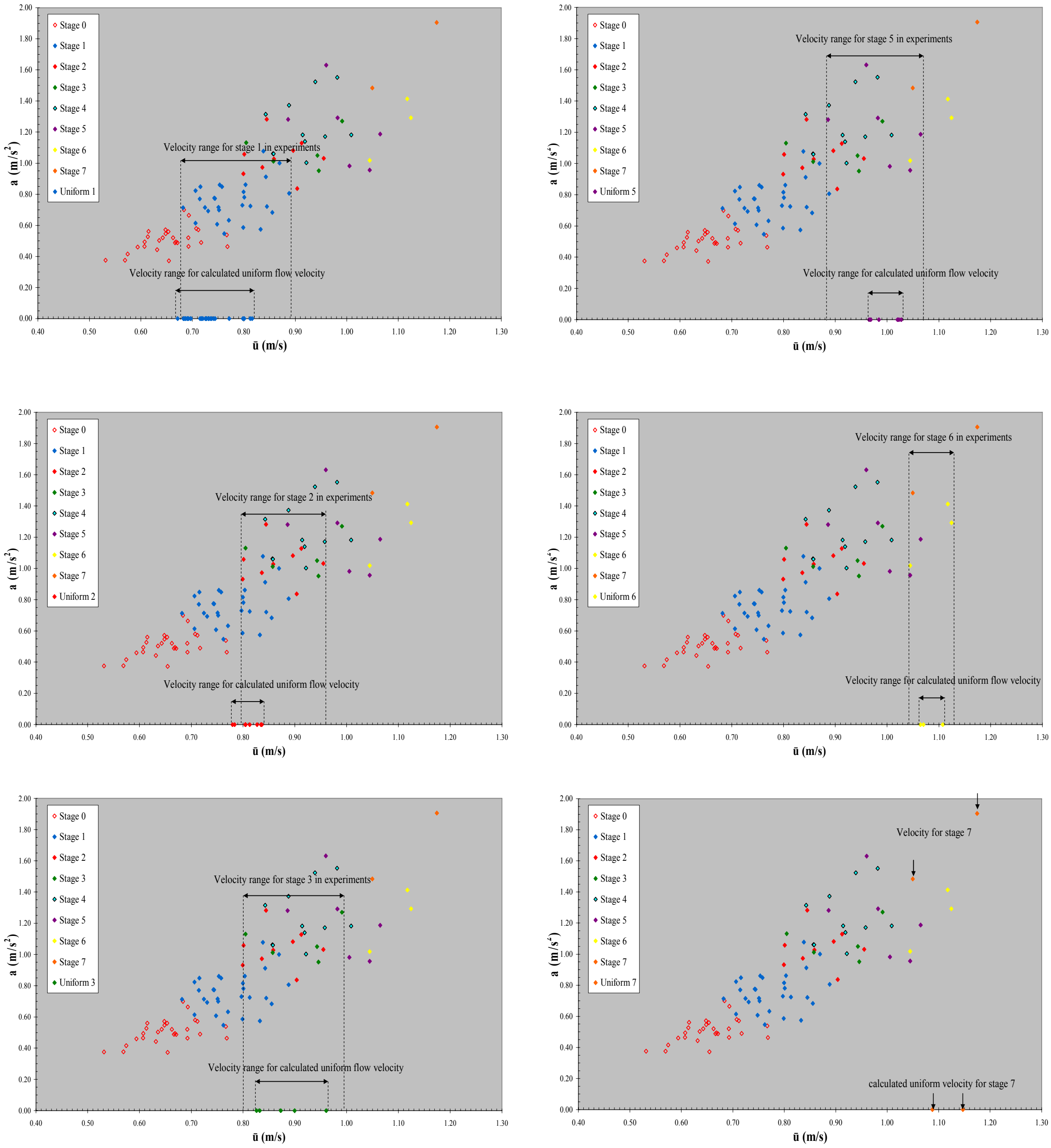

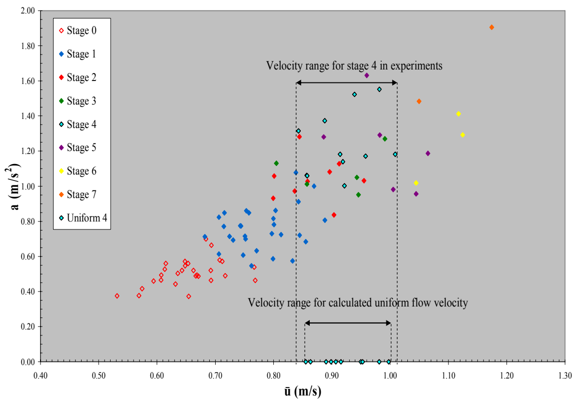

Breusers 7 stages of transport (*distribution 3)*:

- The left column from top to bottom: the shift in velocities for stages 1 to 4 with the calculated uniform flow velocities plotted on the x-axis.
- The right column: the shift in velocities for stages 5, 6 and 7.

Figure 5.11 *Shift in velocities for each stage of transport, distribution 3*

Distribution 3 is an unfavourable distribution when an increase in velocity is sought after. In this case a lot of stone movements are assigned to the early stages of transport which results in a low Shields parameter for frequent stone movements. Consequently the calculated uniform flow velocities will be lower than the calculated velocities with the previous distributions.
Figure 5.11 shows that the ranges for the calculated velocities have moved relatively to the left when compared with *figure 5.4* and *figure 5.8*.
The range of the uniform flow velocities exceeds the left boundary of stages 1 and 2. The ranges for the measured velocities of the other stages of transport enclose the range for the calculated uniform flow velocities. So again here some velocities increase and some decrease.

In *figure* 5.12 the stages of transport are visualized separately for the three different lengths of the tapering.

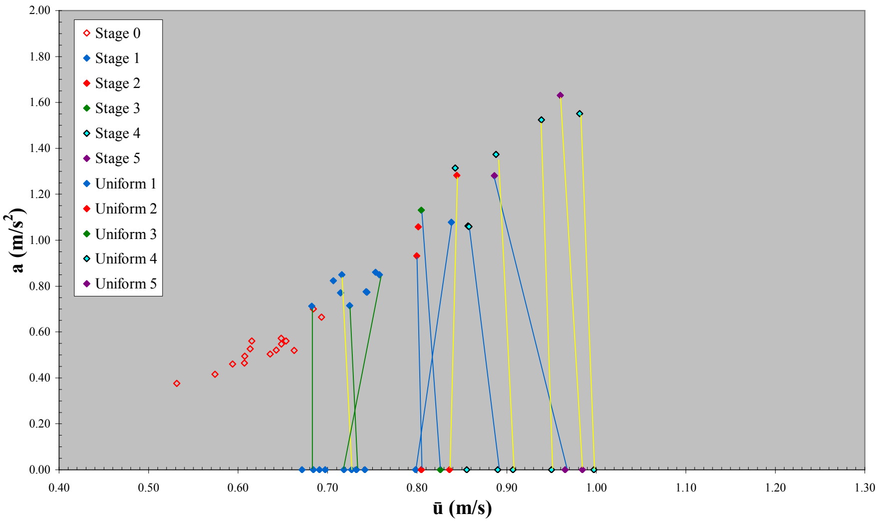

(a) L = 1.50m

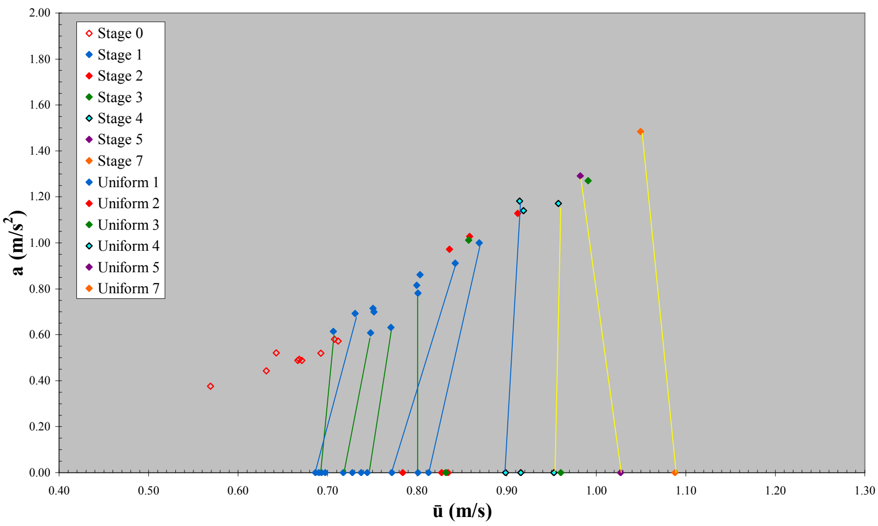

(b) L = 2.00m

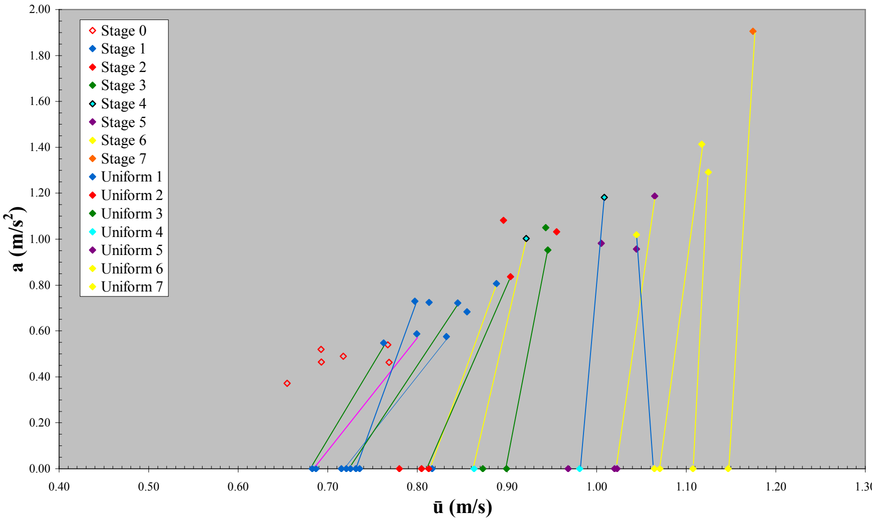

(c) L = 2.50m

Figure 5.12 *Shift in velocities visualized for each length of the tapered section (L = 1.50m, L = 2.00m and L = 2.50m), distribution 3*

Figure 5.12a shows that even with an unfavourable distribution the measured velocities show an increase in velocities when the translation is made between the accelerated situation and the uniform situation.
Figure 5.12b mainly shows a reduction in velocities except for the yellow strip. Here the velocities that are responsible for stone movements are lower than the velocities in a uniform flow for which the same Shields parameter applies.
Figure 5.12c shows a reduction in velocities.

The seven stages by Breusers give a lot of food for thought when choices have to be made as far as the boundaries of a stage of movement are concerned. His experimental data was unobtainable, so it remained a well-thought guess how many stone moves are considered to be “occasional, frequent or continuous movement in some, several or many locations”.

New stages of transport will be defined in *section 5.3.2* in order to simplify the distribution of the amount of stones over the spectrum stages of transport. With the new stages of movement come new distributions.

In these distributions the amount of moved stones are portrayed in the actual numbers of stones that moved out of their strip. It is assumed that the differences in area are small enough that any extra stone moves due to the added area are negligible. This furthermore simplifies the distributions which are made for the velocity-acceleration combinations.

5.3.2 New stages of transport

Here the Shields parameter will be used again as a threshold-of-motion parameter. It is used to indicate the rate of transport.
A threshold of motion will be defined for three stages of transport. For the seven stages of transport, defined by Breusers, it is difficult to quantify the exact amount of stones that belong to a stage of transport. For three stages of transport the choices of boundaries between the stages of transport are less sensitive to interpretations of the definitions of a stage of transport.

Three stages of transport according to Huijsmans:

stage 0.	no movement
stage 1.	occasional movement at some locations
stage 2.	continuous movement across the bed
stage 3.	general transport of the bed

For ψ-values smaller than $\psi = 0.03$ there is no movement. For high Re_* numbers ψ_c becomes constant with a value 0.055. The choice for the value of the first stage of transport has been chosen between these two transitions at a value of $\psi = 0.044$.
De Boer (1998) found that transport of stones completely stops after some hours for ψ-values smaller than 0.06. Above 0.06 the transport goes on continuously. $\psi = 0.060$ seems to be a good value for stage 2, continuous movement across the bed.
As for the last stage of transport the value of the Shields parameter chosen by Breusers is nicely representative for the amount of movement that occurs at a value of $\psi = 0.078$.

Three stages of transport can now be defined with corresponding Shields parameters (Huijsmans):

stage 0.	no movement -	$\psi < 0.03$
stage 1.	occasional movement at some locations -	$\psi = 0.044$
stage 2.	continuous movement across the bed -	$\psi = 0.060$
stage 3.	general transport of the bed -	$\psi = 0.078$

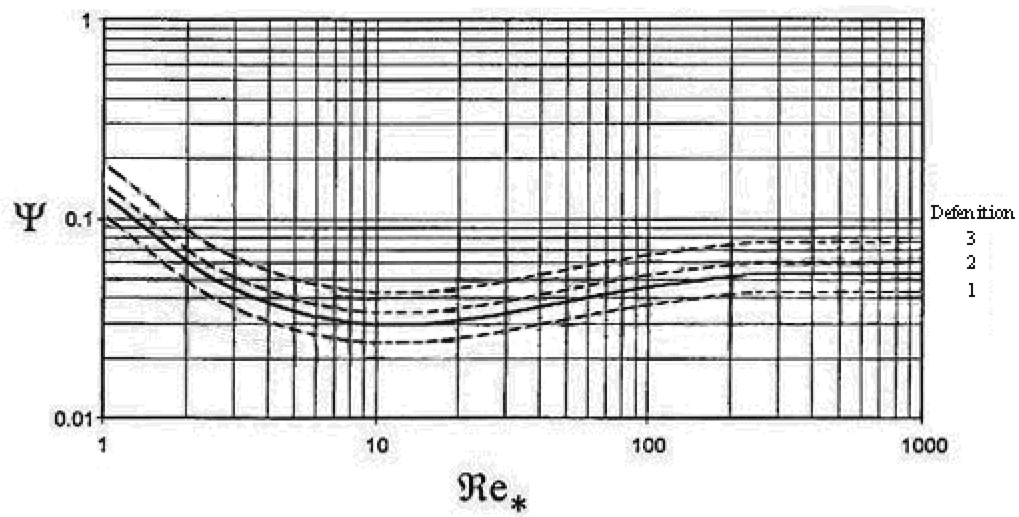

Figure 5.13 *Three stages of transport defined for this thesis*

Distribution 4

For the distributions for the three stages of transport according to Huijsmans the stone moves will not be looked at in terms of stone percentages. The differences in the amount of stones dumped in a strip are assumed negligible.

The following distribution is made for the three stages of transport. Any stone moves less than three stones are considered to belong to stage 0, “no movement”. With a Shields parameter of $\psi = 0.033$ some movement is allowed in design criteria for bed constructions.

The choice of 50 stone moves as the lower limit of stage 3 comes from the attempt to create an increase in velocities when the uniform flow velocities are calculated. The choice of 50 stone moves is quite minimal when considered as “general transport of the bed”. With a low upper limit also less stone moves are ascribed to stages 1 and 2. This would result in a clear increase in velocities even for the tapering with a length of L = 2.50m.

Table 5.4 *Distribution 4 for the three stages of transport according to Huijsmans*

#	Shields parameter	Stone moves
0	$\psi < 0.033$	$\# < 3$
1	$0.033 \leq \psi < 0.055$	$3 \leq \# < 20$
2	$0.055 \leq \psi < 0.075$	$20 \leq \# < 50$
3	$0.075 \leq \psi$	$50 \leq \#$

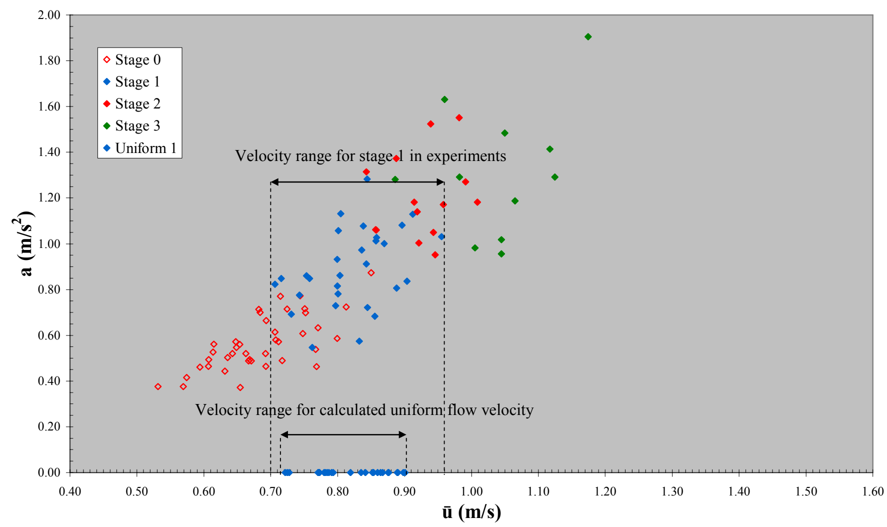

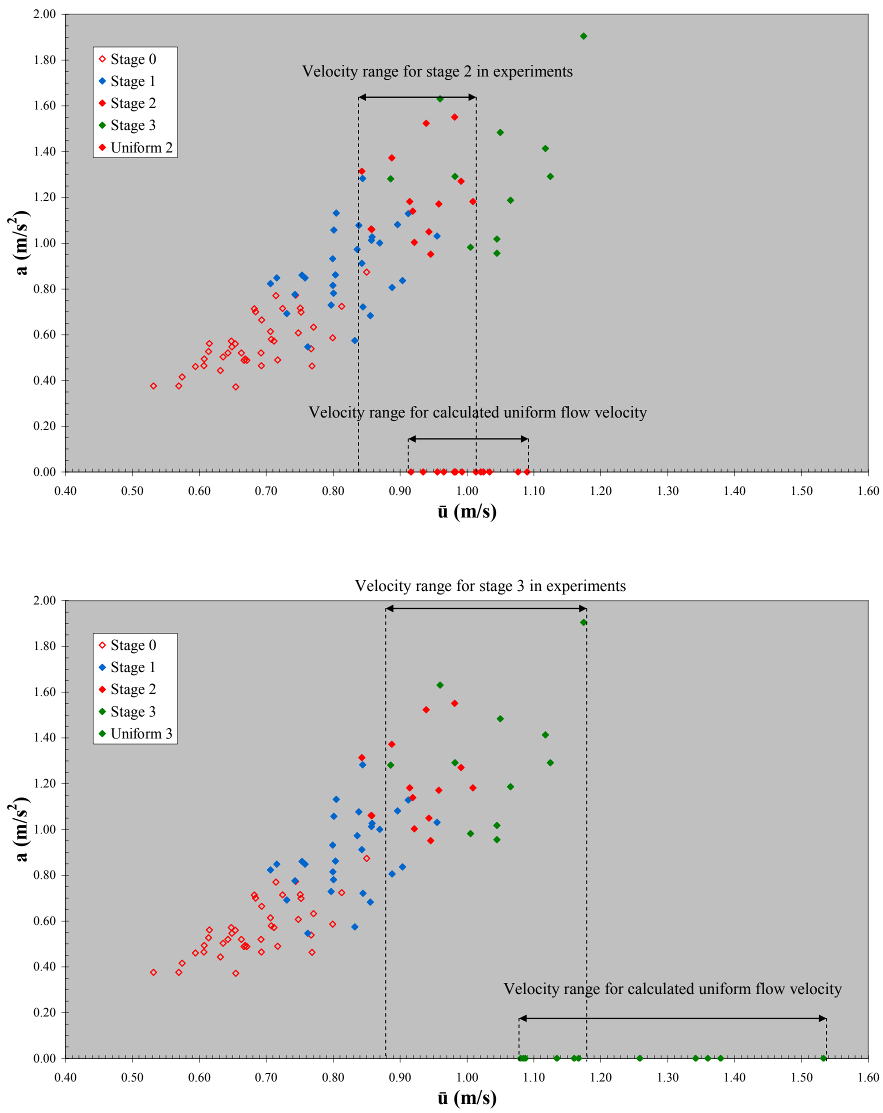

Figure 5.14 *Shift in velocities for the different stages of transport according to Huijsmans, distribution 4*

From these shifts in velocities a number of observations can be made. Stage 1 shows a slight shift to the right, but clearly there are some declines in velocity. The right boundary of the range of velocities for stage 1 has moved to the left. As yet it is not clear whether all three of the accelerated flows show a decline in velocities.
Stage 2 shows an interesting shift to the right. Probably an increase in velocities can be seen for most of the velocity-acceleration combinations.
Stage 3 shows an increase in velocities which seems a bit excessive. This is probably due to the fact that more than 50 stone moves are considered to be general transport in this distribution.

To get a more detailed idea which accelerations are responsible for the increases in velocities the stages of transport are visualized separately for the three different lengths of the tapered sections.

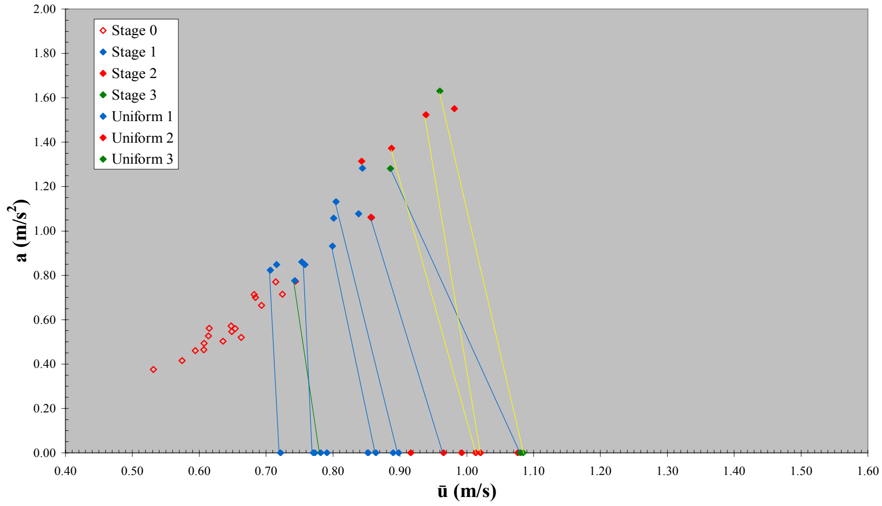

(a) L = 1.50m

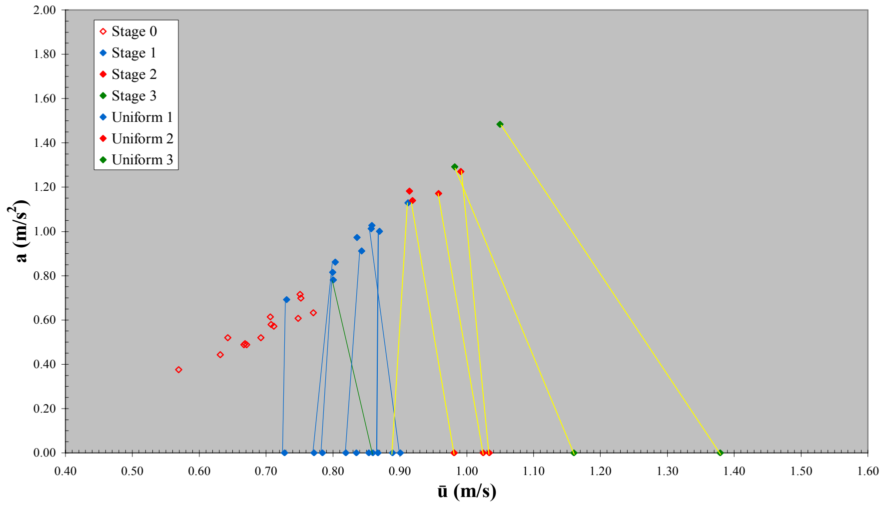

(b) L = 2.00m

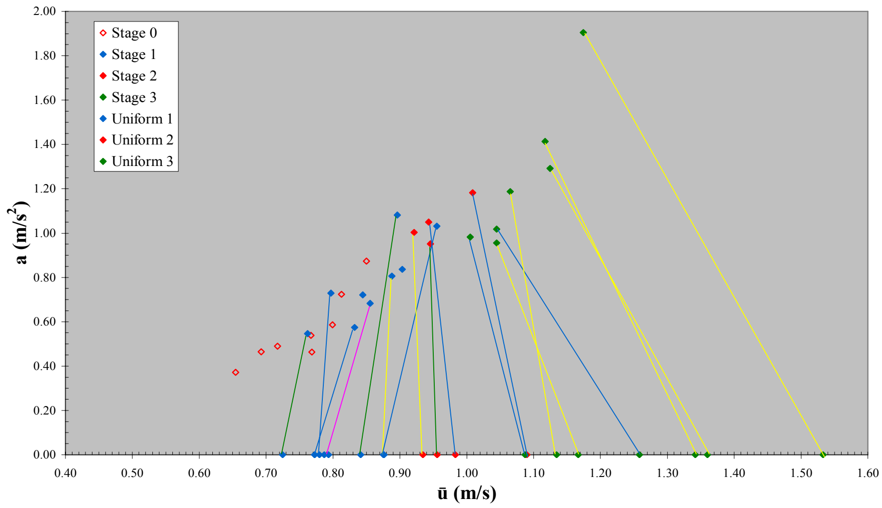

(c) L = 2.50m

Figure 5.15 *Shift in velocities visualized for each length (L = 1.50m, L = 2.00m and L = 2.50m), distribution 4*

Figure 5.15a shows only increases in velocities. The acceleration that occurs in a tapered section of L = 1.50m has a destabilizing effect on the threshold of motion. *Figure 5.15b* shows an increase in velocities for velocity-acceleration combinations higher than $(\bar{a},\bar{u}) = (1.10m/s^2, 0.95m/s)$. Lower velocities-acceleration combinations appear to be otherwise influenced by the acceleration of flow. Stage 1 of transport appears shows a decrease in velocities. Stage 2 starts to show an increase in velocity. *Figure 5.15c* also shows a decline in velocities for stage 1 of transport in the tapered section with a length of L = 2.50m. Stage 2 and stage 3 show an increase in velocities. Stage 3 even shows such an increase in velocities that a high number of stone moves might not be reflected well by this distribution. Since stone moves more than 50 moves already are assigned with high Shields parameters, the calculated uniform velocity will resemble flow conditions with high Shields parameters. If the Shields parameter is chosen to high, the calculated uniform velocity will be too high. It resembles a situation where more stones would have moved.

Distribution 5

This distribution checks whether stage 1 for the tapered section with a length of L = 2.50m can show increases in velocities. Stages 1 of *distribution 4* can be altered by lowering the amount of stone moves for stage 1. Now a single stone move is already considered to be the start of incipient motion.
Also the amount of stones will be heightened for stage 3, which should result in a better representation of the kind of transport which is considered “general transport”.

Table 5.5 *Distribution 5 for the three stages of transport according to Huijsmans*

#	Shields parameter					Stone moves				
0			Ψ	<	0.033			#	<	1
1	0.033	≤	Ψ	<	0.055	1	≤	#	<	20
2	0.055	≤	Ψ	<	0.075	20	≤	#	<	60
3	0.075	≤	Ψ			60	≤	#		

With 60 stone moves considered to be “general transport of the bed” the increase in velocities for stage 3 should be less than the increase in velocities for *distribution 4*.

With this distribution the following shift in velocities for the three stages of transport becomes noticeable, *figure 5.16*.

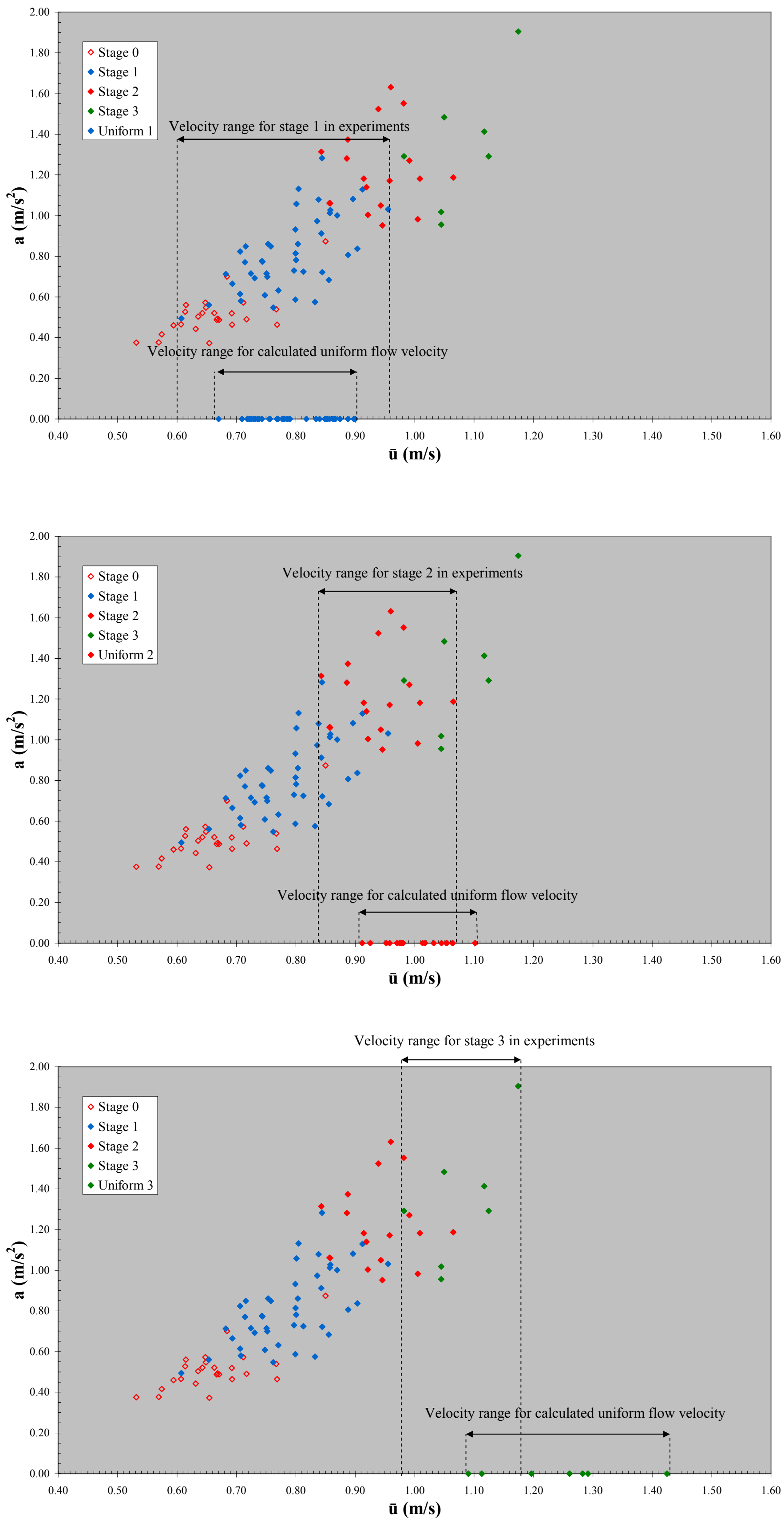

Figure 5.16 *Shift in velocities for the different stages of transport according to Huijsmans, distribution 5*

The shift for the stages of transport in *figure 5.16* in comparison with *figure 5.14* can be explained by the difference in distributions. Less stone moves are assigned to stage 1, which causes the calculated uniform velocities with *distribution 5* to move to the left when compared with *distribution 4*.
Stage 3 has been assigned more stone moves, which causes the shift in velocities to be moved to the left when compared with the shift of stage 3 for *distribution 4*.

The following graph shows the shift in velocities for the three different tapered lengths, *figure 5.17*.

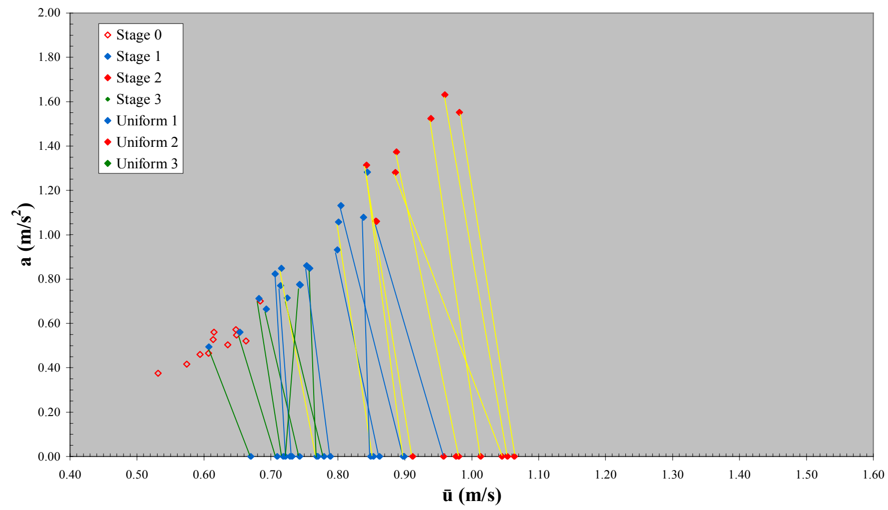

(a) L = 1.50m

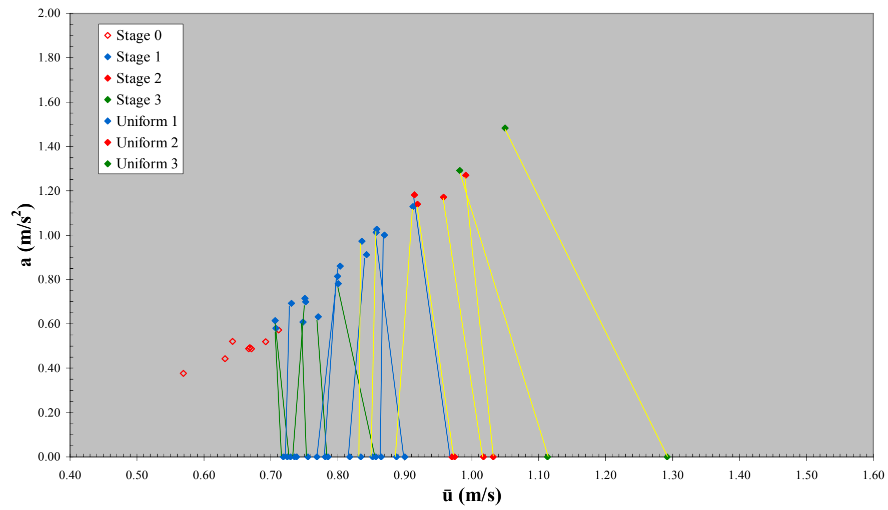

(b) L = 2.00m

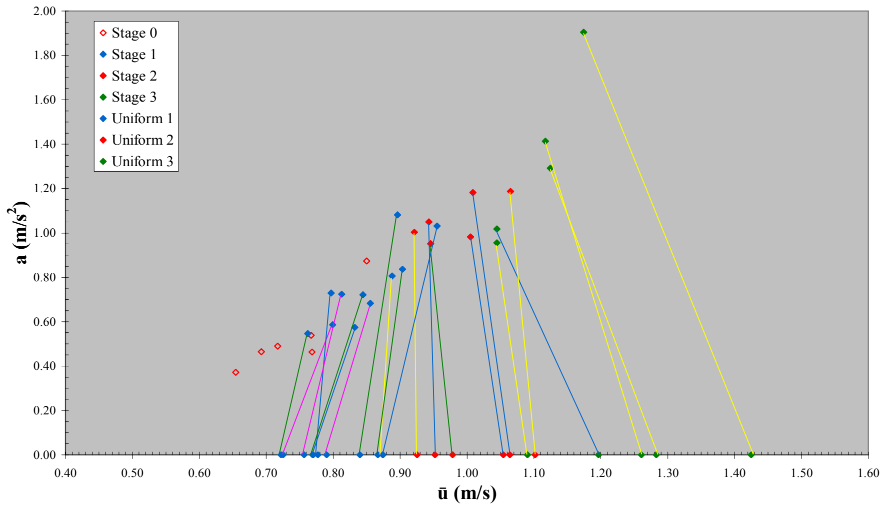

(c) L = 2.50m

Figure 5.17 *Shift in velocities visualized for each length (L = 1.50m, L = 2.00m and L = 2.50m), distribution 5*

Figure 5.17a shows an increase in stone moves due to the influence of acceleration. *Figure 5.17b* shows a general increase in movement due to the influence of acceleration for stage 2 and stage 3 and some decrease in velocities for stage 1. *Figure 5.17c* shows a decline in velocities for stage 1 of transport, which leads us to believe that for the lower velocity-acceleration combinations the acceleration does not have a destabilizing effect on the stability of stones.

Distribution 6

This distribution looks into the velocity-acceleration combinations for which the decrease in calculated uniform velocities changes to an increase in velocities. This change can be noticed between stage 1 and stage 2 of transport. The upper limit of stage 1 has been raised. Furthermore stage 3 has been allowed more stone moves to see if the excessive increase in velocity for stage 3 will be more moderate.

Table 5.6 *Distribution 6 for the three stages of transport by Huijsmans*

#	Shields parameter					Stone moves				
0			ψ	<	0.033			#	<	1
1	0.033	≤	ψ	<	0.055	1	≤	#	<	25
2	0.055	≤	ψ	<	0.075	25	≤	#	<	90
3	0.075	≤	ψ			90	≤	#		

This distribution gives the following shift in velocities, *figure 5.18*.

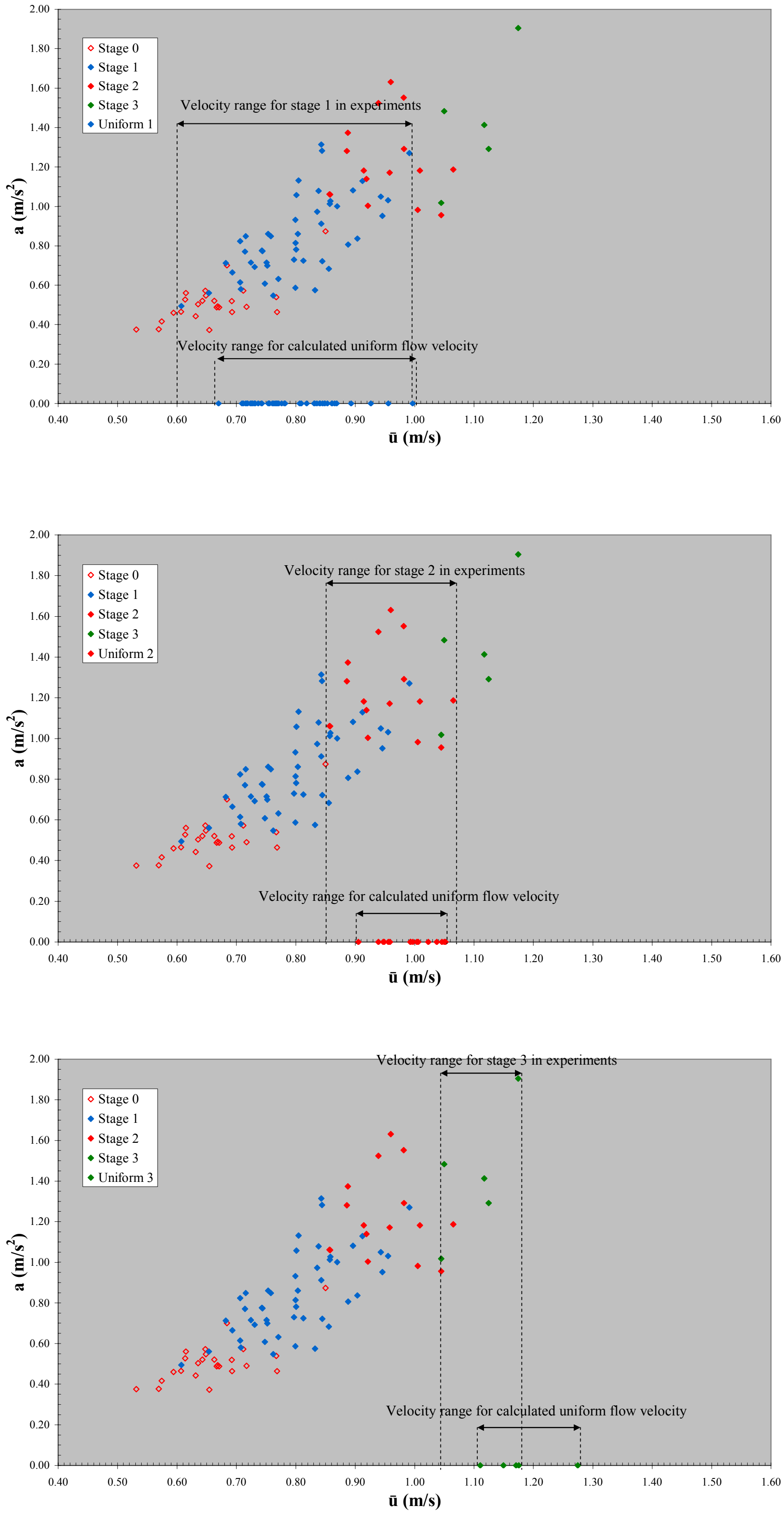

Figure 5.18 *Shift in velocities for the different stages of transport by Huijsmans, distribution 6*

Stage 1 shows a shift forward, but it cannot be seen is from the graph whether this is the case for every tapered section. This will be looked into in *figure 5.19.*
Stage 2 shows a shift forward, which is what can be expected, since more stone moves are assigned to this stage of movement.
Stage 3 does not show such an excessive increase in velocity as *distribution 4* and *distribution 5*.

Allowing for more stone moves to the left boundary of stage 3, results in a better representation of the experiments when a lot of stone moves occur due to high velocities and accelerations.

The differences between the three tapered sections can be seen in *figure 5.19*.

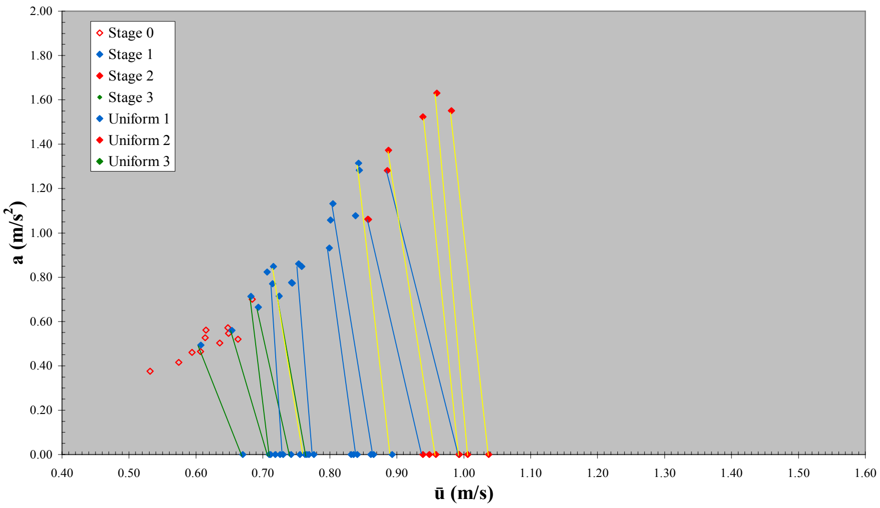

L = 1.50m

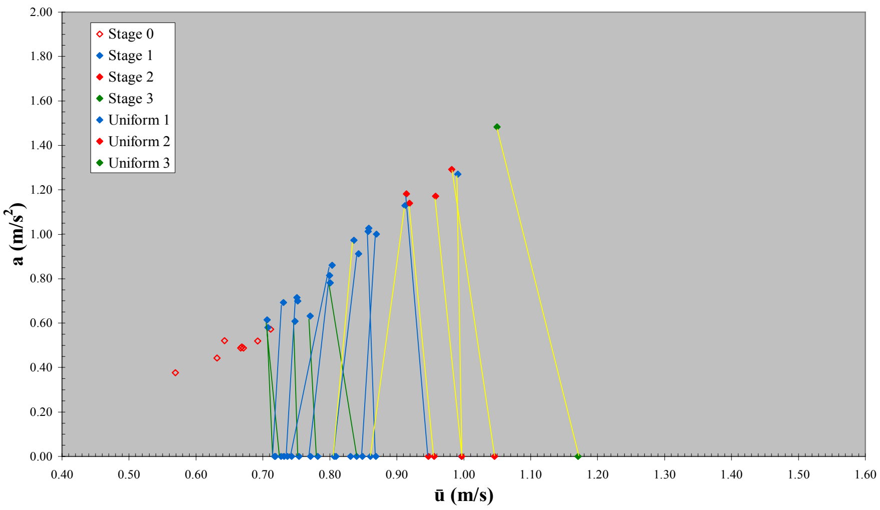

L = 2.00m

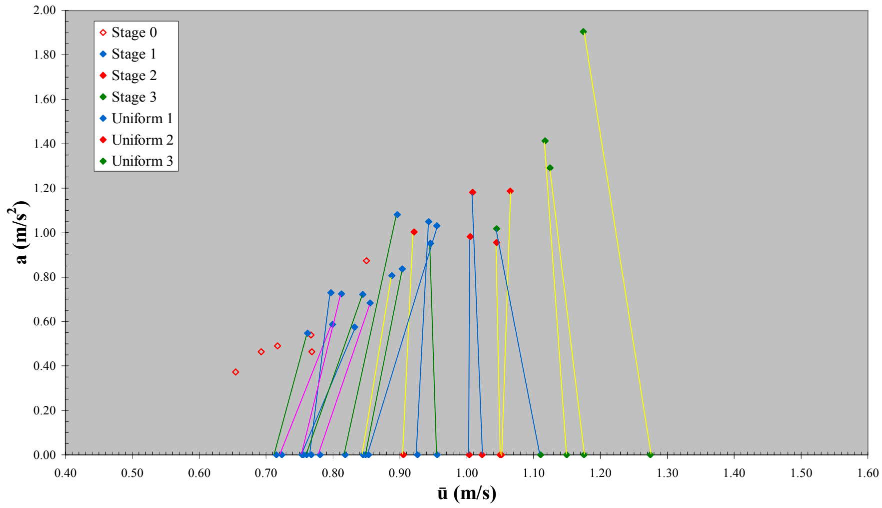

L = 2.50m

Figure 5.19 *Shift in velocities visualized for each length of the tapered section (L = 1.50m, L = 2.00m and L = 2.50m), distribution 6*

Figure 5.19a shows only increase in velocities. The acceleration causes an increase in stone moves.
Figure 5.19b shows that for the higher velocity-acceleration combinations the influence of the acceleration of the flow seems to be disadvantageous to the stability of stones. However, for the lower velocity-acceleration combinations a decline in velocities can be seen.
Figure 5.19c shows a stronger decline in velocities than *figure 5.19b*. The influence of the acceleration of the flow is less than expected.

Judging from shifts in velocities it is not clear if acceleration only causes an increase in stone movements. It appears that for lower velocity-acceleration combinations the acceleration of flow has a stabilizing effect.

In the next section an evaluation is made for the distributions which were used to analyze the data.

5.4 Evaluation

In chapter 5 a method has been applied to compare an accelerated flow with a uniform flow. The basis of this comparison is formed by a study on incipient motion by Breusers (DHL, 1969). Breusers defined 7 stages of transport. These stages of transport reflect the transition between no movement of stones from the bed to general transport of the bed. These stages of transport are correlated with a Shields parameter by the amount of stone moves.

With the help of the definitions given by Breusers a Shields parameter can be assigned to an amount of stones that moved from their strips during an experiment. A distribution is made for the stages of movement in which the stone moves from the experiments are linked to a Shields parameter.

The shear velocity, u_*, can be calculated with a value for the Shields parameter. The theory for the shear velocity assumes that the flow profile is logarithmic. In an accelerated flow this is not the case. A new equilibrium exists for the uniform flow with a new average uniform flow velocity, $\bar{u}_{uniform}$, and a new water depth, h_{strip}.
A shift in velocities between the situations indicates that there is an influence by the acceleration of the flow on the stability of the stones.

These shifts in velocities can be visualized in a number of ways. First the shift in velocities is presented for the different stages of transport. Then the difference in influence between the three tapered lengths is viewed.

Different distributions are made in which the amount of stones assigned to the stages of transport is varied. Different distributions lead to different shifts in velocities. Some distributions show a bigger shift in velocities due to a more favourable distribution of the stones over the different stages of transport.
For the tapered section with a length of L = 2.50m little increase in velocity was noted, in fact more of decline of velocities was noticed.

New stages of transport are defined by Huijsmans in which the original 7 stages of transport are united in three stages of transport. The distribution is simplified and as such less choices of the amount of moved stones that are assigned to a stage of transport have to be made. The shift in velocities for a stage of movement becomes more visible.

The following graph shows the average shift in velocities for the stages of transport by Breusers and Huijsmans:

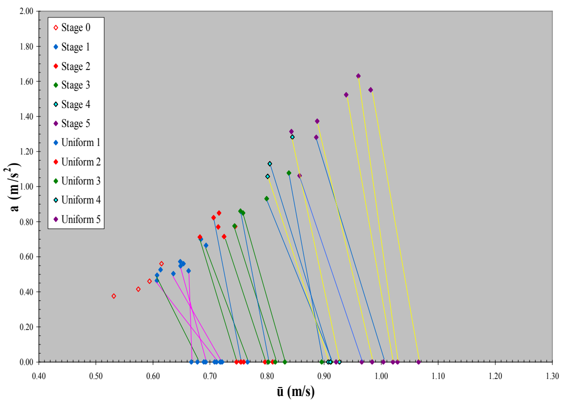

(a)

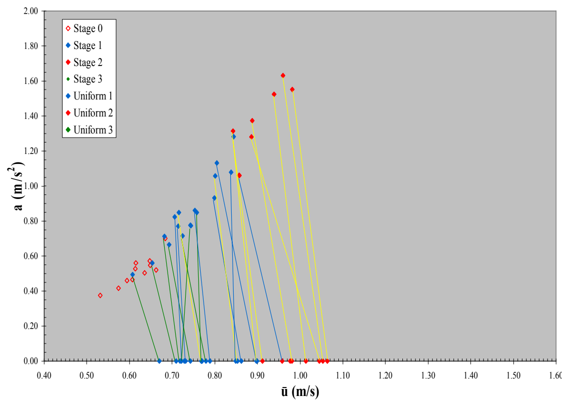

(d)

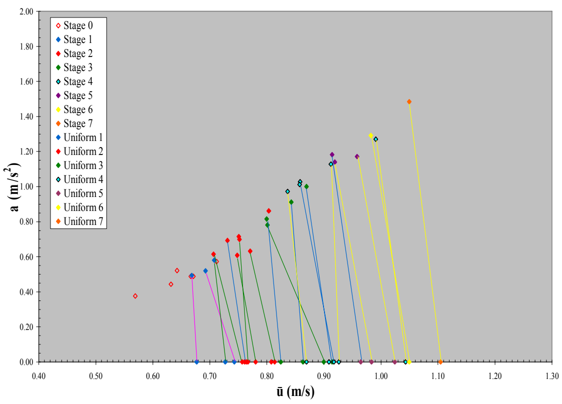

(b)

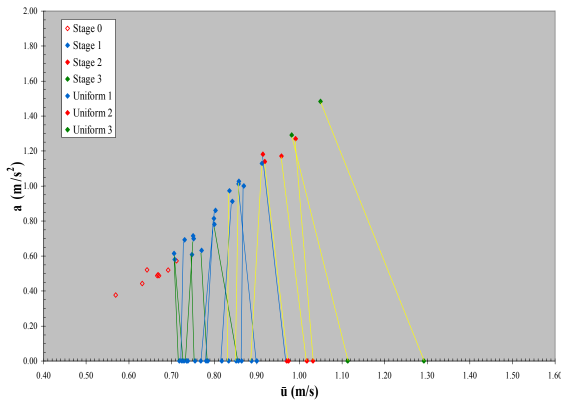

(e)

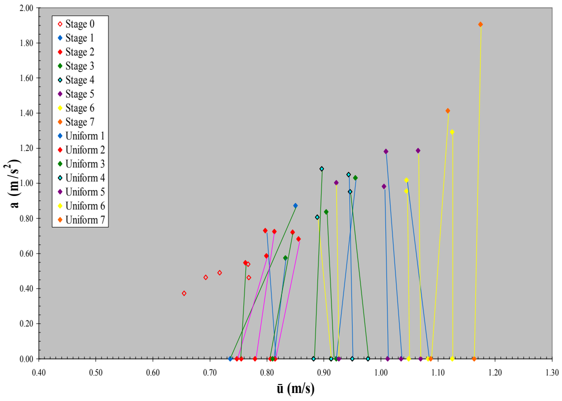

(c)

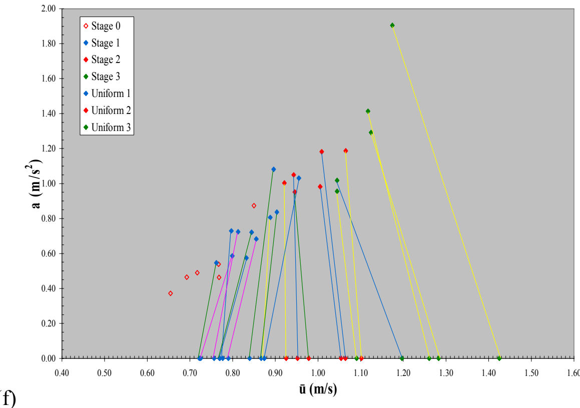

(f)

Figure 5.20 *Shift in velocities for distribution 2 by Breusers, left column: (a.) L = 1.50 m, (b.) L = 2.00m, (c.) L = 2.50m, and distribution 5 by Huijsmans, right column: (d.) L = 1.50m, (e.) L = 2.00m, (f.) L = 2.50m*

From *figure 5.20* can be concluded that the stages of transport defined by Breusers generally show the same shift in velocities as the new stages of transport.
The extent of the influence of acceleration becomes visualized by the difference in shifts in velocities between the three tapered sections.
For the same amount of stone movement to occur in a uniform flow as in the accelerated flow in the flume with a tapered section of L = 1.50m, an average uniform flow velocity is needed that exceeds the average velocity that occurred in the experiments.
The graphs for the tapered section with a length of L = 2.00m generally shows less of an increase in velocities than that of the tapered section with a length of L = 1.50m. This is what was expected, since the acceleration created in this tapered section is less.
The tapered section with a length of L = 2.50 has the least acceleration of flow. Depending on the distribution, which is used, some increase in velocities is achieved for the higher stages of transport. The lower stages of transport do not show an increase in velocities. This leads us to believe that for lower velocity-acceleration combinations the flow acceleration could have a stabilizing effect on the stability of stones.

This assumption can be corroborated by a study done on relative turbulence in a wind tunnel by Reynolds (1977).

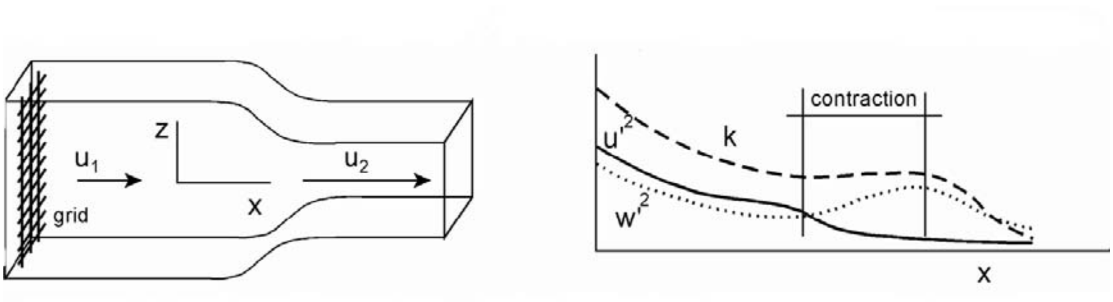

Figure 5.21 Turbulence in wind tunnel contraction (Reynolds, 1977)

As a flow contracts, the relative turbulence decreases. Relative turbulence causes peak velocities that on a micro scale influence the forces on a grain. When the relative turbulence is reduced, the peak velocities are also reduced. This could cause the bed to become more stable.

This seems to be the case when the bed is subjected to a slight acceleration of flow, the velocity-acceleration combinations for the tapering with a length of L = 2.50m. When the acceleration becomes more intense, the acceleration dominates the relative turbulence and an additional acceleration force causes the grain to move before the critical velocity is reached (locally tapered sections with lengths of L = 1.50m and L = 2.00m).

The relative turbulence near the bottom could not be measured with the EMS.

6 Conclusions and recommendations

In this chapter the conclusions, which were drawn throughout the report regarding the influence of acceleration of flow on the threshold of motion, are summarized

Also recommendations for further research on the topic of stability of stones in accelerated flows are given. These recommendations include remarks for further experiments.

Firstly the objectives of this thesis will be revised:

- The objective for following experiments is to record the movement of stones in situations with flow conditions that lie in the interesting regions as shown in *Figure 1.5.*

- The objective for the analysis of the data is to compare the average flow velocity of an accelerated flow with the average flow velocity of a uniform flow for which the same amount of transport of stones occurs as to show the influence of acceleration of flow on the stability of stones.

6.1 Conclusions

It has become evident that the fluid accelerations have an influence on the threshold of motion.

Velocity-acceleration combinations with high velocities and high accelerations show that a higher average uniform flow velocity needed for the same amount of transport to occur.
Velocity-acceleration combinations with low velocities and low accelerations show a lower average uniform flow velocity needed for the same amount of transport to occur.

- A method has been found to compare the flow velocity of an accelerated flow with a uniform flow. This method uses the relation between the amount of moved stones in the experiments and the Shields parameter (Breusers, DHL 1969) to calculate an average flow velocity for a uniform flow, *section 5.2*.

- The influence of the flow acceleration is visualized by a shift in velocities in the velocity-acceleration graph, *figure 5.2*. The calculated uniform flow velocities are plotted on the x-axis in the velocity-acceleration graph.

- The tapered section with a length of L = 1.50m creates the highest acceleration of flow. When a uniform velocity is calculated for which the same amount of stone movement would occur, this velocity exceeds the velocity at which the stones moved from their strips in the experiments.

- The tapered section with a length of L = 2.00m shows an increase in velocities for the higher stages of transport. For the lower stages of transport it depends on the distribution of the amount of stone movements among the stages of transport whether an influence of the acceleration can be noticed. For favourable distributions an increase in velocity can be seen. However, distributions which allow for more stone moves in the early stages of movement show a decline in velocity.

- The tapered section with a length of L = 2.50m only shows an increase in velocity for the highest stage of transport. The gross of the data points show a decline in velocity when an average uniform velocity is calculated for the amount of moved stones.

- There is another effect which is caused by the acceleration of flow. It was believed that acceleration causes the stones to move before a critical velocity is reached. This is the case for velocity-acceleration combinations above a certain velocity-acceleration range, note the increase in velocities as can be seen in *section 5.3*.
  Velocity-acceleration combinations that do not reach these velocities and accelerations show a decline in velocities, *figure 5.20c* and *figure 5.20f*. This indicates that acceleration of flow also can cause a stabilizing effect on the bed.
  Reynolds (1977) showed that, as the acceleration increases, the relative turbulence decreases. Relative turbulence causes peak velocities that on a micro scale influence the forces on a grain. When relative turbulence is reduced, the peak velocities are also reduced. This could cause the bed to become more stable, when subjected to a slight acceleration of flow.

The EMS has restrictions when measuring near the bottom, side walls or the water surface. In these experiments it was not possible to measure the relative turbulence near the bottom.

6.2 Recommendations

Suggestions for new experiments regarding the area of interest for additional velocity-acceleration measurements:

- The range of experimental data that was the objective for additional experiments was not completely achieved. No experiments were done for the region with low velocity and high acceleration combinations. Additional experiments within the range for velocities of [0.70m/s - 0 90m/s] and accelerations of [0.80m/s^2 – 1.40m/s^2] will give more data that can be used to visualize the influence of flow acceleration on the stability of stones.

- The experiments in the tapered section with a length of L = 2.50m showed a decline in velocities. This indicates a stabilizing effect by the acceleration of the flow. Doing experiments in a decelerating flow should show the opposite effect; it should show a destabilizing effect. If this is the case it can be concluded that acceleration of flow can also have a stabilizing effect for areas with slight acceleration of flow

- Measurement in the vertical of the flow profile particularly near the bottom can give more insight in the change of flow profile. These experiments lacked the technical opportunities to fully record the change of flow profile. The bottom part of the flow profile is of interest, because the shear velocity is greatly responsible for the movement of stones. When measuring near the bottom the relative turbulence should also be measured. The relative turbulence also changes when a flow is accelerated. The reduction of relative turbulence could cause the stabilizing effect.
  In addition, with better readings of the flow profile near the bottom, it can be investigated what happens to the height of z_0 when a flow gets accelerated.

Recommendations regarding the experimental set-up:

- Additional experiments in a longer and wider flume would create a larger measurement area. It would be very convenient to have a larger number of stone movements under low-mobility conditions. This could also be achieved by using lighter stones. Lighter stones move sooner than heavier ones and hence flow velocities can be lower.

- Velocity measurements have to be taken with instruments which can measure the velocities more accurately. Preferably with instruments that can measure vertical velocity gradients and that can take measurements nearer to the bottom. It enables the user to find out how the flow profile changes near the bottom as the flow accelerates. It also enables the user to document the turbulence structures which translate into relative turbulence. It also provides you with a chance to get a more accurate reading for z_0 in accelerated flow.

- Recording stone moves in a uniform flow would quantify the definitions for the 7 stages of transport defined by Breusers by verifying the amount of stone moves and their Shields parameters. Video images of the movement of stones in time could also assist to quantify the stages of transport.

List of symbols

Symbol	Definition	Unit
a:	acceleration	[m/s^2]
A:	surface area of the stones	[m^2]
A_D:	exposed surface area (drag force)	[-]
A_L:	exposed surface area (lift force)	[-]
$A_{profile}$:	area of the flow profile	[m^2]
A_{strip}:	area of a strip of stones	[m^2]
B:	width of a cross-section	[m]
B_b:	width of the inflow of the contraction	[m]
B_e:	width of the outflow of the contraction	[m]
B_{strip}:	width of a cross-section at middle of strip	[m]
C_D:	drag coefficient	[-]
C_{L}:	lift coefficient	[-]
C_S:	shear coefficient	[-]
d:	stone diameter	[m]
d_n:	nominal diameter of stone	[m]
d_{n50}:	median nominal diameter of stone	[m]
F:	force	[N]
F_D:	drag force	[N]
F_G:	gravity force	[N]
F_L:	lift force	[N]
F_S:	shear force	[N]
Fr:	Froude number	[-]
g:	gravitational acceleration	[m/s^2]
h:	water depth	[m]
h_{gate}:	gate height	[m]
h_{strip}:	water depth for uniform situation	[m]
k_r:	Nikuradse's roughness coefficient	[-]
k_t:	layer thickness coefficient	[-]
L:	length of the tapered section	[-]
M_{cum}:	cumulative mass of stones	[kg]
M_{dr}:	dry mass	[kg]
M_w:	under-water mass	[kg]
n:	1. number of stones moved	[-]
	2. number of tests	[-]
	3. number of layers	[-]
p:	1. pressure	[N/m^2]
	2. probability	[-]
q:	discharge per meter width	[m^2/s]
Q:	discharge	[m^3/s]
Re:	number of Reynolds	[-]
Re_*:	particle Reynolds number	[-]

S_u:	amount of one layer of dumped stones	[-]
$st\%$:	amount of moved stones in percentages	[-]
t_c:	calculated thickness layer	[m]
t_m:	measured perpendicular thickness layer	[m]
t_t:	theoretical thickness layer	[m]
T:	duration experiment	[s]
u:	flow velocity in x-direction	[m/s]
$\bar{u}$:	depth-averaged flow velocity	[m/s]
u_b:	velocity of the flow near the bottom	[m/s]
$\bar{u}_h$:	calculated velocity using the water depth	[m/s]
$\bar{u}_{uniform}$:	average uniform flow velocity	[m/s]
$\bar{u}_{EMS}$:	velocity measured using EMS	[m/s]
u_*:	shear velocity	[m/s]
u_{*C}:	critical shear velocity	[m/s]
V_s:	volume stone	[m^3]
V:	volume of the stone (d_n^3)	[m^3]
w:	flow velocity in z-direction	[m/s]
W_{eff}:	effective width	[-]
W_{50}:	median nominal weight	[kg]
z:	height of the measurement above the bed	[m]
z_0:	height above bed where velocity is zero	[m]
α:	angle between flume wall and structure	[-]
Δ:	relative density (= (ρ_s-ρ_w) / ρ_w)	[-]
κ:	von Kàrmàn constant (= 0.4)	[-]
ρ_s:	density of stone	[kg/m^3]
ρ_w:	density of water	[kg/m^3]
σ:	standard deviation	[-]
τ_c:	critical shear stress	[N/m^2]
τ_0:	shear stress at the bottom	[N/m^2]
υ:	kinematic viscosity	[m^2/s]
ψ:	Shields parameter	[-]
ψ_c:	critical Shields parameter	[-]

References

BATTJES, J.A., 1997. *Lecture notes CT2100 Vloeistofmechanica.* Delft: Delft Faculty of Civil Engineering and Geosciences

BATTJES, J.A., 2000. *Lecture notes CT3310 Stroming in waterlopen.* Delft: Delft Faculty of Civil Engineering and Geosciences

BOSMA C.F., 2001. *M. Sc.-thesis Porositeit in breuksteenconstructies.* Delft: Delft Faculty of Civil Engineering and Geosciences

BOER, G.M., DE, 1998. *M.Sc. Thesis Transport van stenen van een granulaire bodemverdidiging.* Delft: Delft Faculty of Civil Engineering and Geosciences

BREUSERS, 1969. *Begin van bewegen bodemmateriaal.* Delft: Delft Hydraulic Laboratory (DHL) Report S159-1

CALANTONI, J. AND DRAKE, T.G.8, 2001. *Discrete particle mode for sheet flow sediment transport in the nearshore.* Journal of geophysical research. Vol 106. No C9 pages 19,859-19,869

CIRA/CUR, 1991. *Manual on the use of rock in coastal and shoreline engineering. CUR-Report 154.* Rotterdam: Balkema (ISBN 905410 1024)

CUR REPORT 169, 1995. *Manual on the use of Rock in Hydraulic Engineering*. Gouda: CUR

DESSENS, M. *M. Sc.-thesis The influence of the acceleration of flow on the stability of stones.* Delft: Delft Faculty of Civil Engineering and Geosciences

ENGELUND, F. AND HANSEN, E., 1967. *A monograph on sediment transport.* Copenhagen: Technisk Forlag

FRAAIJ ET AL., 2002. *Experiment manual A CT1120 Materiaalkunde.* Delft: Delft Faculty of Civil Engineering and Geosciences

FORSCHELEN, P., DEC. 1999. *M.Sc. Thesis Transport van granulair bodemmateriaal.* Delft: Delft Faculty of Civil Engineering and Geosciences

HENDRIKS, CH.F. ET AL, 1997. *Lecture notes CT4030 Onderzoeksmethodologie.* Delft: Delft Faculty of Civil Engineering and Geosciences

ELGAR, S. AND HOEFEL, F., 2003. *Wave induced sediment transport and bar migrationecture notes.* Science. Vol. 299 No.C9 pages 1885-1887

LAMMERS, J.C., 1997. *M.Sc. Thesis Shields in de praktijk.* Delft: Delft Faculty of Civil Engineering and Geosciences

KING, R., 1991. *Mach 3.5 boundary-layer transition on a cone at angle of attack. AIAA Paper 91-1804*

PULEO, J.A., 2003. *Fluid acceleration effects on suspended sediment transport in the swash zone.* Mississippi: Naval Research Center

REYNOLDS, A.J., 1977. *Turbulent flow in engineering.* Wiley, London

RIJN, L., VAN, 1989. *Handbook sediment transport by currents and waves.* Delft: Delft Hydraulics Laboratory (DHL)

SCHIERECK, G.J., 2001. *Introduction to Bed, bank and shore protection*. Delft: Delft University Press

SCHOKKING, L.A., 2002. *M.Sc. Thesis Bowthruster-induced Damage.* Delft: Delft Faculty of Civil Engineering and Geosciences

TROMP, M.M.A., 2004. *M.Sc. Thesis The influence that fluid accelerations have on the threshold of motion.* Delft: Delft Faculty of Civil Engineering and Geosciences

Appendix

Appendix A Experimental Set-up

Figure A1 shows the flume with the tapered section near the gate at the end of the flume.

Figure A.1 *The flume with a tapered section near the end*

Placement of the stones

Figure A.2 *The first layer of stones glued to the wooden bottom plates*

The stones are placed using set distances for the measuring area.

Figure A.3 *Dumping of the stones*

The discharge into the flume is regulated by a valve, *figure A4 (left)*, on the inlet pipe. The discharge is measured with a pressure gauge that measures the difference in piezometric head over the orifice plate, *figure A4 (right).*

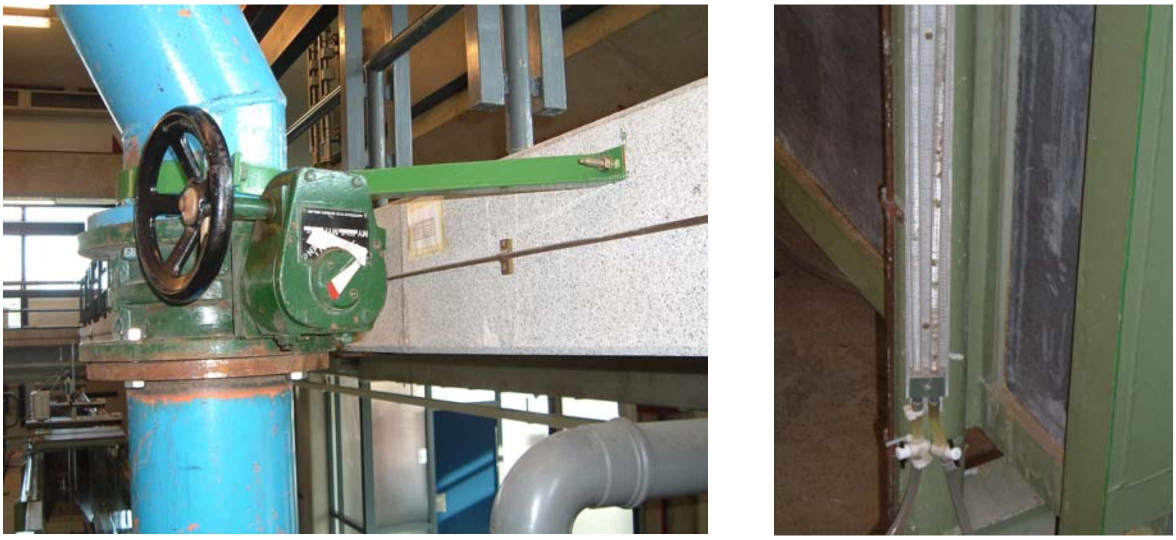

Figure A.4 *Inlet valve (left), pressure gauge for measuring the discharge (right)*

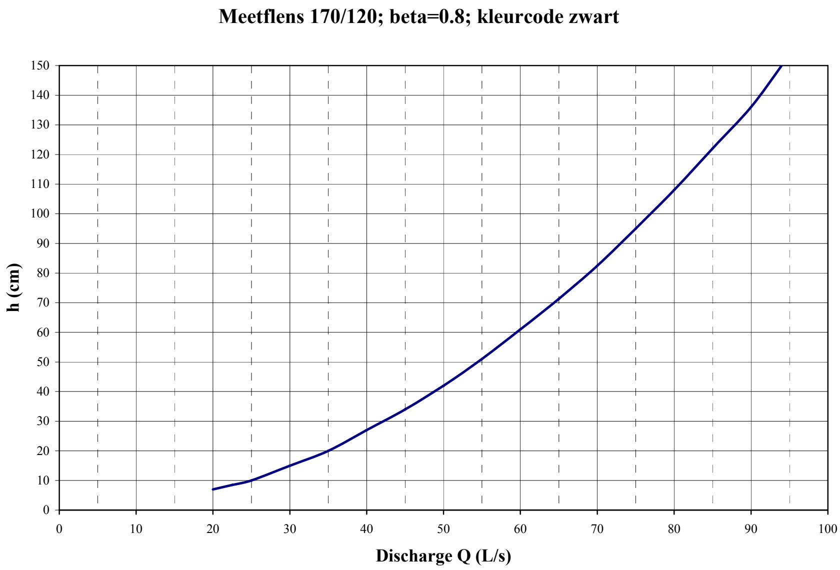

Figure A.5 *Discharge of the flume versus the difference in pressure height of the piezometric plate*

EMS

An Electromagnetic Sensor is used as an Electro-Magnetic Flow meter.

Fluid flow perpendicular to a magnetic field created by a pulsed electromagnet (coil) gives rise to an electric field perpendicular to the flow and magnetic vectors. Measuring the voltage difference between two electrodes senses this electric field. The voltage difference is directly proportional to the flow velocity.

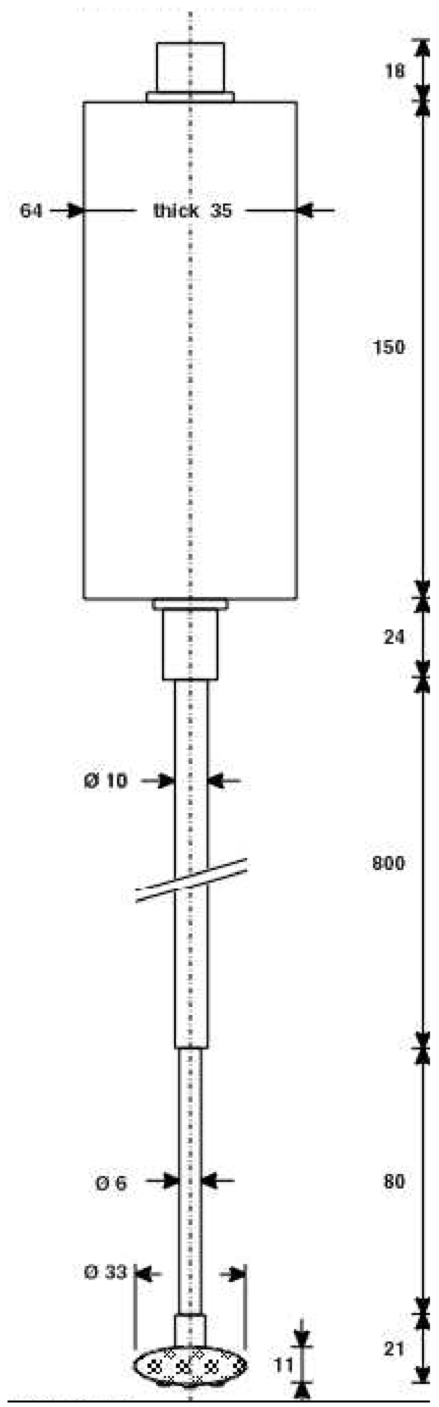

Figure A.6 *The EMS probe*

Appendix B Sieve Curves

The procedure for the selection of the stones with a certain d_{n50} is given in the following steps.

The first four steps are the same all stone sizes:

Step 1 Sieve the stones using two sieves, one with gaps a little larger than the other.
Step 2 Wash the collected stones carefully.
Step 3 Dry the stones.
Step 4 Collect a random large amount of stones from the sieved, washed and dried stones. (≥ 144)
Step 5 Weigh each stone separately using an accurate balance. Weigh each stone dry and under water and register the values.
Step 6 Measure the largest length and the smallest length of each stone using a vernier calliper.
Step 7 Make the following calculations for determining the stone parameters:

$$\rho_s = \rho_w \frac{M_{dr}}{M_w} \tag{3.7}$$

$$V_s = \frac{1}{(\rho_s / M_{dr})} \tag{3.8}$$

$$d_n = \sqrt[3]{V_s} \tag{3.9}$$

M_{dr}:	dry mass	[kg]
M_w:	under-water mass	[kg]
V_s:	volume stone	[m^3]

All the necessary stone parameters can now be calculated.

Dessens (2004) performed the procedures for determining the stones parameters with the following d_{n50} = 0.0082m and d_{n50} = 0.0200m
In *figure B.1* a distribution of the dry mass is plotted versus the percentage of the cumulative weight for the smaller grain size. Also a distribution of the diameter of the grains (d_n) is plotted versus the cumulative weight in *figure B.2*. For the sieve curves of the larger grain size see *The influence of flow acceleration on stone stability* (Dessens, 2004)
For the determination of the stone parameters of the small stones 250 grains were measured.

Table B.1 contains the important parameters for these stones.

Table B.1 *Stone parameters (Dessens, 2004)*

	Small stones	Large stones	Dimension
# stones	250	139	-
M cum.	361.77	2845.6	gr
dn50	0.0082	0.0200	m
ρ av.	2682.2	2682.	kg/m3
W50	1.49	21.422	gr
d85/d15	1.22	1.18	-
Δ	1.67	1.67	-

Now the sieve curves are presented in *figure B.1* and *figure B.2*

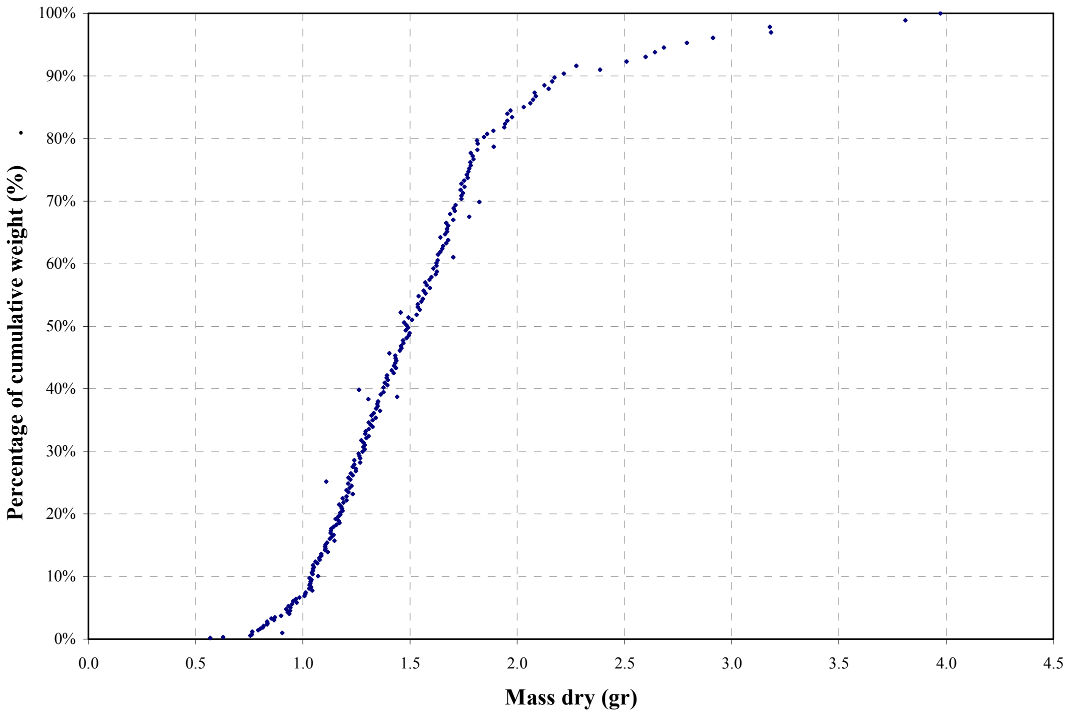

Figure B.1 *Mass distribution small stones, d_{n50} = 0.0082m*

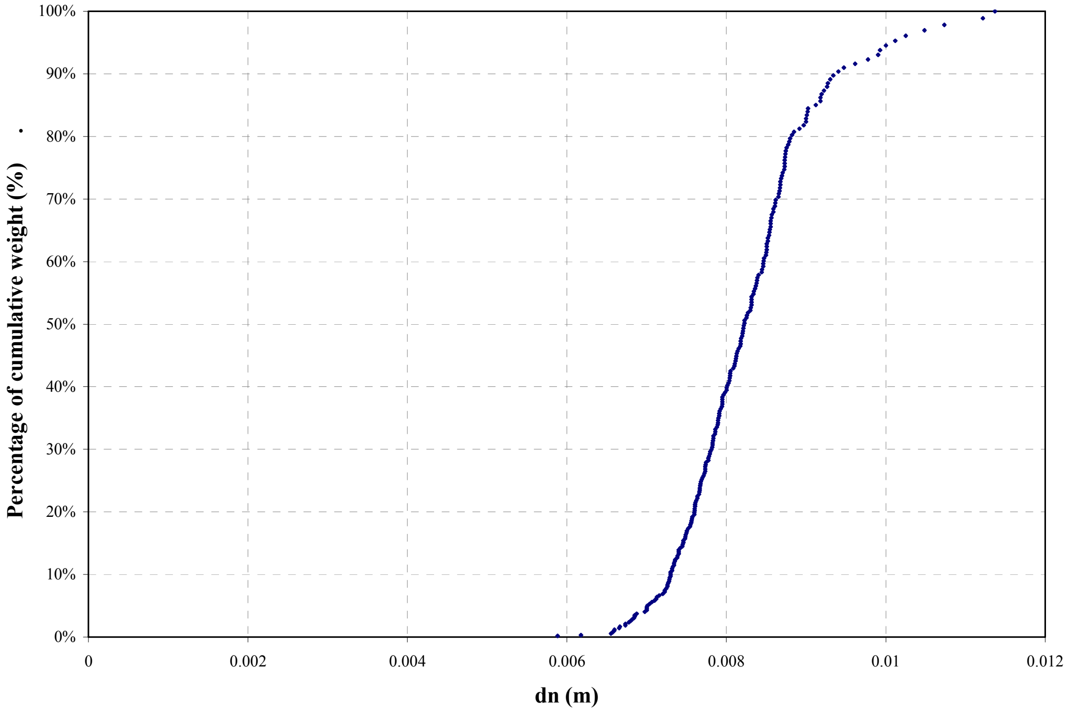

Figure B.2 *d_n distribution small stones, $d_{n50} = 0.0082m$*

Appendix C1 Flow Profiles

Here the velocity profiles for the experiments conducted in the flume with a tapered section of L = 2.50m are displayed.

Series 1: L = 2.50m, Q = 0.04 m3/s, h_{gate} = 0.1890m

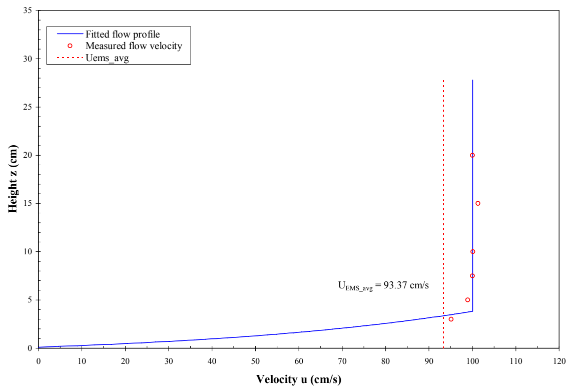

x = 0.00m, h = 27.81cm, $\bar{u}_{EMS}$ = 0.93m/s

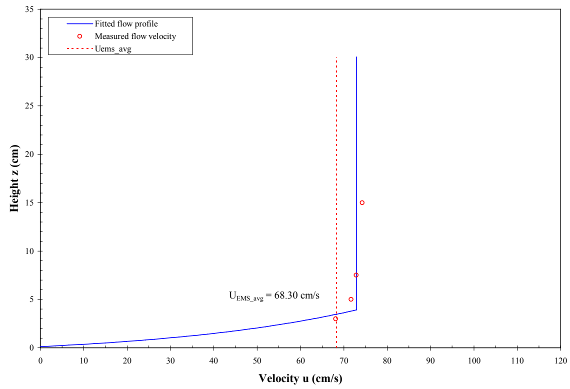

x = 0.30m, h = 30.08cm, $\bar{u}_{EMS}$ = 0.68m/s

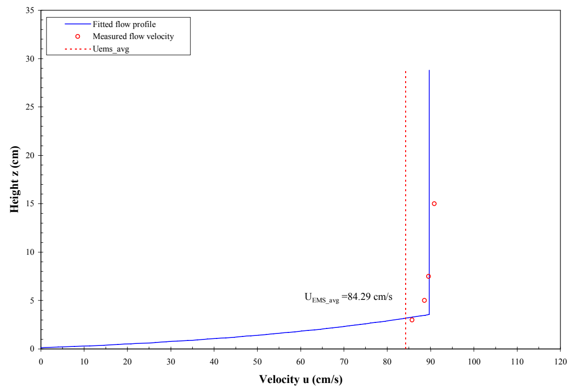

x = 0.10m, h = 28.81cm, $\bar{u}_{EMS}$ = 0.84m/s

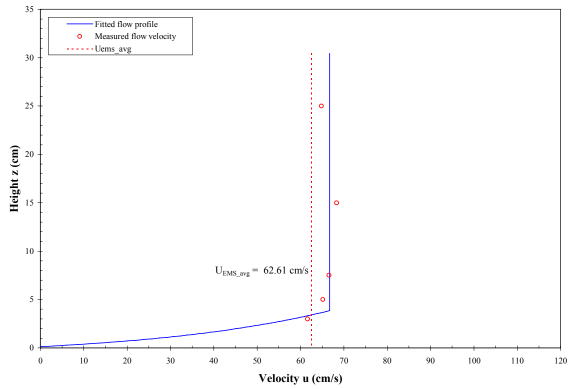

x = 0.40m, h = 30.47cm, $\bar{u}_{EMS}$ = 0.63m/s

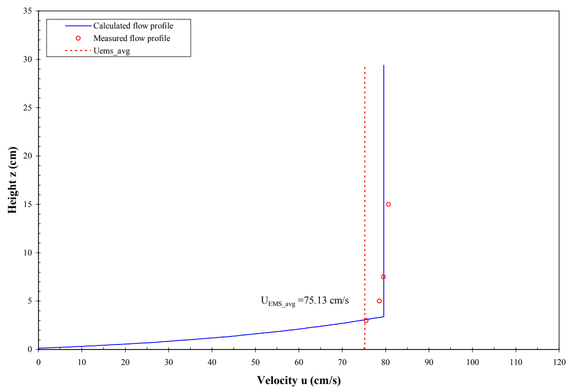

x = 0.20m, h = 29.39cm, $\bar{u}_{EMS}$ = 0.75m/s

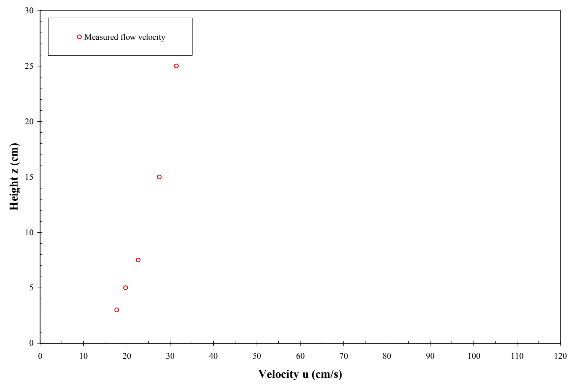

x = 2.50m, h = 32.62cm

Series 2: L = 2.50m, Q = 0.05 m3/s, h_{gate} = 0.1890m

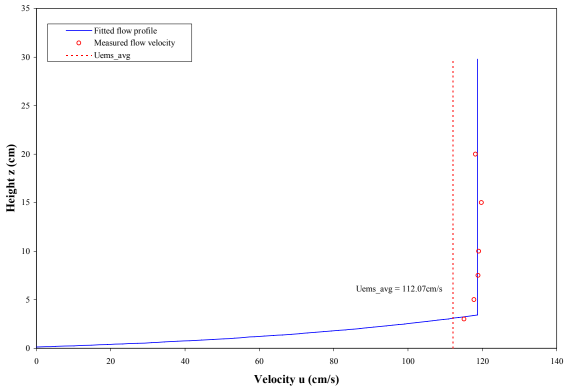

x = 0.00m, h = 29.77cm, $\bar{u}_{EMS}$ = 1.12m/s

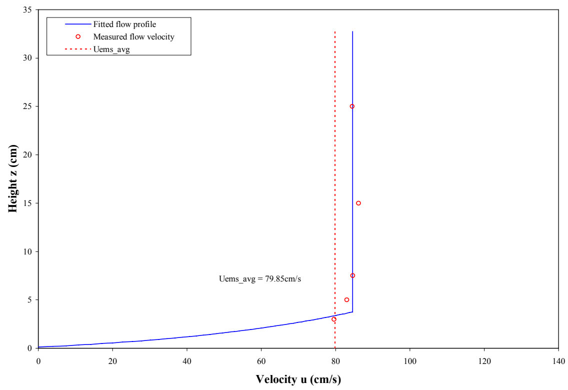

x = 0.30m, h = 32.75cm, $\bar{u}_{EMS}$ = 0.80m/s

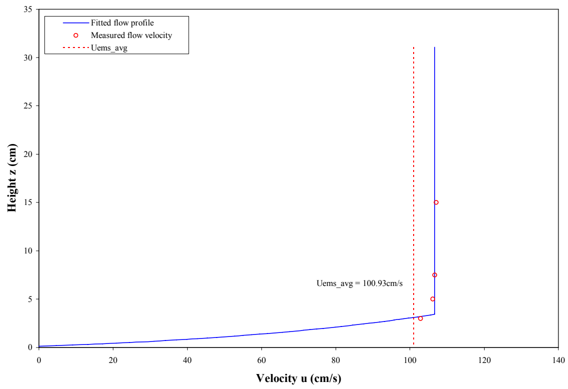

x = 0.10m, h = 31.08cm, $\bar{u}_{EMS}$ = 1.01m/s

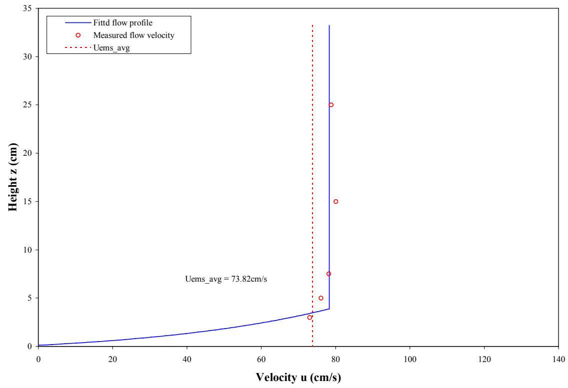

x = 0.40m, h = 33.23cm, $\bar{u}_{EMS}$ = 0.74m/s

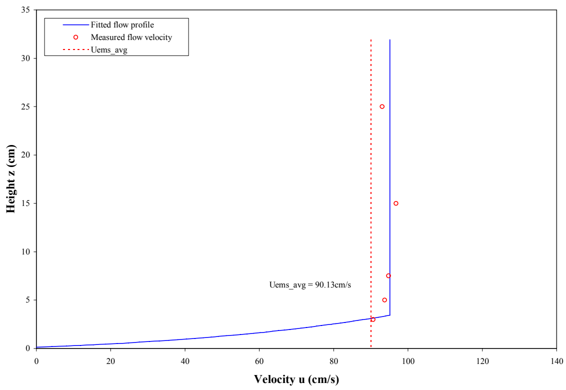

x =0.20m, h = 31.92cm, $\bar{u}_{EMS}$ = 0.90m/s

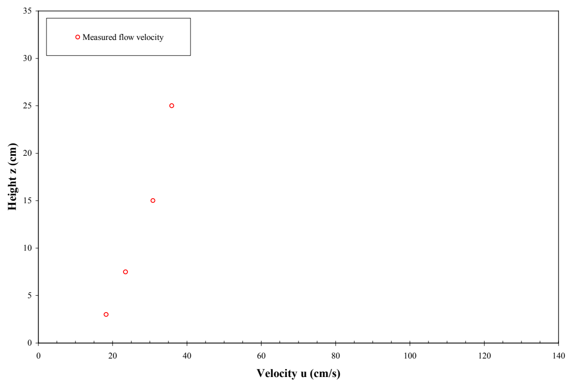

x = 2.50m, h = 35.81cm

Series 3: L = 2.50m, Q = 0.05 m3/s, h_{gate} = 0.1690m

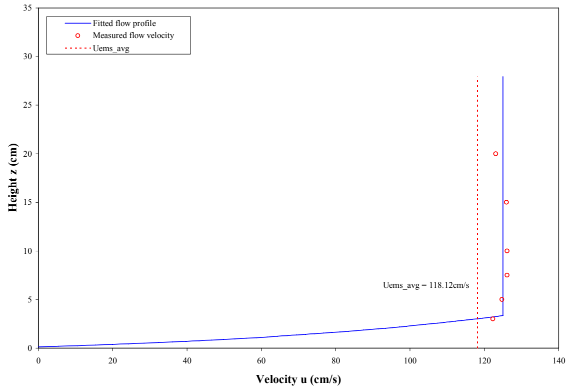

x = 0.00m, h = 27.94cm, $\bar{u}_{EMS}$ = 1.18m/s

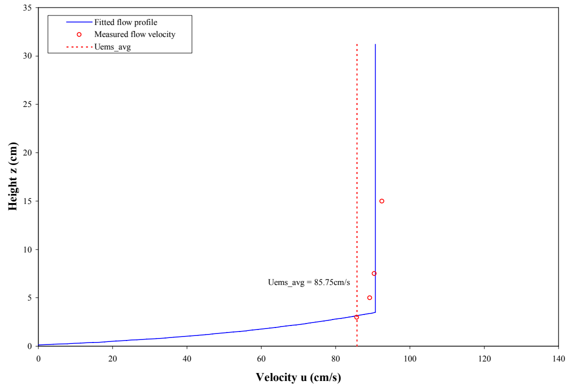

x = 0.30m, h = 31.23cm, $\bar{u}_{EMS}$ = 0.86m/s

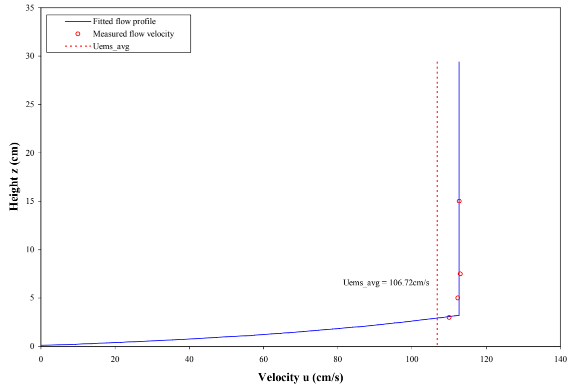

x = 0.10m, h = 29.39cm, $\bar{u}_{EMS}$ = 1.06m/s

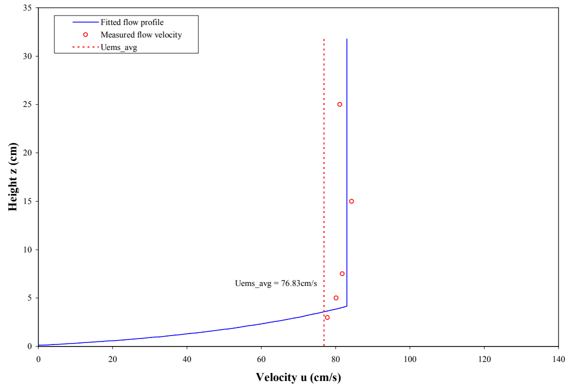

x = 0.40m, h = 31.78cm, $\bar{u}_{EMS}$ = 0.77m/s

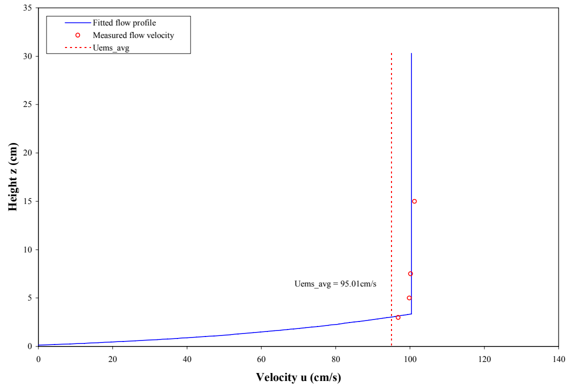

x = 0.20m, h = 30.31cm, $\bar{u}_{EMS}$ = 0.95m/s

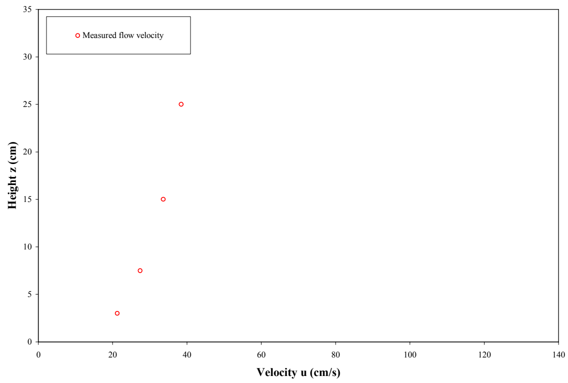

x = 2.50m, h = 34.62cm

Series 4: L = 2.50m, Q = 0.05 m3/s, h_{gate} = 0.1490m

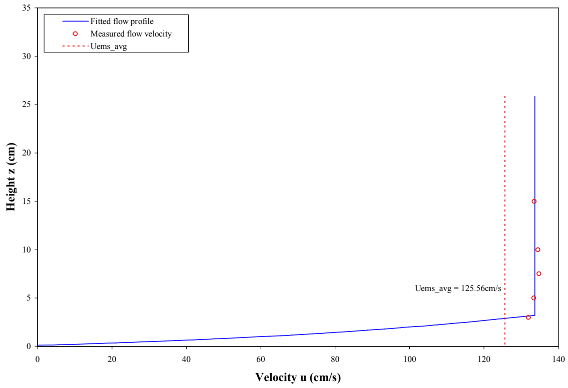

x = 0.00m, h = 25.85cm, $\bar{u}_{EMS}$ = 1.26m/s

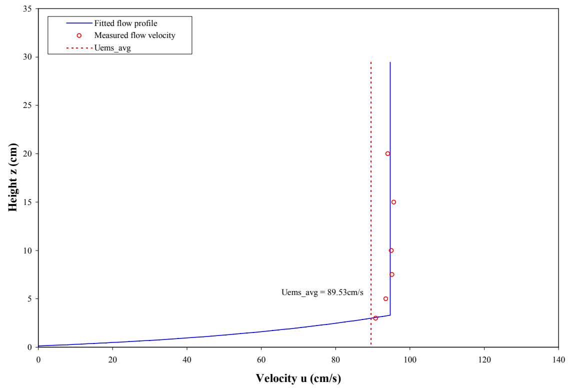

x = 0.30m, h = 29.47cm, $\bar{u}_{EMS}$ = 0.90m/s

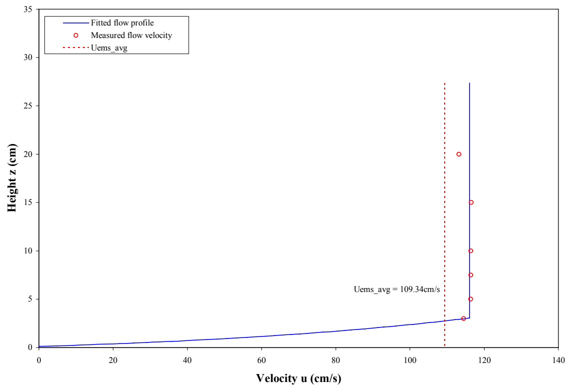

x = 0.10m, h = 27.36cm, $\bar{u}_{EMS}$ = 1.09m/s

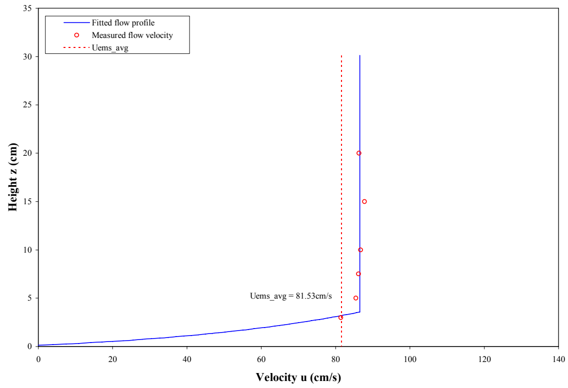

x = 0.40m, h = 30.13cm, $\bar{u}_{EMS}$ = 0.82m/s

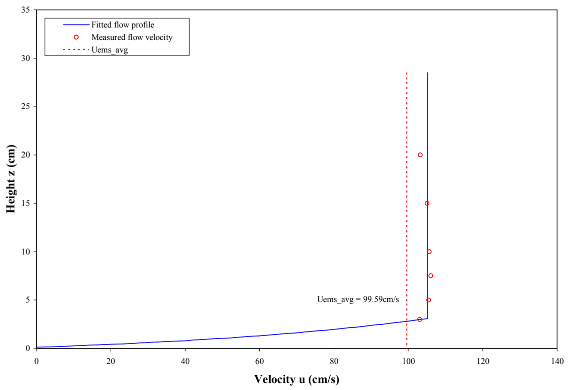

x = 0.20m, h = 28.52cm, $\bar{u}_{EMS}$ = 1.00m/s

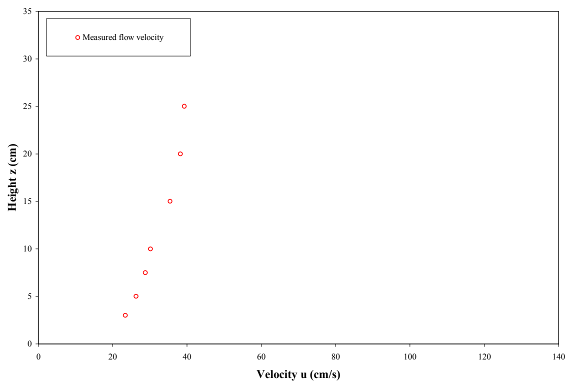

x = 2.50m, h = 33.30cm

Series 5: L = 2.50m, Q = 0.04 m3/s, h_{gate} = 0.1490m

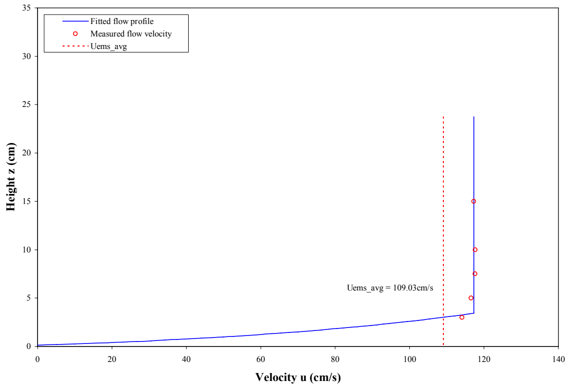

x = 0.00m, h = 23.75cm, $\bar{u}_{EMS}$ = 1.09m/s

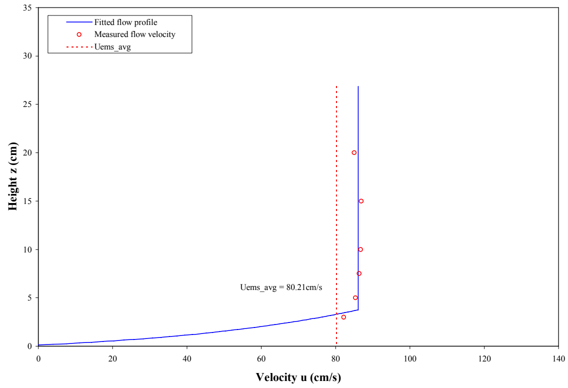

x = 0.30m, h = 26.88cm, $\bar{u}_{EMS}$ = 0.80m/s

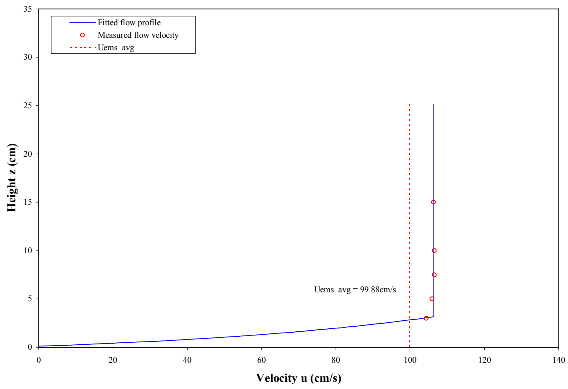

x = 0.10m, h = 25.15cm, $\bar{u}_{EMS}$ = 1.00m/s

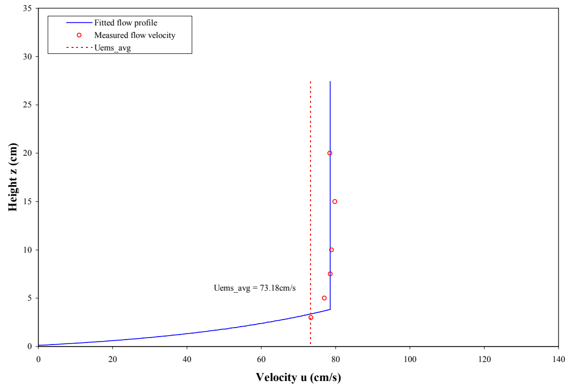

x = 0.40m, h = 27.42cm, $\bar{u}_{EMS}$ = 0.73m/s

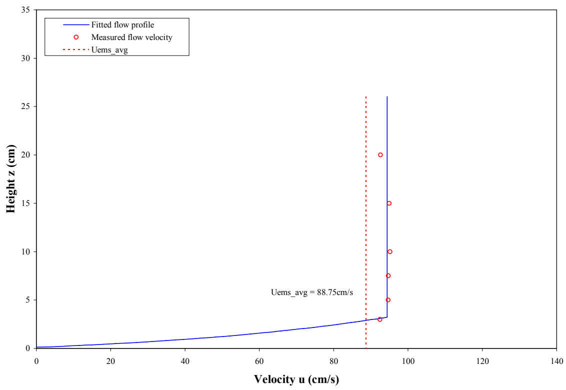

x = 0.20m, h = 26.05cm, $\bar{u}_{EMS}$ = 0.89m/s

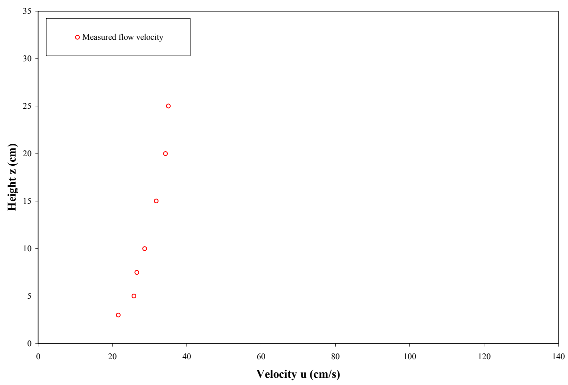

x = 2.50m, h = 30.07cm

Series 6: L = 2.50m, Q = 0.04 m3/s, h_{gate} = 0.1290m

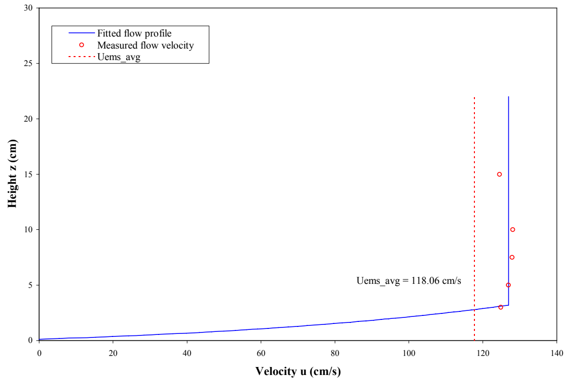

x = 0.00m, h = 22.01cm, $\overline{u}_{EMS}$ = 1.18m/s

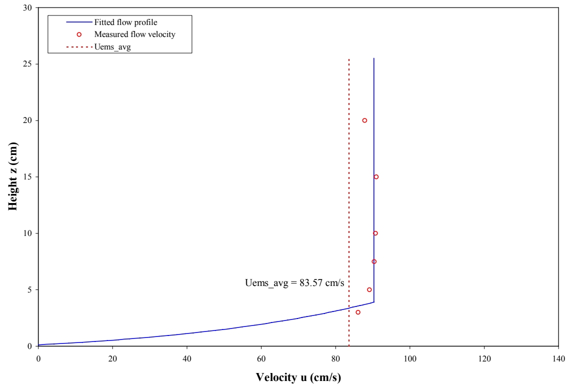

x = 0.30m, h = 25.52cm, $\overline{u}_{EMS}$ = 0.84m/s

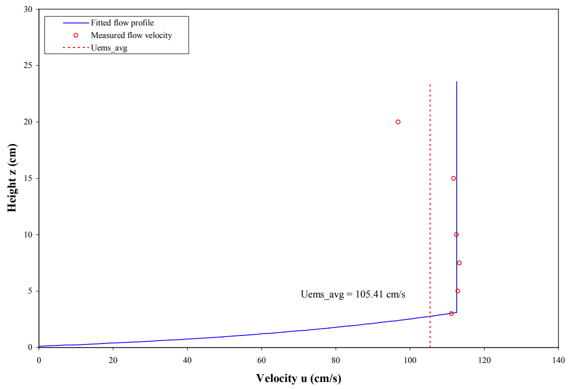

x = 0.10m, h = 23.57cm, $\overline{u}_{EMS}$ = 1.05m/s

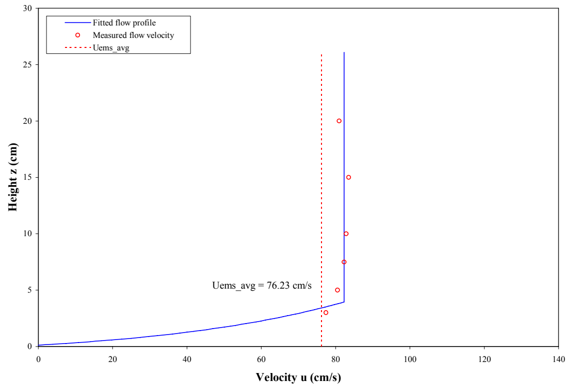

x = 0.04m, h = 26.10cm, $\overline{u}_{EMS}$ = 0.76m/s

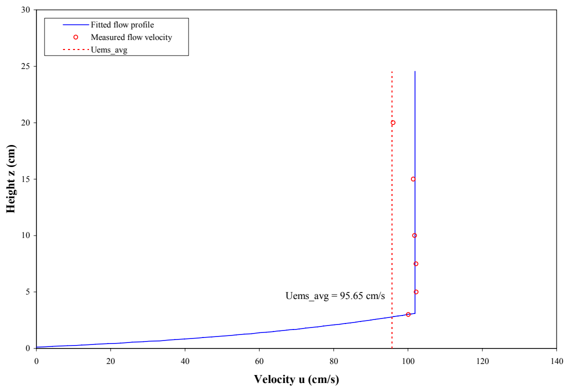

x = 0.20m, h = 24.57cm, $\overline{u}_{EMS}$ = 0.96m/s

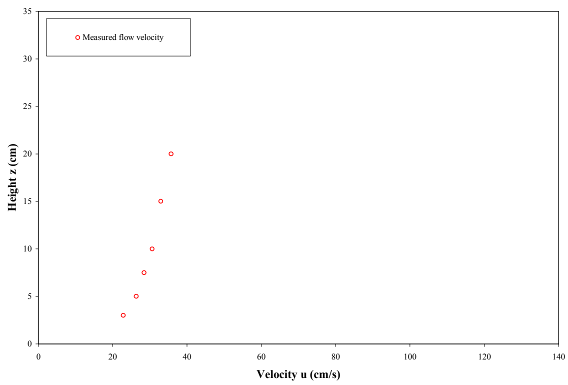

x = 2.50m, h = 28.91cm

Series 7: L = 2.50m, Q = 0.03 m3/s, h_{gate} = 0.1290m

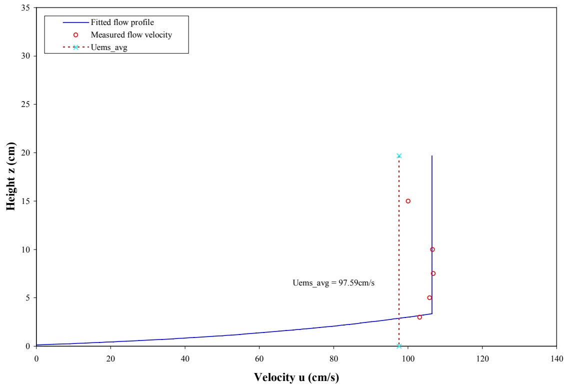

x = 0.00m, h = 19.69cm, $\bar{u}_{EMS}$ = 0.98m/s

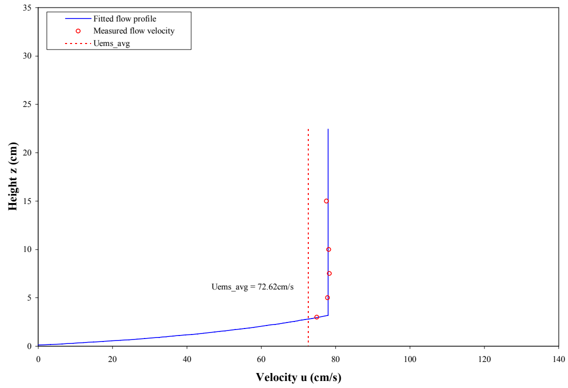

x = 0.30m, h = 22.44cm, $\bar{u}_{EMS}$ = 0.73m/s

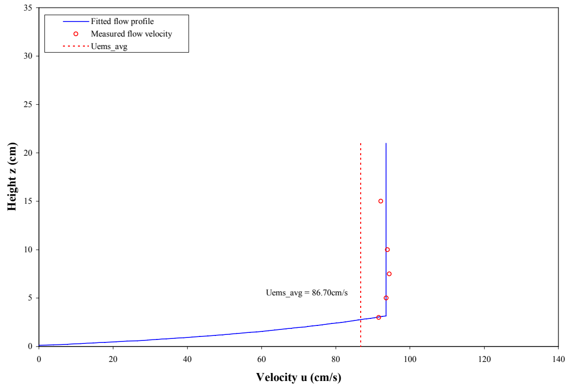

x = 0.10m, h = 20.99cm, $\bar{u}_{EMS}$ = 0.87m/s

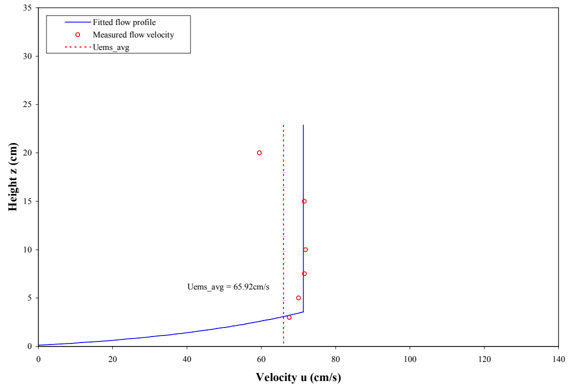

x = 0.40m, h = 22.88cm, $\bar{u}_{EMS}$ = 0.66m/s

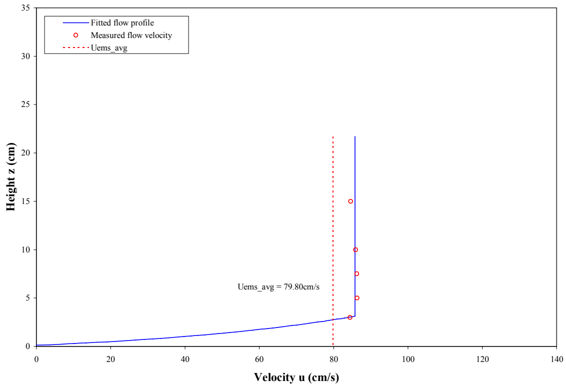

x = 0.20m, h = 21.71cm, $\bar{u}_{EMS}$ = 0.80m/s

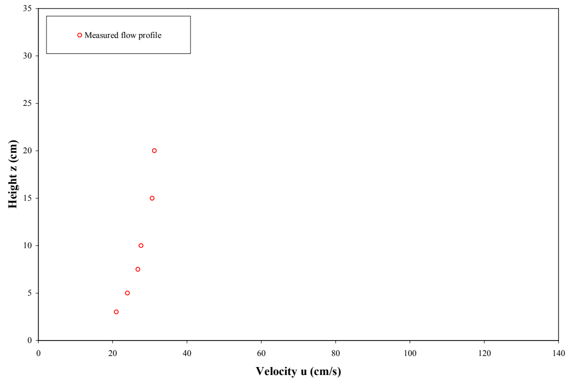

x = 2.50m, h = 25.05cm

Appendix C2 Determination of z_0

To determine the value of z_0 the flow velocity of an undisturbed flow at the beginning of the tapered section is plotted versus the logarithmic height of the velocity measurement.
Through the data points a straight line is drawn and the value for z_0 can be determined where $u = 0$ and $z = 0$ through:

$$\ln z = \kappa \frac{u}{u_*} + \ln z_0 = \kappa \frac{1}{u_*} u + \ln z_0 = au + b \qquad \text{(A.1)}$$

An average value for z_0 is calculated for both estimations of the level of the bed ($1.17 \text{x} 10^{-2}$m / $1.30 \text{x} 10^{-2}$m above the bottom plates) and for the different lengths of the tapering.

The following graphs show the flow profiles plotted on a logarithmic scale.

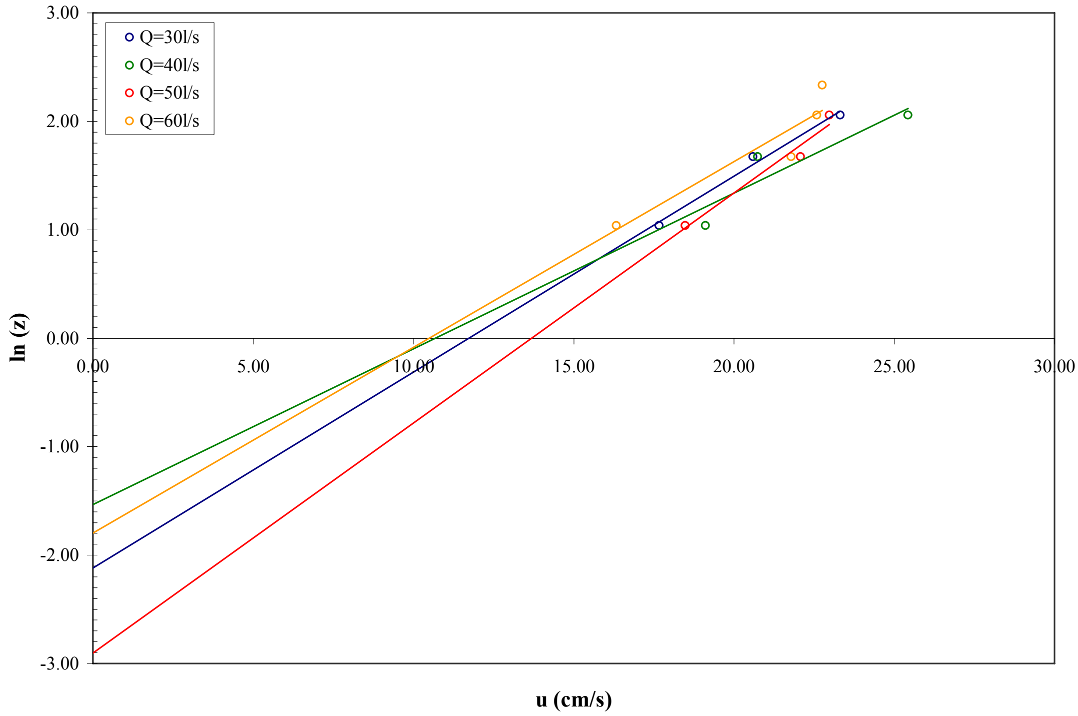

Figure C.1 *Determination of z_0 with a level of the bed (z =0.00m) at $1.17*10^{-2}$m above the bottom plates for L= 1.50m*

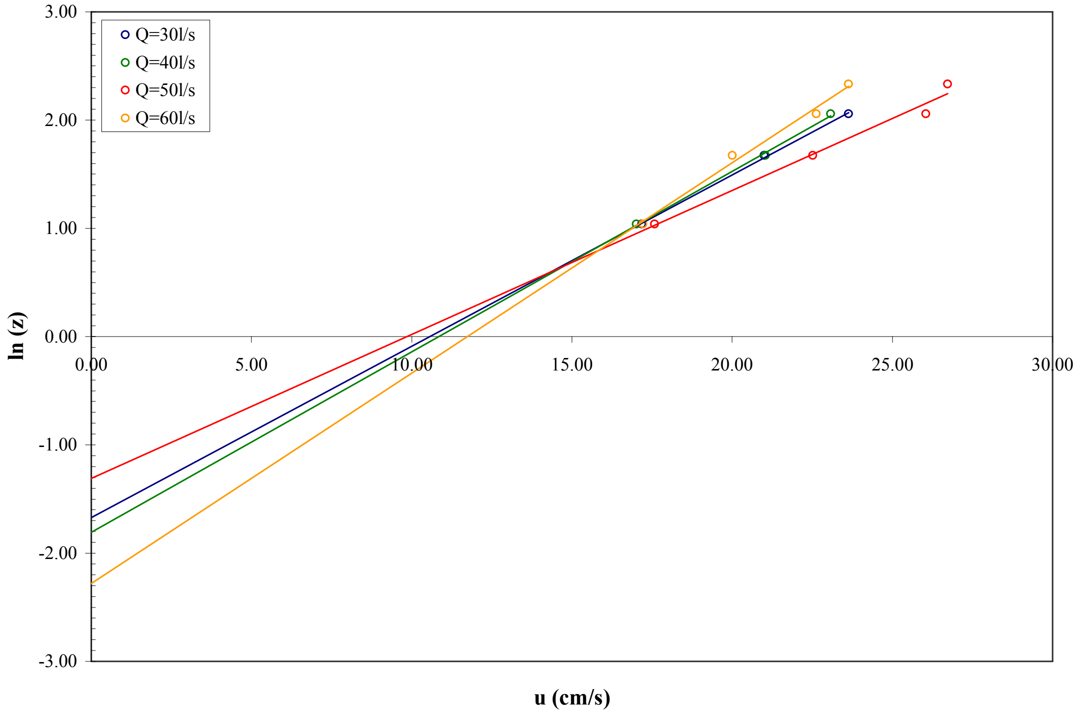

Figure C.2 *Determination of z_0 with a level of the bed (z =0.00m) at $1.17*10^{-2}$m above the bottom plates for L= 2.00m*

For *figure C.1* and *figure C.2* the values of z_0 are determined as shown in the table below. With the level of the bed set at 1.17×10^{-2}m above the bottom plates the average value of z_0 in the experiments, conducted by Dessens, is found to be z_0 = 1.56×10^{-3}m above z = 0.00m.

Table C.1 *Values of z_0 with a level of the bed at 1.17×10^{-2}m above the wooden plates for L = 1.50m and L = 2.00m (Dessens)*

L (m)	Q (m3/s)	delta z (m)	z_0 (m)	h (m)	ū (m/s)
1.50	0.03	0.01174	0.0012	0.258	0.243
1.50	0.04	0.01174	0.0022	0.323	0.257
1.50	0.05	0.01174	0.0006	0.378	0.273
1.50	0.06	0.01174	0.0031	0.436	0.283
2.00	0.03	0.01174	0.0019	0.261	0.24
2.00	0.04	0.01174	0.0016	0.325	0.255
2.00	0.05	0.01174	0.0027	0.383	0.27
2.00	0.06	0.01174	0.001	0.44	0.281
		Average z_0	0.00156		

The two series in grey were not used by Dessens to calculate the averaged z_0 because or differing values with other datasets, Dessens (2004).
The next figures show the flow profiles plotted on a logarithmic scale for the level of the bed at 1.30×10^{-2}m above the bottom plates.

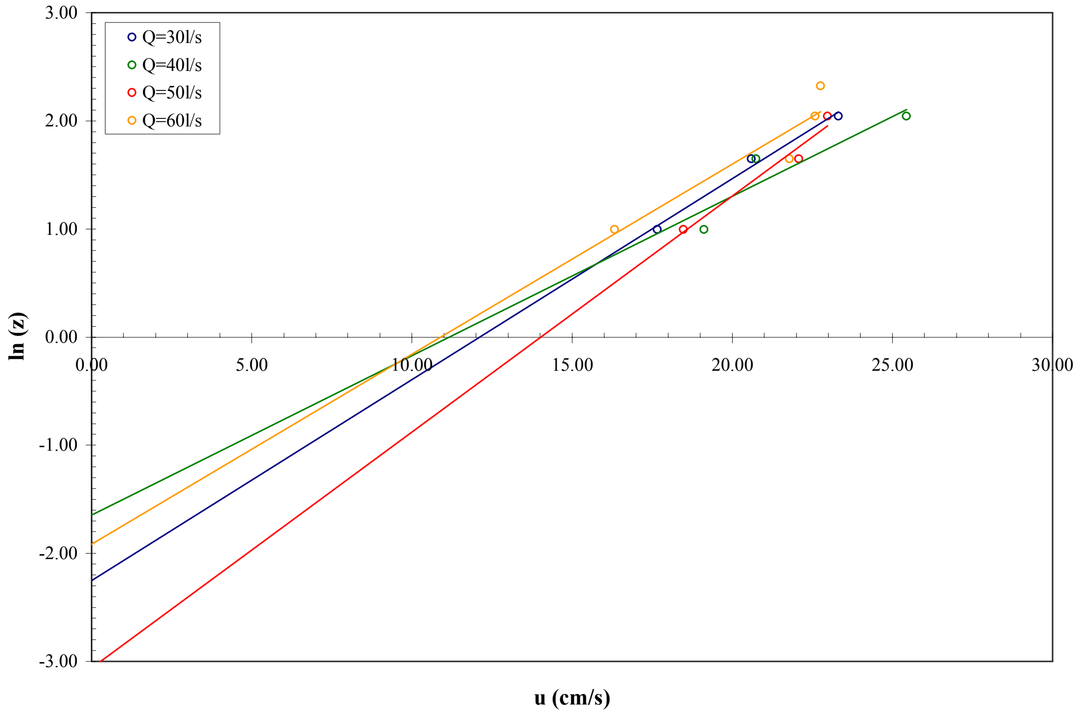

Figure C.3 *Determination of z_0 with the level of the bed (z =0.00m) at 1.30*10^{-2}m above the bottom plates for L= 1.50m*

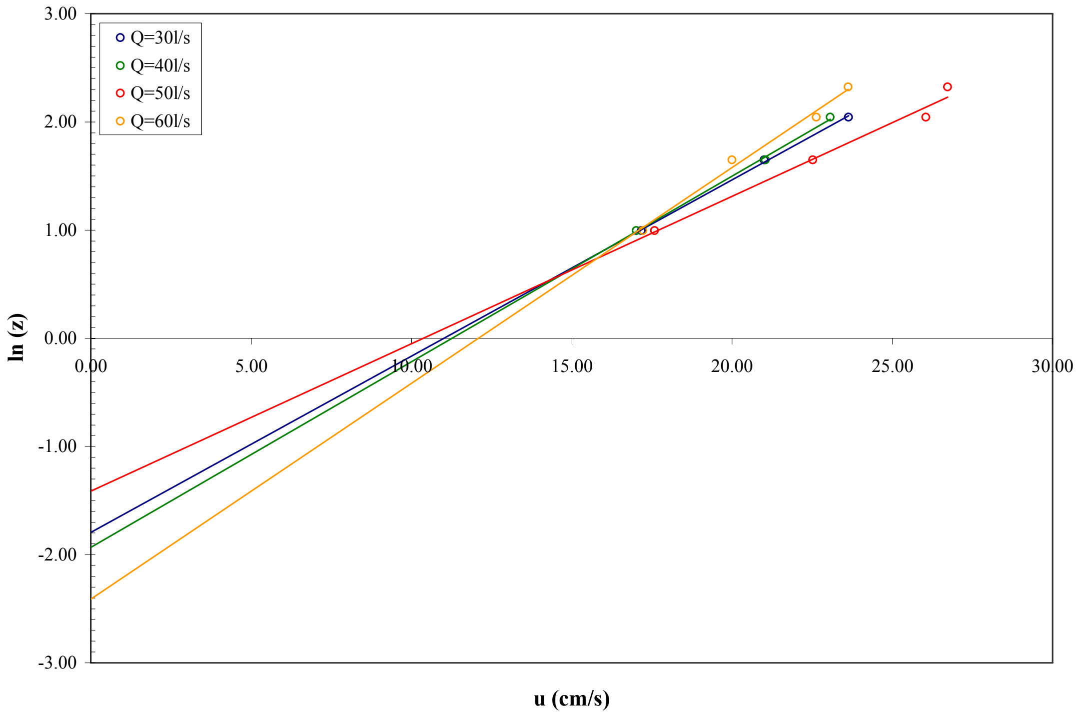

Figure C.4 *Determination of z_0 with the level of the bed (z =0.00m) at 1.30*10^{-2}m above the bottom plates for L= 2.00m*

With the level of the bed set at 1.30x10^{-2}m above the bottom plates the average value of z_0 for the experiments, conducted by Dessens, is found to be z_0 = 1.17x10^{-3}m above z = 0.00m, as shown in *table C.2*.
The data series in grey were disregarded.

Table C.2 *Values of z_0 with a level of the bed at 1.30x10^{-2}m above the bottom plates for L = 1.50m and L = 2.00m (Dessens)*

L (m)	Q (m3/s)	delta z (m)	z0 (m)	h (m)	ū (m/s)
1.50	0.03	0.01297	0.0011	0.257	0.246
1.50	0.04	0.01297	0.0017	0.321	0.259
1.50	0.05	0.01297	0.0005	0.377	0.275
1.50	0.06	0.01297	0.0015	0.434	0.285
2.00	0.03	0.01297	0.0017	0.26	0.243
2.00	0.04	0.01297	0.0013	0.324	0.258
2.00	0.05	0.01297	0.0024	0.381	0.271
2.00	0.06	0.01297	0.0009	0.438	0.282
		Average z_0	0.00117		

In the following graph, *figure C.5,* the flow profiles, taken from the experiments conducted by Huijsmans, are plotted on a logarithmic scale with the level of the bed set at 1.17x10^{-2}m above the bottom plates.

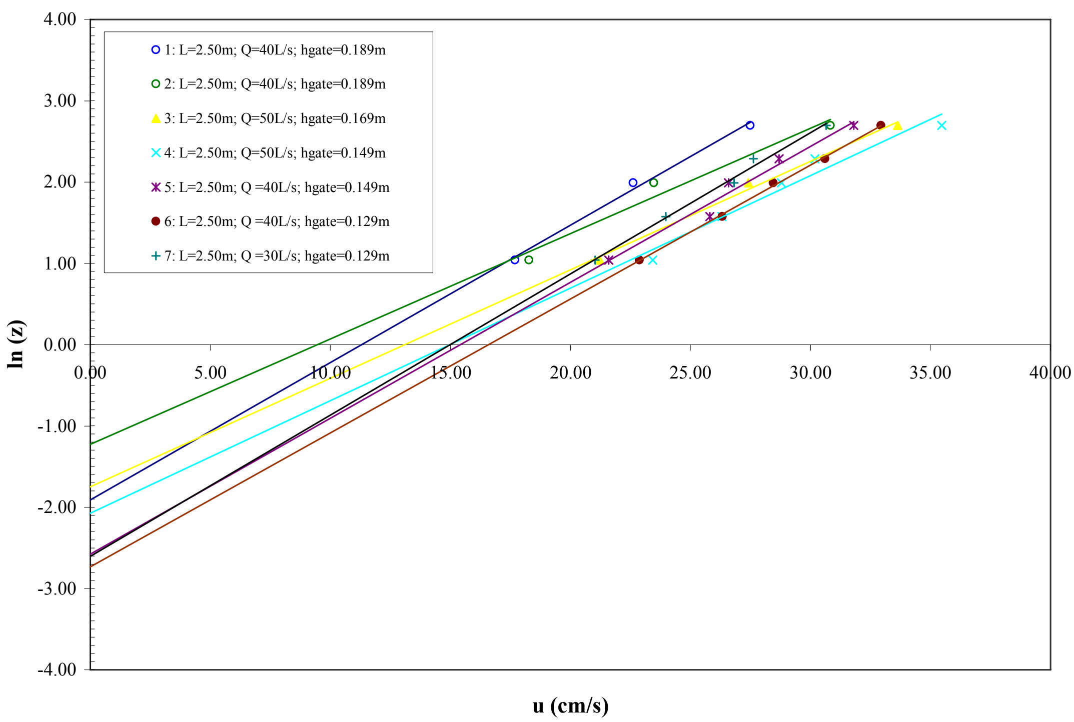

Figure C.5 *Determination of z_0 with a level of the bed (z =0.00m) at 1.17*10^{-2}m above the bottom plates for L= 2.50m*

Table C.3 *Values of z_0 with a level of the bed set at $1.17x10^{-2}$m above the bottom plates for L = 2.50m*

Series	L (m)	Q (m3/s)	delta z (m)	z0 (m)	h (m)	ū (m/s)
1	2.50	0.04	0.01174	0.0019	0.328	0.244
2	2.50	0.04	0.01174	0.0037	0.359	0.223
3	2.50	0.05	0.01174	0.0022	0.348	0.288
4	2.50	0.05	0.01174	0.0018	0.335	0.298
5	2.50	0.04	0.01174	0.0010	0.301	0.266
6	2.50	0.04	0.01174	0.0008	0.291	0.275
7	2.50	0.03	0.01174	0.0006	0.253	0.237
			Average z_0	0.00172		

With the level of the bed set at $1.17x10^{-2}$m above the bottom plates the average value of z_0 is found to be $z_0 = 1.72x10^{-3}$m above z = 0.00m, *table C.3*.

In *figure C.6* the flow profiles by Huijsmans are plotted on a logarithmic scale for a level of the bed set at $1.30x10^{-2}$m above the bottom plates.

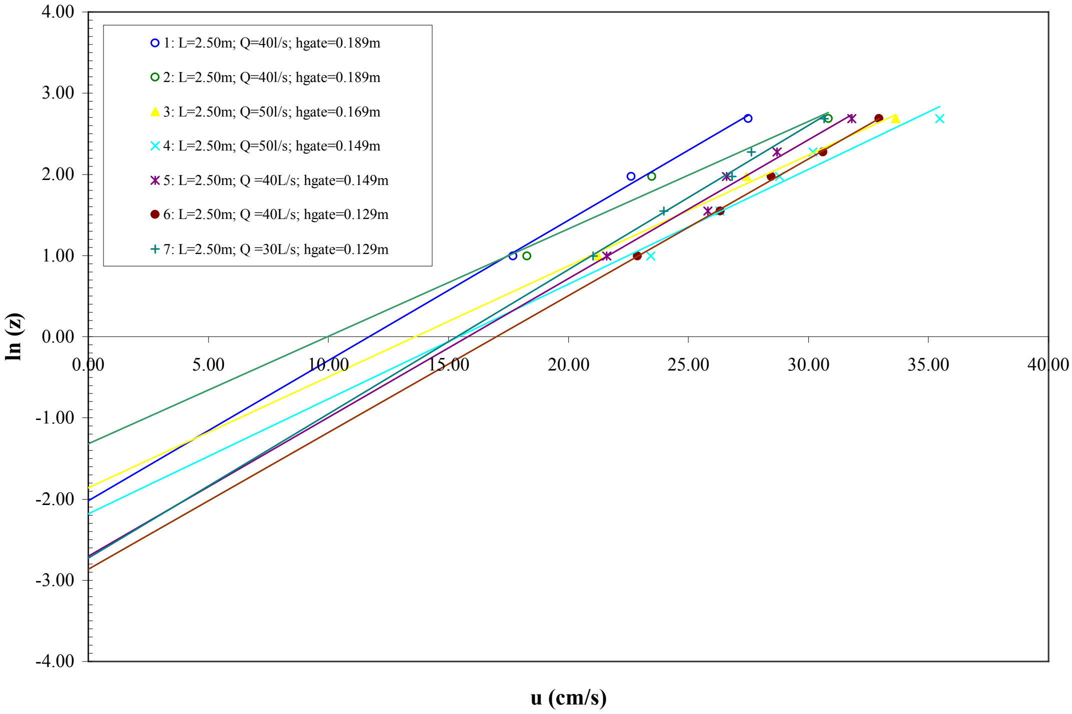

Figure C.6 *Determination of z_0 with a level of the bed (z =0.00m) at $1.30*10^{-2}$m above the bottom plates for L= 2.50m*

This results in an average value of z_0 = 1.57x10^{-3}m above z = 0.00m.

Table C.4 *Values of z_0 with a level of the bed set at 1.30x10^{-2}m above the bottom plates for L = 2.50m (Huijsmans)*

Series	L (m)	Q (m3/s)	delta z (m)	z0 (m)	h (m)	ū (m/s)
1	2.50	0.04	0.01297	0.0017	0.326	0.245
2	2.50	0.04	0.01297	0.0034	0.358	0.223
3	2.50	0.05	0.01297	0.0020	0.346	0.289
4	2.50	0.05	0.01297	0.0017	0.334	0.299
5	2.50	0.04	0.01297	0.0009	0.299	0.267
6	2.50	0.04	0.01297	0.0007	0.289	0.277
7	2.50	0.03	0.01297	0.0005	0.252	0.239
			Average z_0	0.00157		

Appendix C3 Stone moves

			stone moves in experiment								dumped
strip	ū	a	1	2	3	4	5	6	avg	%	tot.
L = 1.50m											
yellow	0.84	1.31	27	41	26	7	28	17	24.3	10.81	225
blue	0.71	0.82	1	5	2	2	8	5	3.8	1.53	250
green	0.61	0.49	1	1	0	1	2	1	1.0	0.36	277
pink	0.53	0.38	0	0	0	0	0	0	0.0	0.00	306
yellow	0.94	1.52	32	17	12	20	41	35	26.2	11.63	225
blue	0.80	0.93	10	5	5	10	13	15	9.7	3.87	250
green	0.69	0.66	2	0	2	2	2	0	1.3	0.48	277
pink	0.61	0.46	3	1	0	0	0	0	0.7	0.22	306
yellow	0.98	1.55	19	50	21	48	24	20	30.3	13.48	225
blue	0.84	1.08	9	6	4	8	4	6	6.2	2.47	250
green	0.72	0.71	2	2	2	0	1	2	1.5	0.54	277
pink	0.64	0.50	0	1	1	0	0	0	0.3	0.11	306
yellow	0.89	1.37	25	21	20	41	33	34	29.0	12.89	225
blue	0.75	0.86	4	3	8	9	6	7	6.2	2.47	250
green	0.65	0.56	1	2	0	1	2	0	1.0	0.36	277
pink	0.57	0.42	1	0	0	0	0	0	0.2	0.05	306
yellow	-	-	137	123	210	191	173	187	170.2	75.63	225
blue	0.89	1.28	63	36	83	53	55	56	57.7	23.07	250
green	0.76	0.85	6	2	6	10	8	4	6.0	2.17	277
pink	0.66	0.52	0	0	1	0	1	0	0.3	0.11	306
yellow	-	-	200	206	203	100	110	165	164.0	72.89	225
blue	0.86	1.06	21	63	50	12	22	40	34.7	13.87	250
green	0.74	0.78	5	9	11	6	6	4	6.8	2.47	277
pink	0.65	0.55	1	0	1	1	1	1	0.8	0.27	306
yellow	-	-	123	102	102	94	107	71	137.0	60.89	225
blue	0.86	1.06	41	13	40	23	35	7	26.5	10.60	250
green	0.74	0.77	3	3	2	3	0	1	2.0	0.72	277
pink	0.65	0.57	2	2	0	0	0	0	0.7	0.22	306
yellow	0.80	1.06	10	5	7	5	17	17	10.2	4.52	225
blue	0.68	0.70	0	3	1	0	0	0	0.7	0.27	250
green	0.59	0.46	0	0	0	0	0	1	0.2	0.06	277
pink	-	-	0	0	0	0	0	0	0.0	0.00	306

yellow	0.96	1.63	70	42	46	46	59	46	51.5	22.89	225
blue	0.80	1.13	20	21	12	11	21	15	16.7	6.67	250
green	0.68	0.71	2	0	3	1	4	3	2.2	0.78	277
pink	-	-	0	2	0	0	0	0	0.3	0.11	306
yellow	0.84	1.28	20	19	8	7	15	12	13.5	6.00	225
blue	0.71	0.77	4	1	0	0	2	2	1.5	0.60	250
green	0.62	0.56	0	0	0	0	1	0	0.2	0.06	277
pink	-	-	0	0	0	0	0	0	0.0	0.00	306
yellow	0.72	0.85	1	1	9	3	2	3	3.2	1.41	225
blue	0.61	0.53	0	1	0	0	2	0	0.5	0.20	250
green	-	-	0	1	0	0	0	0	0.2	0.06	277
pink	-	-	0	0	0	0	0	0	0.0	0.00	306
	L = 2.00m										
yellow	0.84	0.97	21	8	9	21	5	15	13.2	5.80	227
blue	0.73	0.69	4	5	2	5	5	3	4.0	1.63	246
green	0.64	0.52	0	0	0	0	0	1	0.2	0.06	278
pink	0.57	0.38	0	0	0	0	0	0	0.0	0.00	251
yellow	0.91	1.13	9	17	25	11	9	9	13.3	5.87	227
blue	0.80	0.81	6	5	11	3	3	2	5.0	2.03	246
green	0.71	0.58	1	0	1	1	2	1	1.0	0.36	278
pink	0.63	0.44	0	0	1	0	1	0	0.3	0.13	251
yellow	0.92	1.14	22	30	42	16	19	27	26.0	11.82	220
blue	0.80	0.86	2	4	5	3	6	4	4.0	1.63	245
green	0.71	0.61	2	2	2	2	2	2	2.0	0.75	265
pink	-	-	2	0	0	0	0	0	0.3	0.11	290
yellow	1.05	1.48	125	156	112	160	162	149	144.0	65.45	220
blue	0.91	1.18	32	24	22	34	36	33	30.2	11.77	245
green	0.80	0.78	10	7	6	6	10	8	7.8	2.96	265
pink	0.71	0.57	0	1	0	0	0	0	0.2	0.06	290
yellow	0.86	1.03	10	10	11	3	21	5	10.0	4.55	220
blue	0.75	0.72	1	3	1	2	2	1	1.7	0.68	245
green	0.67	0.49	0	0	1	0	0	0	0.2	0.06	265
pink	-	-	0	0	0	0	0	0	0.0	0.00	290
yellow	0.98	1.29	86	71	66	53	89	69	72.3	32.88	220
blue	0.86	1.01	18	5	17	7	36	15	16.3	6.67	245
green	0.75	0.70	4	1	3	5	0	2	2.5	0.94	265
pink	0.67	0.49	0	0	1	0	1	0	0.3	0.11	290

yellow	0.96	1.17	20	25	18	36	49	10	26.3	11.60	227
blue	0.84	0.91	9	4	4	8	6	1	5.3	2.17	246
green	0.75	0.61	2	0	1	3	2	1	1.5	0.54	278
pink	0.67	0.49	0	0	0	0	0	0	0.0	0.00	251
yellow	0.99	1.27	25	21	18	11	33	20	21.3	9.40	227
blue	0.87	1.00	5	10	10	5	6	6	7.0	2.85	246
green	0.77	0.63	1	2	4	1	2	2	2.0	0.72	278
pink	0.69	0.52	0	0	0	1	1	1	0.5	0.20	251
L = 2.50m											
yellow	0.89	0.81	9	23	13	13	8	8	12.3	5.14	240
blue	0.80	0.73	6	4	3	5	4	6	4.7	1.79	260
green	0.72	0.49	1	0	0	0	0	0	0.2	0.06	260
pink	0.65	0.37	0	0	0	0	0	0	0.0	0.00	320
yellow	1.06	1.19	10	54	87	79	33	45	51.3	21.39	240
blue	0.96	1.03	8	13	7	8	13	10	9.8	3.78	260
green	0.85	0.87	0	0	1	1	1	0	0.5	0.19	260
pink	0.77	0.46	0	0	0	0	0	0	0.0	0.00	320
yellow	1.12	1.29	173	133	116	127	72	72	115.5	48.13	240
blue	1.01	1.18	69	41	34	40	22	59	44.2	16.99	260
green	0.90	0.84	18	14	7	8	6	8	10.2	3.91	260
pink	0.81	0.72	3	2	2	2	1	2	2.0	0.63	320
yellow	1.17	1.90	181	205	195	175	163	161	180.0	75.00	240
blue	1.04	1.02	95	116	105	102	55	75	91.3	35.13	260
green	0.95	0.95	17	35	19	29	19	24	23.8	9.17	260
pink	0.86	0.68	9	6	3	4	1	5	4.7	1.46	320
yellow	1.04	0.96	82	79	58	82	50	90	73.5	30.63	240
blue	0.94	1.05	29	22	18	26	9	33	22.8	8.78	260
green	0.84	0.72	3	3	6	10	5	0	4.5	1.73	260
pink	0.77	0.54	2	0	0	0	0	0	0.3	0.10	320
yellow	1.12	1.41	132	120	100	112	135	180	129.8	54.10	240
blue	1.01	0.98	71	72	29	36	40	80	54.7	21.03	260
green	0.90	1.08	29	8	5	5	6	12	10.8	4.17	260
pink	0.80	0.59	2	3	2	2	2	0	1.8	0.57	320
yellow	0.92	1.00	42	27	34	14	29	25	28.5	11.88	240
blue	0.83	0.57	3	1	3	10	17	11	7.5	2.88	260
green	0.76	0.55	2	1	0	2	12	6	3.8	1.47	260
pink	0.69	0.46	0	0	0	0	0	1	0.2	0.05	320

Appendix C4 Choice of z_0

The uniform flow velocities have been calculated with a value for z_0 of $z_0 = 1.17\text{x}10^{-3}$m, *section 4.1.2.* This is the z_0, which has been determined with the uniform flow profiles as the flow enters the tapered section.

It wasn't possible to measure near enough to the bottom in the accelerated flow to see what happens to the bottom part of the flow profile. Since the flow contraction causes the boundary layer thickness to reduce, it is unlikely that the value for z_0 should increase. To see what happens to the shift in velocities when a higher value z_0 is applied, the uniform velocities are calculated with another value for z_0.

Boutovski, 1998, found for a bed in a flume experiment: $k_r \approx 6\ d_{n50}$. This would result in z_0 of $z_0 = 1.62\text{x}10^{-3}$m.

To see if the value of z_0 affects the shift in velocities, the shift in velocities has been calculated for a value z_0 of $z_0 = 1.62\text{x}10^{-3}$m.

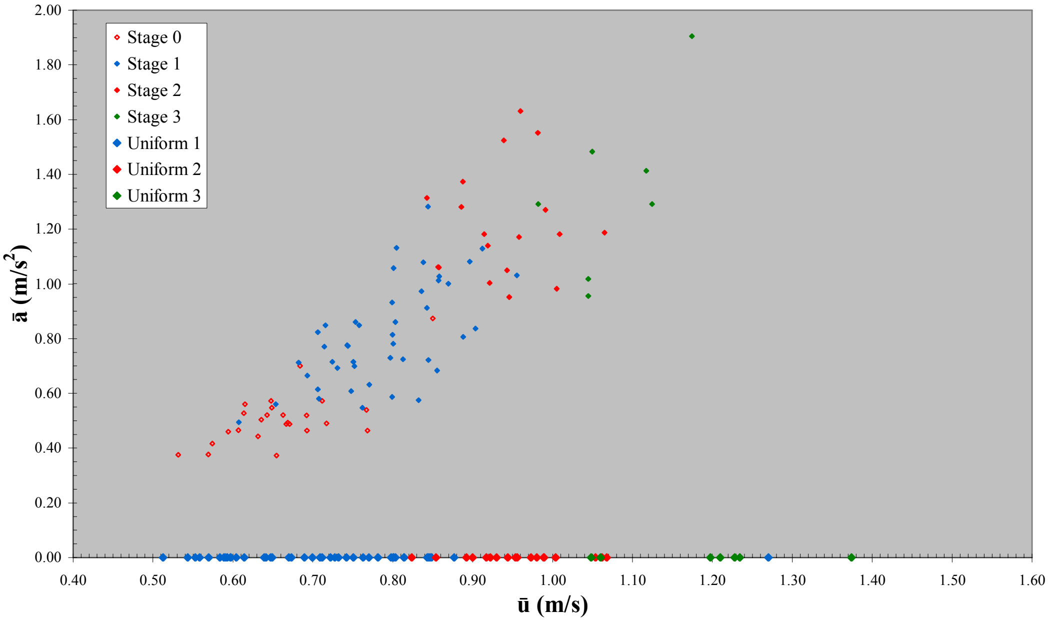

Figure C.7 *Shift in velocities for distribution 5 with $z_0 = 1.64\text{x}10^{-3}$m.*

The shift in velocities will be shown for the three different lengths of the tapered section calculated with a value for z_0 of $z_0 = 1.17\text{x}10^{-3}$m in the left column and a value for z_0 of $z_0 = 1.62\text{x}10^{-3}$m in the right column are given in the next graph, *figure C.8.*

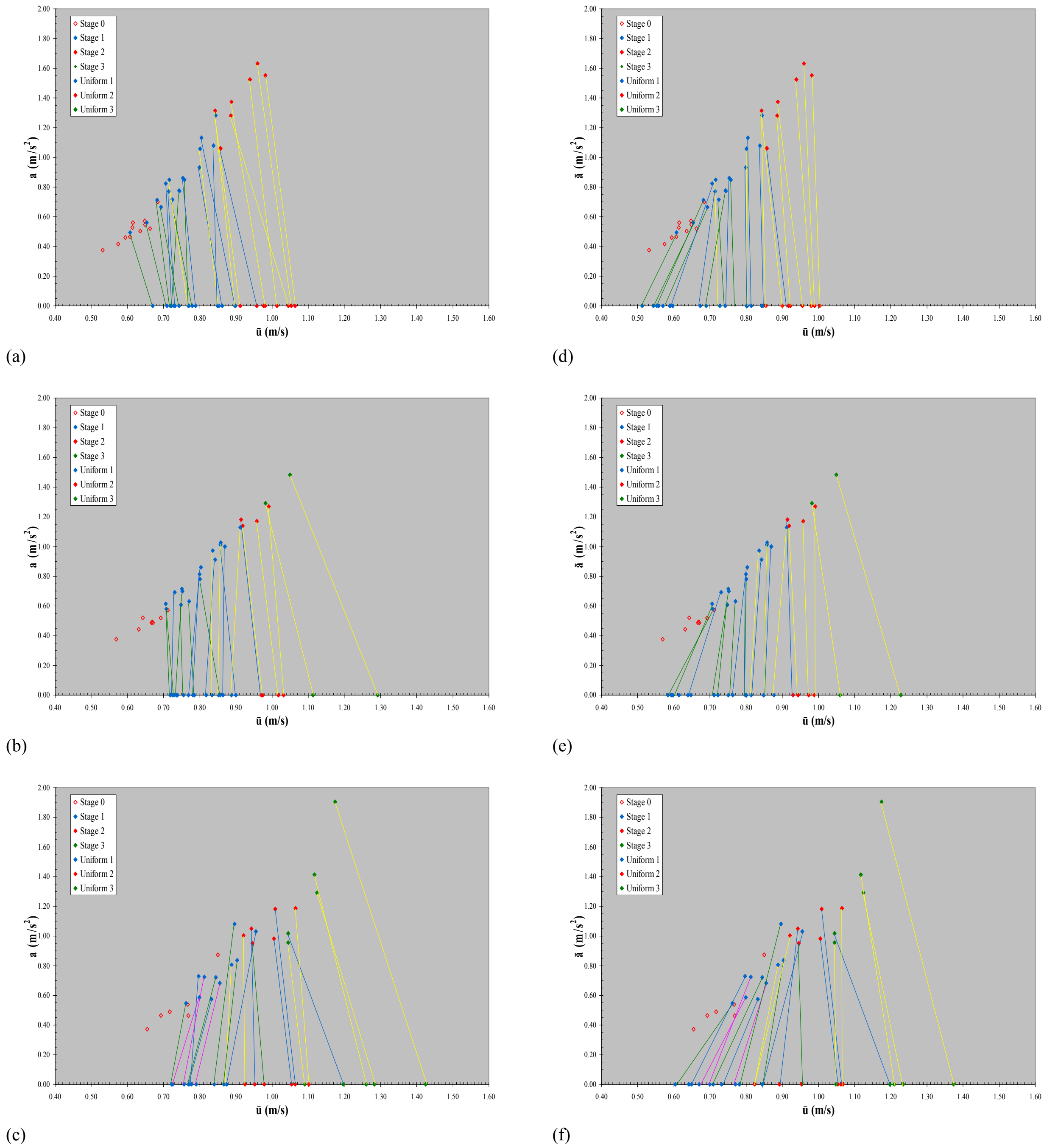

Figure C.8 *Shift in velocities for distribution 5 according to Huijsmans, left column: $z_0 = 1.17x10^{-3}$m ((a.) L = 1.50 m, (b.) L = 2.00m, (c.) L = 2.50m), right column: $z_0 = 1.62x10^{-3}$m ((d.) L = 1.50m, (e.) L = 2.00m, (f.) L = 2.50m)*

The choice of z_0 does have an effect on the shift in velocities. With a higher z_0 flow acceleration does not have such impact on the stability of stones. The shift in velocities has shifted to the left compared to the shift with a z_0 of $z_0 = 1.17x10^{-3}$m

More accurate readings near the bed in the accelerated flow can give insight in how the height of z_0 is affected by the acceleration of the flow.